



**TECHNICAL REPORT 5-4829-03-1**  
TXDOT PROJECT NUMBER 5-4829-03

# Soil-Geosynthetic Interaction Test to Develop Specifications for Geosynthetic-Stabilized Roadways

Gholam H. Roodi  
Jorge G. Zornberg  
Mahmoud M. Aboelwafa  
James R. Phillips  
Liming Zheng  
Jose Martinez

August 2017; Published May 2018

<http://library.ctr.utexas.edu/ctr-publications/5-4829-03-1.pdf>



Technical Report Documentation Page

1. Report No. FHWA/TX-18/5-4829-03-1		2. Government Accession No.	3. Recipient's Catalog No.	
4. Title and Subtitle Soil-Geosynthetic Interaction Test to Develop Specifications for Geosynthetic-Stabilized Roadways		5. Report Date August 2017; Published May 2018		
		6. Performing Organization Code		
7. Author(s) Gholam H. Roodi, Jorge G. Zornberg, Mahmoud M. Aboelwafa, James R. Phillips, Liming Zheng, Jose Martinez		8. Performing Organization Report No. 5-4829-03-1		
9. Performing Organization Name and Address Center for Transportation Research The University of Texas at Austin 3925 W. Braker Lane, 4th floor Stop D9300 Austin, TX 78759		10. Work Unit No. (TRAIS)		
		11. Contract or Grant No. 5-4829-03		
12. Sponsoring Agency Name and Address Texas Department of Transportation Research and Technology Implementation Office P.O. Box 5080 Austin, TX 78763-5080		13. Type of Report and Period Covered Technical Report September 2015–August 2017		
		14. Sponsoring Agency Code		
15. Supplementary Notes Project performed in cooperation with the Texas Department of Transportation and the Federal Highway Administration.				
16. Abstract A comprehensive soil-geosynthetic interaction testing program was conducted to determine the stiffness of the soil-geosynthetic composite ( $K_{SGC}$ ) for a wide range of geosynthetics. The tests were conducted after establishment of test configurations that were found suitable for specification of geosynthetic-stabilized base roadways. Field performance of experimental test sections that were constructed using the same geosynthetics as those tested in the experimental program was also evaluated. By comparing the field performances to the $K_{SGC}$ values obtained using soil-geosynthetic interaction tests, a threshold value for selection of geosynthetics for base stabilization was identified. Recommendations were made to implement findings of this project into TxDOT DMS-6240.				
17. Key Words Geosynthetics, geogrids, geotextiles, stabilization, reinforcement, soil-geosynthetic interaction, pavements, expansive clay subgrades, reinforced unbound base course, small pullout test, stiffness		18. Distribution Statement No restrictions. This document is available to the public through the National Technical Information Service, Springfield, Virginia 22161; www.ntis.gov.		
19. Security Classif. (of report) Unclassified	20. Security Classif. (of this page) Unclassified	21. No. of pages 112	22. Price	



**THE UNIVERSITY OF TEXAS AT AUSTIN  
CENTER FOR TRANSPORTATION RESEARCH**

## **Soil-Geosynthetic Interaction Test to Develop Specifications for Geosynthetic-Stabilized Roadways**

Gholam H. Roodi  
Jorge G. Zornberg  
Mahmoud M. Aboelwafa  
James R. Phillips  
Liming Zheng  
Jose Martinez

---

CTR Technical Report:	5-4829-03-1
Report Date:	August 2017: Published May 2018
Project:	5-4829-03
Project Title:	Implementation of Geosynthetic-Reinforced Unbound Base Courses
Sponsoring Agency:	Texas Department of Transportation
Performing Agency:	Center for Transportation Research at The University of Texas at Austin

Project performed in cooperation with the Texas Department of Transportation and the Federal Highway Administration.

Center for Transportation Research  
The University of Texas at Austin  
3925 W. Braker Lane, Stop D9300  
Austin, TX 78759

<http://ctr.utexas.edu/>

## **Disclaimers**

---

**Author's Disclaimer:** The contents of this report reflect the views of the authors, who are responsible for the facts and the accuracy of the data presented herein. The contents do not necessarily reflect the official view or policies of the Federal Highway Administration or the Texas Department of Transportation (TxDOT). This report does not constitute a standard, specification, or regulation.

**Patent Disclaimer:** There was no invention or discovery conceived or first actually reduced to practice in the course of or under this contract, including any art, method, process, machine manufacture, design or composition of matter, or any new useful improvement thereof, or any variety of plant, which is or may be patentable under the patent laws of the United States of America or any foreign country.

Notice: The United States Government and the State of Texas do not endorse products or manufacturers. If trade or manufacturers' names appear herein, it is solely because they are considered essential to the object of this report.

## **Engineering Disclaimer**

---

NOT INTENDED FOR CONSTRUCTION, BIDDING, OR PERMIT PURPOSES.

Research Supervisor: Dr. Jorge Zornberg

## **Acknowledgments**

---

The authors are thankful for the support provided by TxDOT Project Director, Mr. Richard Izzo (Construction Division), for the efficient technical and logistical guidance. We would also like to acknowledge the help of Joe Adams (RTI), Jimmy Si (Construction Division), Brett Haggerty (Construction Division), Mike Arellano (Austin District), and Gisel Carrasco (Austin District). Their prompt assistance has facilitated enormously the successful completion of this implementation project.

# Table of Contents

---

Chapter 1. Objectives and Scope of the Report .....	1
Chapter 2. Refinements in the Soil-geosynthetic Interaction Test Procedure and Data Analysis .....	3
2.1. Introduction.....	3
2.2. Refinements in the Testing Procedure .....	3
2.2.1. Refinement in the Telltales Attachment Procedure .....	3
2.2.2. Refinement of Grip Setup .....	4
2.2.3. Refinement of Boundary Conditions .....	5
2.2.4. Refinement of the Normal Pressure System .....	6
2.3. Refinement of Data Analysis .....	6
2.3.1. Factors Evaluated in the Refinement Process .....	6
2.3.2. Final Protocol Adopted for Data Analysis .....	8
2.4. Summary and Conclusions .....	9
Chapter 3. Experimental Program: Production of Soil-geosynthetic Interaction Data using Small-scale Device .....	10
3.1. Introduction.....	10
3.2. Material Properties.....	10
3.2.1. Baseline Geosynthetics .....	10
3.2.2. Characterization of Geosynthetics in accordance with TxDOT Specifications .....	15
3.2.3. Backfill Materials.....	16
3.3. Scope of Testing Program.....	18
3.3.1. Geosynthetic Specimen Dimensions.....	18
3.3.2. Confining Pressure (Normal Stress) .....	18
3.3.3. Geosynthetic Orientation .....	19
3.3.4. Testing Displacement Rate .....	19
3.3.5. Testing Matrix.....	19
3.4. Test Results.....	19
3.4.1. Effect of Backfill Materials .....	20
3.4.2. Effect of Normal Stress.....	22
3.4.3. Effect of Test Direction.....	24
3.5. Summary and Conclusions .....	25
Chapter 4. Field Monitoring Program.....	27
4.1. Introduction.....	27
4.2. Performance Evaluation Program .....	27

4.2.1. Visual Condition Surveys .....	28
4.2.2. Total Station Surveys .....	31
4.2.3. PMIS Data.....	35
4.3. Field Performance of Experimental Test Sections .....	38
4.3.1. Identification of Field Test Sections .....	38
4.3.2. Site 1: Farm-to-Market Road 2 (FM 2).....	41
4.3.3. Site 2: Farm-to-Market Road 1644 (FM 1644).....	43
4.3.4. Site 3: Farm-to-Market Road 1915 (FM 1915).....	46
4.3.5. Site 4: Farm-to-Market Road 1774 (FM 1774).....	49
4.3.6. Site 5: State Highway 21 (SH 21).....	52
4.3.7. Site 6: Farm-to-Market Road 2924 (FM 2924).....	57
4.3.8. Site 7: Farm-to-Market Road 1979 (FM 1979).....	61
4.3.9. Site 8: Cabeza Road .....	64
4.3.10. Site 9: Farm-to-Market Road 972 (FM 972).....	68
4.3.11. Site 10: Turnersville Road .....	73
4.4. Summary and Conclusions .....	79
Chapter 5. Specifications for Selection of Geosynthetic for Base Stabilization of Roadways Subjected to Environmental Loads .....	81
5.1. Introduction.....	81
5.2. Review of the Existing Specifications .....	81
5.3. Experimental Program to Produce Soil-geosynthetic Interaction Data .....	83
5.3.1. Geosynthetic Products .....	83
5.3.2. Test Configurations.....	87
5.3.3. Sources of Uncertainty in the Test Results .....	87
5.3.4. Data Reduction Protocol .....	88
5.4. Establishment of Threshold Value for $K_{SGC}$ .....	89
5.4.1. Comparison of $K_{SGC}$ Values .....	89
5.4.2. Qualitative Evaluation of Field Performance.....	91
5.4.3. Recommended Threshold Value for $K_{SGC}$ .....	92
5.5. Refinement of TxDOT DMS-6240.....	92
5.5.1. Alternative 1 – Two Geogrid Grades: Types 1 and 2 .....	93
5.5.2. Alternative 2 – Three Geogrid Grades: Types 1, 2, and 3 .....	94
Chapter 6. Conclusions .....	97
References.....	98



## List of Figures

---

Figure 2.1 Refinement in the telltale attachment procedure: a) old procedure; b) refined procedure.....	4
Figure 2.2 Grip setup .....	4
Figure 2.3 Knurled rod adopted in the refined testing procedure .....	5
Figure 2.4 Refinement of boundary condition: a) old procedure; b) refined procedure .....	5
Figure 2.5 Refined normal pressure control system .....	6
Figure 2.6 Example test results showing the impact of data smoothing procedure.....	8
Figure 2.7 Impact of refinement in the data analysis (sample results) .....	9
Figure 3.1 Baseline biaxial integrally formed geogrid from polypropylene: GG 1.....	11
Figure 3.2 Baseline triangular integrally formed geogrid from polypropylene: GG 2.....	12
Figure 3.3 Baseline biaxial woven geogrid from polyester: GG 3 .....	13
Figure 3.4 Baseline biaxial laser-bonded geogrid from polypropylene: GG 4.....	14
Figure 3.5 Baseline woven geotextile: GT 1 .....	15
Figure 3.6 Backfill materials used in the experimental program: a) AASHTO No. 8; b) AASHTO No. 8-Truncated; c) Monterey No. 30 Sand.....	17
Figure 3.7 Soil particle size distribution curves of the backfill materials used in the experimental program.....	18
Figure 3.8 $K_{SGC}$ values obtained for the baseline geosynthetics using various backfill materials: a) AASHTO No. 8; b) AASHTO No. 8-Truncated; c) Monterey No. 30 Sand.....	21
Figure 3.9 $K_{SGC}$ values obtained for the baseline geosynthetics using various normal stresses: a) 1 psi; b) 3 psi; c) 5 psi. ....	23
Figure 3.10 Comparison of $K_{SGC}$ values obtained for the baseline geosynthetics in cross-machine and machine directions using AASHTO No. 8-Truncated backfill materials under 3 psi .....	25
Figure 4.1 Measurements of rutting in the FM2 pavement .....	29
Figure 4.2 Example analysis for comparative evaluation of performance in geosynthetic-stabilized versus non-stabilized test sections .....	31
Figure 4.3 Non-uniform environmental loading imposed to road structures by expansive subgrades (Roodi and Zornberg, 2012).....	32

Figure 4.4 Conceptual model for generating environmentally induced longitudinal cracks in pavements.....	32
Figure 4.5 Marking transverse test sections a) Marking a stripe with duct tape; b) Painting the stripe with white spray paints; c) Painting circular orange marks on the white stripe .....	33
Figure 4.6 Using total station and prism to monitor vertical deformation of the marked transverse sections .....	34
Figure 4.7 Total station survey of the marked sections in the field.....	34
Figure 4.8 Example transverse profile of the road surface generated using total station data .....	35
Figure 4.9 Example analysis for comparative evaluation of performance in geosynthetic-stabilized versus non-stabilized test sections using PMIS data.....	37
Figure 4.10 Location of FM 2 and the rehabilitation area .....	41
Figure 4.11 Design profile of FM 2 before reconstruction.....	42
Figure 4.12 Location of the test sections at FM 2.....	42
Figure 4.13 Four repair schemes used in the FM2 project .....	42
Figure 4.14 Percentage of environmental longitudinal cracks at the FM2 test sections .....	43
Figure 4.15 Location of the test sections at FM 1644.....	44
Figure 4.16 Layout of the test sections at FM 1644 .....	44
Figure 4.17 Design of the test sections at FM 1644 .....	45
Figure 4.18 Percentage of environmental longitudinal cracks at the FM1644 test sections .....	45
Figure 4.19 Example pictures from test sections at FM 1644: a) Section 2 (geosynthetic-stabilized section); b) Section 4 (control section).....	46
Figure 4.20 Extensions and designs of the test sections at FM 1915 .....	47
Figure 4.21 Percentage of environmental longitudinal cracks at FM 1915 test sections .....	48
Figure 4.22 Example pictures from test sections at FM 1915: a) Section 1 (geosynthetic-stabilized section); b) Section 2 (control section).....	48
Figure 4.23 Extensions and designs of the test sections in FM 1774 .....	49
Figure 4.24 Example pictures of the field performance of the test section stabilized using GG 4: a) longitudinal crack on the pavement; b) slippage between longitudinal and transverse ribs at junction of geogrid .....	50

Figure 4.25 Example picture of the field performance of the test section stabilized using GG 1 at FM 1774 .....	51
Figure 4.26 Condition score of the test sections at FM 1774 from 1995 to 2014.....	52
Figure 4.27 Location of SH 21 and the test sections .....	53
Figure 4.28 Layout of test sections at SH 21 .....	53
Figure 4.29 Test sections design in the SH21 reconstruction project: a) before reconstruction; b) after reconstruction.....	54
Figure 4.30 Percentage of environmental longitudinal cracks at SH21 test sections.....	55
Figure 4.31 Example pictures from test sections at SH 21: a) Section 1; b) Section 4; c) Section 5; d) Section 3.....	56
Figure 4.32 Design of test sections at FM 2924 .....	57
Figure 4.33 Layout of the test sections at FM 2924 .....	58
Figure 4.34 Example pictures of the longitudinal cracks developed at the edges of test sections at FM 2924 .....	59
Figure 4.35 Elevation of marked transverse sections at FM 2924 from 2015 to 2017: a) Transverse Section 2; b) Transverse Section 4; c) Transverse Section 6 .....	60
Figure 4.36 Location of FM 1979 relative to San Marcos and Martindale .....	61
Figure 4.37 Layout of test sections at FM 1979 .....	62
Figure 4.38 Percentage of environmental longitudinal cracks at the FM1979 test sections .....	62
Figure 4.39 Transverse Section 3 at FM 1979: a) variation of the elevation from 2015 to 2017 from data recorded using total station; b) picture of the transverse section .....	63
Figure 4.40 Variation of the road elevation at Transverse Section 7.....	64
Figure 4.41 Location of Cabeza Rd. relative to Nordheim.....	64
Figure 4.42 Location of test sections along Cabeza Rd.....	65
Figure 4.43 Layout of test sections at Cabeza Rd.....	65
Figure 4.44 Design of test sections at Cabeza Rd.: a) Section 1 (geosynthetic-stabilized); b) control; c) geosynthetic-stabilized .....	66
Figure 4.45 Percentage of environmental longitudinal cracks at SH21 test sections.....	67
Figure 4.46 Example pictures of longitudinal cracks in control section at Cabeza Rd. ....	67

Figure 4.47 Transverse Section 5 at Cabeza Rd. located within test Section 3: a) variation of the elevation from 2015 to 2016 from data recorded using total station; b) picture of the transverse section.....	68
Figure 4.48 Layout of test sections at FM 972 .....	69
Figure 4.49 Results of total station surveys and road conditions at FM 972.....	72
Figure 4.50 Layout of test sections at Turnersville Road .....	73
Figure 4.51 Results of total station surveys and road conditions in Turnersville Road.....	77
Figure 4.52 Percentage of environmental longitudinal cracks at Turnersville Road test sections .....	78
Figure 4.53 Example pictures of longitudinal cracks observed at Turnersville Road test sections in 2017 .....	78
Figure 5.1 Interaction test conducted using Mylar sheets as an index for a product with particularly weak interaction properties .....	84
Figure 5.2 The $K_{SGC}$ values obtained for the identified geosynthetics using test configurations recommended for TxDOT specifications .....	90
Figure 5.3 Alternative 1 - Adopting two geogrid grades in the refined TxDOT DMS-6240 specification .....	93
Figure 5.4 Refinement in TxDOT DMS-6240 specification according to Alternative 1.....	94
Figure 5.5 Alternative 2 - Adopting three geogrid grades in the refined TxDOT DMS-6240 specifications.....	95
Figure 5.6 Refinement in TxDOT DMS-6240 specification according to Alternative 2.....	96

## List of Tables

---

Table 3.1: Geosynthetic products used in small pullout testing program.....	11
Table 3.2. Index Properties of GG 1 .....	12
Table 3.3. Index Properties for GG 2.....	13
Table 3.4. Index Properties of GG 3 .....	13
Table 3.5. Index Properties of GG 4 .....	14
Table 3.6. Index Properties of GT 1 .....	15
Table 3.7: Characterization of geosynthetics in accordance with TxDOT DMS-6240.....	16
Table 3.8: Soil-geosynthetic interaction testing matrix using the baseline geosynthetics.....	19
Table 4.1: Example visual condition survey data collected as part of the monitoring program .....	31
Table 4.2. Example results from total station surveys .....	35
Table 4.3. Example PMIS data collected as part of the monitoring program.....	37
Table 4.4: Main features of the identified field test sections.....	39
Table 4.5: Characterization of geosynthetics used in the field test sections in accordance with the requirements of TxDOT DMS-6240.....	40
Table 4.6. Main features of three test sections constructed at FM 1915 .....	47
Table 4.7. Summary of monitoring program and results for transverse test sections in FM 972—Segment II.....	71
Table 4.8. Summary of monitoring program and results for transverse test sections in Turnersville Road.....	76
Table 5.1 Geogrid requirements in accordance with TxDOT DMS-6240.....	82
Table 5.2 Geogrid requirements in accordance with TxDOT DMS-6270.....	83
Table 5.3: Characterization of the selected geosynthetic reinforcements in accordance with the requirements of DMS-6240 .....	85
Table 5.4: Final testing matrix for the additional ten geosynthetics.....	87
Table 5.5 Qualitative field performance of geosynthetics as compared to their $K_{SGC}$ value.....	92

# Chapter 1. Objectives and Scope of the Report

This document reports on the activities that have been accomplished in implementation Project 5-4829-03. The primary objective of this project was to implement the analytical model and the testing procedure developed in research Project 0-4829 (Zornberg et al., 2012a and b) in TxDOT specifications for selection of geosynthetic for base-stabilization of roadways subjected to environmental loads. As part of research Project 0-4829, an analytical model was developed to evaluate soil-geosynthetic interaction under small displacements. Specifically, the soil-geosynthetic interaction under small displacements was characterized by an index parameter referred to as the stiffness of the soil-geosynthetic composite ( $K_{SGC}$ ) (Zornberg et al., 2017; Roodi and Zornberg, 2017; Roodi, 2016). A testing procedure, referred to as the geosynthetic composite stiffness test, was developed to characterize  $K_{SGC}$ . This test mobilizes interaction mechanisms between soil and geosynthetics, similar to those mobilized in the conventional pullout test. However, the focus of the data collection and analysis has been on the onset of movement along the geosynthetic. Specifically, the relationship between load per unit width of the geosynthetic ( $T$ ) and displacements along the geosynthetic ( $u$ ) has been determined for displacements ranging from 0.1 to 1 mm. The slope of the linear relationship defined between  $T^2$  and  $u$  along the confined length of the geosynthetic has been defined as  $K_{SGC}$ .

This report details the complementary soil-geosynthetic interaction testing program conducted to characterize the stiffness of soil-geosynthetic composite ( $K_{SGC}$ ) for a wide range of geosynthetics, backfill materials, normal stresses, and geosynthetic orientations. The tests were conducted at the Geosynthetics Laboratory at The University of Texas at Austin. This document also reports the results of a complementary field monitoring program to collect information on the performance of geosynthetic-stabilized roadway sections under environmental loads as compared to the counterpart non-stabilized sections. The data produced in the experimental program along with the performance data obtained from field monitoring program was used to support refinement of TxDOT specifications for selection of geosynthetics for base-stabilization of roadways subjected to environmental loads.

Chapter 2 details the refinements made in the soil-geosynthetic interaction test procedure and in the procedure adopted to analyze and report the test results. Chapter 3 discusses the experimental testing program conducted using a wide range of geosynthetics, backfill materials, normal pressures, and geosynthetic orientations. Findings from evaluation of the data obtained in this experimental

program resulted the final test configurations to be used for selection of geosynthetics for base stabilization. Chapter 4 reports the information collected from geosynthetic-stabilized field sections as compared to that in non-stabilized (control) test sections. Chapter 5 details the activities completed to refine TxDOT specifications for selection of geosynthetics for base-stabilization of roadways subjected to environmental loads. This included conducting additional soil-geosynthetic interaction tests using 15 geosynthetics typically used for base stabilization of roadways. Then, based on the relevant field performance of the test sections constructed using the geosynthetics, limits of acceptable  $K_{SGC}$  values were established. Chapter 6 summarizes the findings obtained from various tasks of the project.

# **Chapter 2. Refinements in the Soil-geosynthetic Interaction Test Procedure and Data Analysis**

## **2.1. Introduction**

---

The soil-geosynthetic interaction test procedure and data analysis were originally developed in research Project 0-4829 (Zornberg et al., 2012a). As part of the activities conducted in this implementation Project 5-4829-03, the test procedure and data analysis were reevaluated and refined. The primary objective of the refinements was to minimize scatter in the test results and, consequently, improve the quality of test data. The refined procedure and data process were found to be particularly suitable to be implemented by geosynthetic laboratories. This chapter details the main refinements that were made in the test procedure and data analysis.

## **2.2. Refinements in the Testing Procedure**

---

This section describes the refinements made in the testing procedure.

### **2.2.1. Refinement in the Telltales Attachment Procedure**

The telltale attachment procedure was refined to minimize scatter in the test results. The old technique involved tying a cobalt-based alloy steel wire of 0.016 in. (0.4 mm) in diameter around geosynthetic junctions and securing the steel wire end inside a crimped ferrule (Figure 2.1a). Although this technique could provide a high-performance telltale attachment, the quality of the attachment relied on the operator's skill.

An alternative telltale attachment procedure was adopted that involved using an epoxy resin. The cobalt-alloy steel wires were also replaced by reusable zinc-galvanized steel wires of 0.041 in. (1.04 mm) in diameter. The new wires were hooked to the longitudinal ribs at the junction and the epoxy was applied to secure the attachment (Figure 2.1b). After the test is completed, the wires may be detached from the specimen by heating the epoxy.



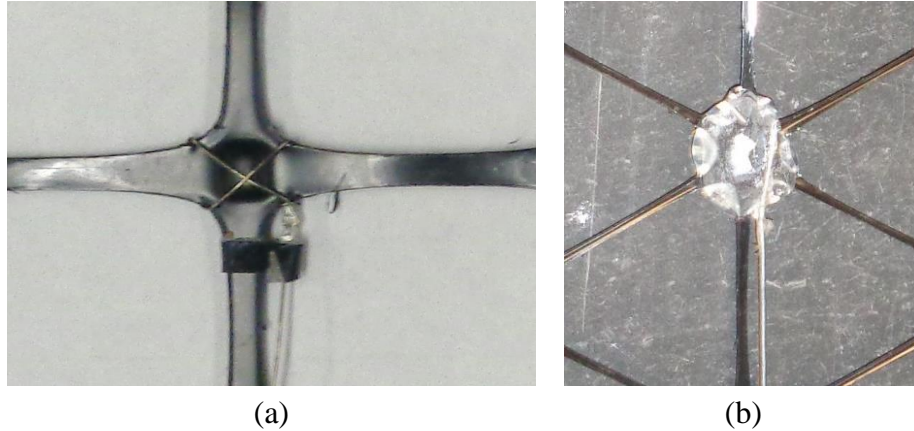


Figure 2.1 Refinement in the telltale attachment procedure: a) old procedure; b) refined procedure.

### 2.2.2. Refinement of Grip Setup

A potential source for the scatter among the test results was identified as the grip setup. The grip setup adopted in the test included a metal rod that was screwed to the roller grip as presented in Figure 2.2. The geosynthetic was inserted through the space between the metal rod and the roller grip and screws were tightened to secure the geosynthetic. To prevent slippage of the geosynthetic during pullout, sandpapers were glued to the rod and to the roller grip to provide friction with the geosynthetic. However, uneven gripping and sliding of the geosynthetic out of the grip setup were identified as sources of scatter in the test results.

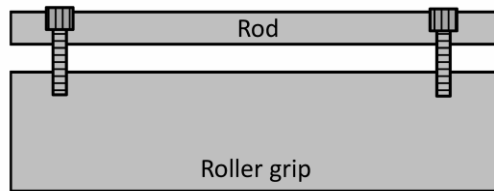


Figure 2.2 Grip setup

An assessment had previously conducted on potential impacts that tightening the screws of the rod (in an attempt to prevent slippage of the specimen during the test) may have on the test results. It was found that both excessively tightening and uneven tightening of the screws can adversely impact the test results. As both screws were tightened with excessive but even torque, the rod tended to bend in the center, leading to a looser grip of the geosynthetic in the center in relation to the edges. This could result in uneven pullout of the specimen, leading to erroneous displacement readings at the center of the specimen. The same problem was observed when excessive uneven torque was applied to the screws, but the location of the looser grip of the geosynthetic would change to a closer location to the screw with higher torque applied. This could also lead to uneven pullout of the specimen. Both situations could compromise the repeatability of the test results. As a

refinement in the gripping procedure, use of a torque wrench was adopted in all tests to minimize uneven gripping of geosynthetic specimens. The torque value was accordingly adjusted to avoid excessive tightening of the screws.

Sliding of the geosynthetic during the test was also found in cases where sandpapers failed to provide adequate friction to prevent sliding or in cases where the glue used to attach sandpapers to the metal rod failed. As an additional refinement in the grip setup, the smooth metal rod and sandpapers were replaced by a knurled rod (Figure 2.3). This refinement provided higher and more uniform friction along the gripping rod and eliminated the uncertainties arise from gluing sandpapers to the rod.

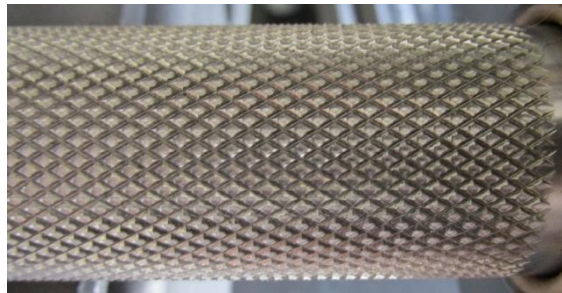


Figure 2.3 Knurled rod adopted in the refined testing procedure

### 2.2.3. Refinement of Boundary Conditions

An additional refinement was made in the boundary condition used on the internal walls of the box. The old procedure (Figure 2.4a), which involved using two layers of Mylar sheets and grease, was replaced by one layer of Mylar sheet attached to the internal walls using double-sided tape (Figure 2.4b). The new procedure reduced the box preparation time. Furthermore, as the grease was not used in the new procedure, the aggregate was protected from mixing with grease, which was found to be one of the sources for scatter in the test results. As the refined procedure provided the same soil-Mylar interface in the boundaries, test results were found not to be sensitive to this boundary condition.



(a)



(b)

Figure 2.4 Refinement of boundary condition: a) old procedure; b) refined procedure

## 2.2.4. Refinement of the Normal Pressure System

A comprehensive investigation was conducted to refine the normal pressure system. Specifically, several shapes and materials were tested for the air bladder incorporated inside the box lid to apply normal pressure. The main objective of the refinements was to provide a normal pressure that is uniformly distributed over the soil surface. Air tubes and connections were also upgraded to minimize the blockage in the air transfer route. As part of the refinement, three air pressure gauges were also adopted in the testing procedure to monitor the air pressure all along the air transfer route. A digital gage accurate to three decimal digits was used to control the pressure provided by the air pressure source. Two additional air pressure gages were also used on the box lid to measure the pressure at two locations including 1) before the air enters the air bladder and 2) where the air is distributed inside the air bladder and is being applied to the soil (Figure 2.5).



Figure 2.5 Refined normal pressure control system

## 2.3. Refinement of Data Analysis

An overview of the refinements made in the data analysis is presented in this section. As part of the refinement process, several factors that may affect the accuracy or scatter in the results of the soil-geosynthetic interaction tests were studied. The procedure that eventually adopted for data analysis was that minimized the scatter in the reported values for the stiffness of the soil-geosynthetic composite ( $K_{SGC}$ ). The main factors evaluated in the process and the final protocol adopted in the data analysis are discussed next.

### 2.3.1. Factors Evaluated in the Refinement Process

#### 2.3.1.1. Characterization of the $K_{SGC}$ at the Center of the Specimens

To identify the best approach to report the final  $K_{SGC}$  value, four approaches were evaluated:

- Approach 1: The  $K_{SGC}$  value was obtained using interpolation of the data recorded at the two telltales located on both sides around the specimen center.
- Approach 2: The  $K_{SGC}$  value was obtained using extrapolation of the data recorded at the two telltales located closest, but on one side of the specimen center.
- Approach 3: The  $K_{SGC}$  value was obtained using the data recorded at the closest telltale to the specimen center.
- Approach 4: The  $K_{SGC}$  value was obtained using regression of the data recorded at the three middle telltales.

Results obtained from all approaches were compared. While all approaches should theoretically result the same value for  $K_{SGC}$ , variation among the values obtained using different approaches were used to identify outlier results.

### **2.3.1.2. Effect of Data Smoothing Procedure**

As the raw data recorded by the sensors involved inevitable noises, data smoothing procedures were used to minimize the impact of noises on interpretation of the data. The data smoothing procedure adopted in this project involved a moving average technique in which each data point was replaced by a value that was obtained by averaging the data over a larger time span. The effect of data smoothing procedure was evaluated by comparing the  $K_{SGC}$  values obtained using the raw data with those obtained using various averaging spans. Specifically, the averaging span was changed from 10 points to 300 points and changes in the  $K_{SGC}$  value were evaluated. After extensive evaluation of the data recorded for various geosynthetic products, a moving average span of 250 data points was adopted in the final data analysis procedure. Figure 2.6 presents an example plot of the raw data versus the smoothed data using a moving average of 250 data points.

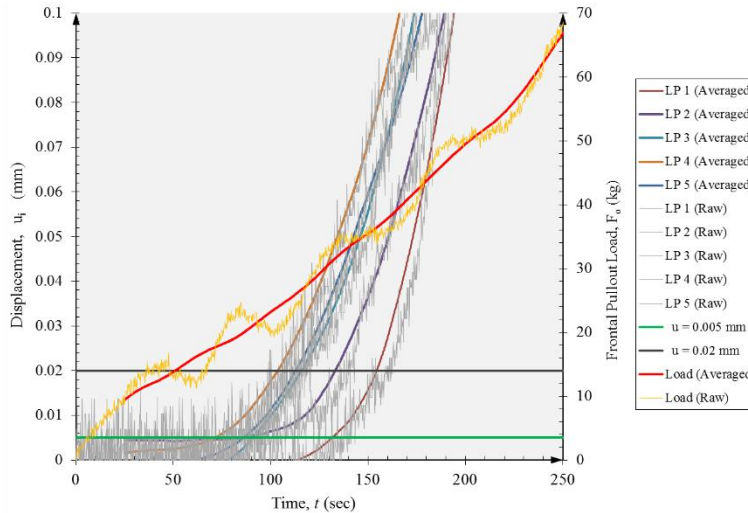


Figure 2.6 Example test results showing the impact of data smoothing procedure

### 2.3.1.3. Effect of Displacement Trigger Values

Since the  $K_{SGC}$  index is determined at the onset of the telltale movements, capturing small displacements is an essential part of the data acquisition. However, it is equally important not to misinterpret the noise recorded by the linear potentiometers as actual tell-tale movements at the onset of the displacement. Furthermore, the displacements that are accounted for in the estimation of  $K_{SGC}$  should correspond to those mobilized by soil-geosynthetic interaction; that means displacements that are realized by relatively small unit tensions (e.g., following initial adjustment of the geosynthetic after applying a seating load) should not be used.

An extensive evaluation of the test data obtained for various geosynthetics was conducted to identify the displacement range at which  $K_{SGC}$  should be reported. Specifically, sensitivity of  $K_{SGC}$  to the displacement value at which each tell-tale was first triggered was evaluated. The displacement trigger value was changed from 0.0002 to 0.0016 in. (0.005 to 0.04 mm) and  $K_{SGC}$  was estimated from the triggering displacement to a maximum displacement of 0.04 to 0.12 in. (1 to 3 mm). The procedure adopted in the final data analysis protocol involved estimation of  $K_{SGC}$  from a triggering displacement of 0.0008 in. (0.02 mm) up to the maximum displacement of 0.04 in. (1 mm). However, the  $K_{SGC}$  values obtained using smaller and larger triggering displacements were also evaluated in each test.

### 2.3.2. Final Protocol Adopted for Data Analysis

All factors evaluated in the refinements of the data analysis procedure were incorporated in an automated Microsoft Excel spreadsheet that was used in the analysis of the test results. Figure 2.7 shows sample results of the analysis obtained after using the automated spreadsheet for a soil-geosynthetic interaction test. The

$K_{SGC}$  value reported under the Final Protocol column corresponds to the value obtained using the final configurations adopted in the data analysis. The values presented under other columns summarize the estimated  $K_{SGC}$  using configurations other than those in the baseline case. The percentage values presented in the bottom row highlights the sensitivity of the reported  $K_{SGC}$  to changes in various parameters involved in the data analysis.

	Final Protocol	Impact of Extrapolation	Impact of Using Avg of LPs 2,3,4	Impact of Using Only LP 3	Impact of Smoothing			Impact of Triggering Point of LPs		
$K_{SGC}$	14.5	14.1	15.1	14.5	15.1	14.9	14.5	16.0	15.5	13.0
% Change	0%	-3%	4%	0%	4%	3%	0%	10%	7%	-10%

Figure 2.7 Impact of refinement in the data analysis (sample results)

## 2.4. Summary and Conclusions

Several refinements were made in the soil-geosynthetic interaction test to facilitate testing procedure and to minimize uncertainties associated with boundary conditions, normal pressure systems, and a low-skill test operator. The original procedure adopted to analyze the test data was also refined and a final protocol for data analysis was established. The refinements adopted in this chapter resulted in reduced scatter in the experimental results as discussed in the next chapter.

# **Chapter 3. Experimental Program: Production of Soil-geosynthetic Interaction Data using Small-scale Device**

## **3.1. Introduction**

---

This chapter reports on the experimental testing program aimed at establishing the soil-geosynthetic interaction test configurations to be used for TxDOT specifications for selection of geosynthetics for base-stabilization of roadways subjected to environmental loads. Specifically, five geosynthetics were tested, which were aimed at resulting in minor, moderate, and excellent improvement in the pavement performance. The selected geosynthetics were characterized according to the physical requirements of the current TxDOT Department Material Specifications DMS-6240 for Geogrid for Base/Embankment Reinforcement. Three backfill materials with different ranges of particles sizes were also identified. The backfill materials were characterized in accordance with the AASHTO Soil Classification System and the Unified Soil Classification Systems (USCS). Soil-geosynthetic interaction tests were conducted using combination of the geosynthetics and the backfill materials to characterize the stiffness of the soil-geosynthetic composite. Additional testing programs were also conducted to evaluate the effect on the results of the normal stress (confining pressure) and of the geosynthetic orientation (cross-machine and machine directions). The results obtained in the testing program were used to establish the test configurations to be used for TxDOT specifications.

## **3.2. Material Properties**

---

Characteristics of the geosynthetics and backfill materials used in the testing program are discussed in this section.

### **3.2.1. Baseline Geosynthetics**

A total of five geosynthetics (referred to as baseline geosynthetics) were used. The geosynthetic products were aimed at resulting in minor, moderate, and excellent improvement in pavement performance. The expected performance of the geosynthetic products was assumed on the basis of the field performance data collected as part of the field monitoring program of this project. Four geogrids and one geotextile were used. The products were selected with a wide range of physical and mechanical properties and with various manufacturing processes to allow evaluation of the impact on the results of these factors. Table 3.1 summarizes the main features of the five geosynthetics used in this program along with the expected

improvement in the field performance from their use in roadways. Characteristics of each geosynthetics are discussed next.

**Table 3.1: Geosynthetic products used in small pullout testing program**

Geosynthetic Name	Geosynthetic Type	Manufacturing Processes	Polymer Type	Expected performance
GG 1	Biaxial Geogrid	Extruded (Homogenous)	Polypropylene (PP)	Excellent
GG 2	Triangular Geogrid	Extruded (Homogenous)	Polypropylene (PP)	Excellent
GG 3	Biaxial Geogrid	Woven with Coated Yarn	Polyester (PET)	Moderate
GG 4	Biaxial Geogrid	Laser Welded	Polypropylene (PP)	Poor
GT 1	Woven Geotextile	Woven	Polypropylene (PP)	Excellent

### 3.2.1.1. GG 1

GG 1 is a biaxial polypropylene geogrid that is integrally formed by punch-and-drawn and extrusion process (Figure 3.1). It has been used in several TxDOT field test sections including FM 2, FM1915, and SH 21. As a result of the immense familiarity of TxDOT and the project team with this product, it was used as one of the baseline geogrids in the soil-geosynthetic interaction testing programs. Index properties of this geosynthetic are presented in Table 3.2.

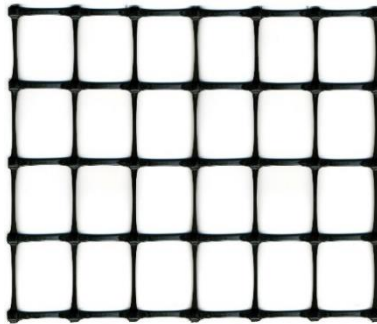


*Figure 3.1 Baseline biaxial integrally formed geogrid from polypropylene: GG 1*



**Table 3.2. Index Properties of GG 1**

Characteristics		Units	MD	CD	
Mechanical Properties	Tensile Strength - ASTM 6637	@ 0.5% Strain	kN/m (lb/ft)	-	-
		@ 2% Strain	kN/m (lb/ft)	4.1 (280)	6.6 (450)
		@ 5% Strain	kN/m (lb/ft)	8.5 (580)	13.4 (920)
		Ultimate	kN/m (lb/ft)	12.4 (850)	19.0 (1,300)
	Junction Efficiency (%)	(%)	93	-	
Flexural Stiffness		mg-cm	250,000	-	
Geometric Properties	Aperture Dimensions		mm (in)	25 (1.0)	33 (1.3)
	Minimum Rib Thickness		mm (in)	0.76 (0.03)	0.76 (0.03)
	Rib Width		mm (in)	3.2 (.125)	3.2 (.125)
Polymer Type		Polypropylene			
Manufacturing Process		Integrally Formed Biaxial Geogrid			

**3.2.1.2. GG 2**

GG 2 is a triangular polypropylene geogrid manufactured from a punched polypropylene sheet, oriented in three directions (Figure 3.2). The use of triangular geogrids has recently gained momentum in the geosynthetic-stabilized roadways across Texas. Therefore, TxDOT would particularly benefit from the results obtained in the soil-geosynthetic interaction tests using this product as compared to other products. Primary evaluation of the test sections constructed using GG 2 has indicated an excellent performance under environmental loads. Index properties of this geosynthetic are presented in Table 3.3.

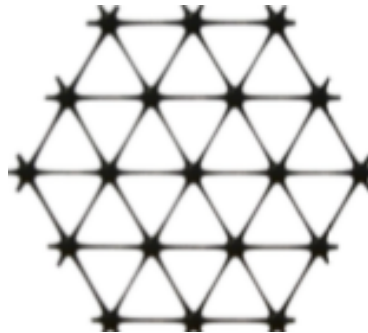


*Figure 3.2 Baseline triangular integrally formed geogrid from polypropylene: GG 2*

**Table 3.3. Index Properties for GG 2**

Characteristics		Units	Longitudinal	Diagonal	Transverse	General
Geometric Properties	Rib Pitch <sup>(1)</sup>	mm (in)	40 (1.60)	40 (1.60)	-	-
	Mid-Rib Depth <sup>(1)</sup>	mm (in)	-	1.6 (0.06)	1.4 (0.06)	-
	Mid-Rib Width <sup>(1)</sup>	mm (in)	-	1.0 (0.04)	1.2 (0.05)	-
	Aperture Shape	-	-	-	-	Triangular
Structural Integrity	Junction Efficiency	%	-	-	-	93
	Radial Stiffness @ 0.5% Strain <sup>(2)</sup>	kN/m (lb/ft)	-	-	-	300 (20,580)
Polymer Type		Polypropylene				
Manufacturing Process		Integrally Formed Triaxial Geogrid				

(1) Nominal Dimensions

(2) Radial Stiffness determined from tensile stiffness measured in any in-plane axis. Testing in accordance with ASTM D6637.

### 3.2.1.3. GG 3

GG 3 is a woven geogrid made of high molecular weight multifilament polyester yarns (Figure 3.3). The yarns are woven into a stable network and placed under tension. The polyester yarns are PVC coated to help prevent degradation. This product has not been widely used by TxDOT. Index properties of this geosynthetic are presented in Table 3.4.

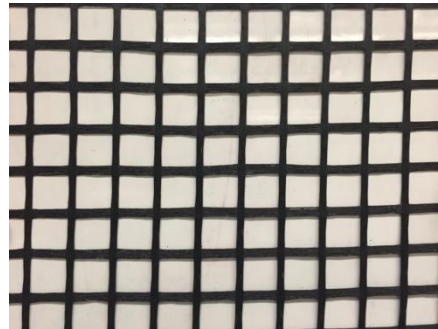


*Figure 3.3 Baseline biaxial woven geogrid from polyester: GG 3*

**Table 3.4. Index Properties of GG 3**

Characteristics		Units	MD	CD	
Mechanical Properties	Tensile Strength - ASTM 6637	@ 1% Strain	kN/m (lb/ft)	-	-
		@ 2% Strain	kN/m (lb/ft)	7.7 (526)	8.4 (578)
		@ 5% Strain	kN/m (lb/ft)	11.5 (792)	15.2 (1,042)
		Ultimate	kN/m (lb/ft)	34.9 (2,388)	56.5 (3,870)
	FHWA Sum of Junctions - Efficiency		%	201	100
Junction Strength (Ultimate)		kN/junction (lb/junction)	0.87 (59.4)	0.69 (47.6)	
Geometric Properties	Aperture Dimensions		mm (in)	25 (1.0)	25 (1.0)
	Minimum Rib Thickness		mm (in)	1.1 (0.04)	1.1 (0.04)
	Rib Width		mm (in)	5.4 (0.21)	6.6 (0.26)
Polymer Type		Polyester			
Manufacturing Process		Woven Polyester Yarns			

### 3.2.1.4. GG 4

GG 4 is a biaxial polypropylene geogrid manufactured by laser bonding longitudinal and transverse ribs (Figure 3.4). It has been used in the field test sections constructed in FM 1774. Due to its different manufacturing procedure as a welded geogrid, the mechanistic behavior of this geogrid might differ from the extruded and woven geogrids discussed earlier. Therefore, selection of this geogrid allowed evaluation of the impact of manufacturing process on the test results. Furthermore, the research team expected to capture a comparatively low value of composite stiffness as the section built using this product in the field has exhibited a comparatively poor performance. Index properties of this geosynthetic are presented in Table 3.5.



Figure 3.4 Baseline biaxial laser-bonded geogrid from polypropylene: GG 4

**Table 3.5. Index Properties of GG 4**

Characteristics		Units	MD	CD	
Mechanical Properties	Tensile Strength - ASTM 6637	@ 1% Strain	kN/m (lb/ft)	5.2 (356)	-
		@ 2% Strain	kN/m (lb/ft)	8.2 (563)	-
		@ 5% Strain	kN/m (lb/ft)	15.1 (1,031)	-
		Ultimate	kN/m (lb/ft)	24.2 (1,658)	-
	Junction Strength (Ultimate)	kN (lbs)	0.70 (157)	-	
Junction Strength (Ultimate)	kN/m (lb/ft)	14.0 (958)	-		
Geometric Properties	Aperture Dimensions	mm (in)	41 (1.61)	41 (1.61)	
	Minimum Rib Thickness	mm (in)	0.6 (0.02)	0.45 (0.02)	
	Rib Width	mm (in)	8.9 (0.35)	9.1 (0.36)	
Polymer Type		Polypropylene			
Manufacturing Process		Laser Welded Biaxial Geogrid			

### 3.2.1.5. GT 1

GT 1 is a geotextile created from high-tenacity polypropylene filaments formed into a weave to provide reinforcement strength integrated with water flow and soil retention (Figure 3.5). This product has been used in the SH21 rehabilitation project. Selection of this product allowed capturing any alternate mechanisms

involved in soil-geotextile interaction as compared to those involved in soil-geogrid interaction. Index properties of this geosynthetic are presented in Table 3.6.

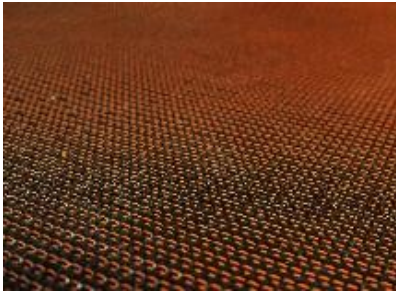


Figure 3.5 Baseline woven geotextile: GT 1

**Table 3.6. Index Properties of GT 1**

Characteristics		Units	MD	CD	
Mechanical Properties	Tensile Strength - ASTM 4595	@ 1% Strain	kN/m (lb/ft)	-	-
		@ 2% Strain	kN/m (lb/ft)	350 (24,000)	1,313 (90,000)
		@ 5% Strain	kN/m (lb/ft)	-	-
		Ultimate	kN/m (lb/ft)	-	-
	Flow Rate ASTM D 4491		l/min/m <sup>2</sup> (gal/min/ft <sup>2</sup> )	3056 (75)	
	Permittivity ASTM D 4491		sec <sup>-1</sup>	1.0	
	Apparent Opening Size (AOS) ASTM D 4751		mm (U.S. Sieve)	0.43 (40)	
Polymer Type		Polypropylene Filaments			
Manufacturing Process		Woven Filaments			

### 3.2.2. Characterization of Geosynthetics in accordance with TxDOT Specifications

The selected geosynthetics were characterized according to the physical requirements of the then-existing TxDOT Department Material Specifications DMS-6240 for Geogrid for Base/Embankment Reinforcement. The requirements involved only geometrical or in-isolation (i.e., without involvement of surrounding soil) properties of the geosynthetics including aperture size, percent open area, thickness of the ribs, tensile modulus, and junction efficiency. Table 3.7 summarizes characteristics of the selected geosynthetics as compared to the requirements by TxDOT DMS-6240.

**Table 3.7: Characterization of geosynthetics in accordance with TxDOT DMS-6240**

DMS-6240 Material Requirements for Type 1 Geogrid								
Geosynthetics	Aperture Size in., (mm)	Percent Open Area, %	Minimum Thickness of Ribs and Junctions, in. (mm)			Tensile Modulus @2% strain, kips/ft, (kN/m)		Junction Efficiency, % of rib ultimate tensile strength
			MD Ribs	CMD Ribs	Junctions	MD	CMD	
	1.0-2.0 (25-51)	> 70%	0.03 (0.77)	0.025 (0.64)	0.06 (1.50)	>14 (205)	>14 (205)	> 90%
GG 1	1.0x1.3 (25x33)	75%	0.03 (0.76)	0.03 (0.76)	0.06 (1.50)	14 (205)	22.5 (330)	93%
GG 2	1.6x1.6x1.6 (40x40x40)	>70%	0.07 (1.8) In diagonal	0.06 (1.5) In transverse	0.13 (3.4)	20.5 (300) (Radial stiffness @ 0.5% strain)		93%
GG 3	1.0x1.0 (25x25)	>70%	> 0.03 (0.77)	> 0.03 (0.77)	> 0.06 (1.5)	26.3 (385)	28.9 (422)	100% in CD 201% in MD
GG 4	1.73x1.73 (44x44)	75%	> 0.03 (0.77)	> 0.03 (0.77)	> 0.06 (1.5)	20.5 (300)	68.5 (500)	35%
GT 1	--	--	--	--	--	24 (350)	90 (1313)	--

### 3.2.3. Backfill Materials

The backfill materials used in the soil-geosynthetic interaction testing program represent various particle sizes of base materials ranging from fine gravel to medium size sand. Specifically, two gravel and one sand backfill materials were used.

A gravel backfill material was obtained from Martin Marietta Sand and Gravel Quarry in Garfield, Texas. It involved a clean, river-washed pea gravel with rounded particles (Figure 3.6a). This gravel contained particles passing a 3/8” sieve and included portions retained in all sieves up to Sieve No. 16. This soil was referred to as AASHTO No. 8 because it conformed to the specifications of this class of aggregates as specified in AASHTO M43 (AASHTO 2013) and ASTM D448 (ASTM 2012). The average specific gravity of this soil is 2.65 and is classified as poorly graded gravel (GP) according to the USCS [ASTM D2487 (ASTM 2011)] and as Group A-1-a according to the AASHTO classification system [AASHTO M145 (AASHTO 2012); ASTM D3282 (ASTM 2015)].

The second gravel backfill material was obtained after sieving AASHTO No. 8 backfill using 1/4” (6.35 mm) and Sieve No. 4 (4.75 mm). The portion remained between the two sieves, which represented a comparatively more uniformly graded gravel, was used as the second backfill material referred to herein as AASHTO No. 8-Truncated (Figure 3.6b).

The third backfill material used in the experimental program consisted of a clean poorly graded sand, known as Monterey No. 30 sand (Zornberg et al., 1998b). The

sand has a uniform soil particle size distribution, with particle sizes smaller than 0.762 mm, and is composed of medium to fine and subangular to subrounded particles. The mean particle size ( $D_{50}$ ), coefficient of uniformity ( $C_u$ ), and coefficient of curvature ( $C_c$ ) were determined to be 0.44 mm, 1.6, and 1.0, respectively. Monterey No. 30 sand is classified as poorly graded sand (SP), according to the USCS [ASTM D2487 (ASTM 2011)], and as Group A-1-b, according to the AASHTO classification system [AASHTO M145 (AASHTO 2012); ASTM D3282 (ASTM 2015)].

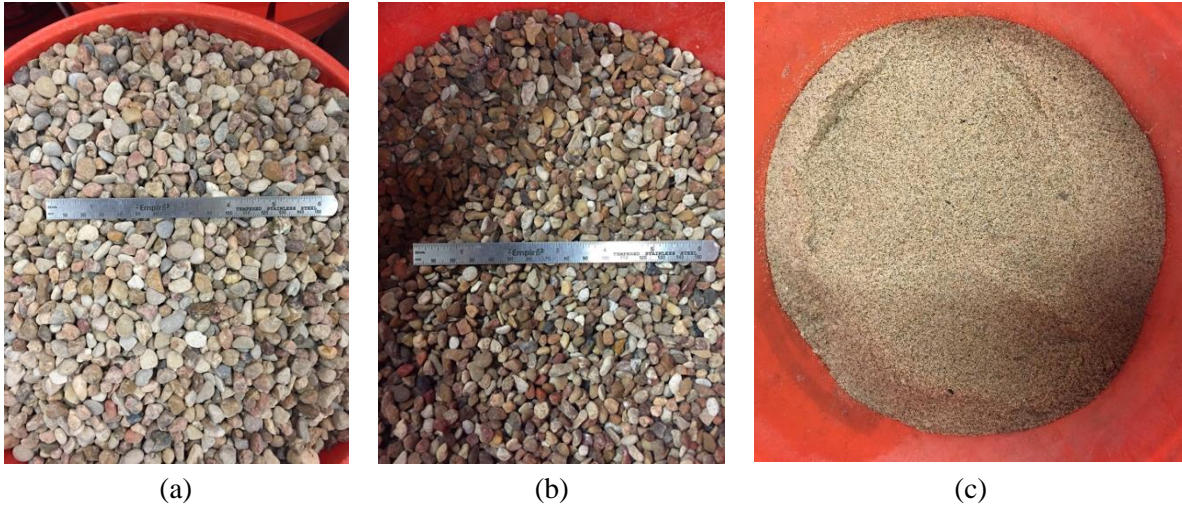


Figure 3.6 Backfill materials used in the experimental program: a) AASHTO No. 8; b) AASHTO No. 8-Truncated; c) Monterey No. 30 Sand

The AASHTO No. 8 and AASHTO No. 8-Truncated backfill materials were placed dry and the Monterey sand was placed with a moisture content of 1.5 to 2%. The target dry unit weight of the backfill materials was 103.4 pcf (16.24 kN/m<sup>3</sup>). The particle size distribution curves of the three backfill materials are presented in Figure 3.7.



### 3.3.3. Geosynthetic Orientation

The baseline geosynthetics were tested in both cross-machine and machine directions. While the soil-geosynthetic interaction in the geosynthetic cross-machine direction is expected to be predominant in the performance of the geosynthetic-stabilized roadways under environmental loads, both cross-machine and machine directions are expected to be important in the performance under traffic loads.

### 3.3.4. Testing Displacement Rate

According to American Society for Testing and Material (ASTM) Standard Test Method for Measuring Geosynthetic Pullout Resistance in Soil (ASTM D6706), the displacement rate that shall be used for pullout testing is 0.04 in/min (1 mm/min). An experimental program was conducted to evaluate the effect of displacement rate on the soil-geosynthetic interaction results. It was found that although displacement rate may slightly change the absolute value of the index parameter, it does not change comparative evaluation among various geosynthetics. Eventually, the displacement rate recommended by ASTM D6706 (i.e., 0.04 in/min [1 mm/min]) was adopted in the soil-geosynthetic interaction testing program in this project.

### 3.3.5. Testing Matrix

Considering various combinations of backfill materials (AASHTO No. 8, AASHTO No. 8-Truncated, and Monterey No. 30), confining pressures (1, 3, and 5 psi), and geosynthetic orientations (cross-machine and machine directions) the testing matrix adopted to produce data to support TxDOT specification of geosynthetic-stabilized base roadways are summarized in Table 3.8. Repeat tests were conducted for each testing configuration to reach an acceptable range of error. Eventually, over 400 soil-geosynthetic interaction tests were conducted. Results obtained in the experimental program are discussed in the next section.

**Table 3.8: Soil-geosynthetic interaction testing matrix using the baseline geosynthetics**

No. of Backfill Materials	No. of Confining Pressures	No. of Test Direction	No. of Geosynthetics	No. of Repeats	Total No. of Tests
3	3	2	5	≥4	≥400

## 3.4. Test Results

Findings obtained from comparison of the  $K_{SGC}$  values among various test configurations are discussed in this section.



### 3.4.1. Effect of Backfill Materials

Results of the soil-geosynthetic interaction tests conducted using various backfill materials are presented in Figure 3.8a, b, and c, for AASHTO No. 8, AASHTO No.8-Truncated, and Monterey Sand, respectively. The trends observed among the  $K_{SGC}$  values of the four baseline geogrids were similar between the two gravel backfills (i.e., AASHTO No. 8 and AASHTO No.8-Truncated) (Figure 3.8a and b). Specifically, using either of the gravel backfills the four baseline geogrids could be ranked from the highest  $K_{SGC}$  to the lowest  $K_{SGC}$  as GG 2, GG 1, GG 3, and GG 4.

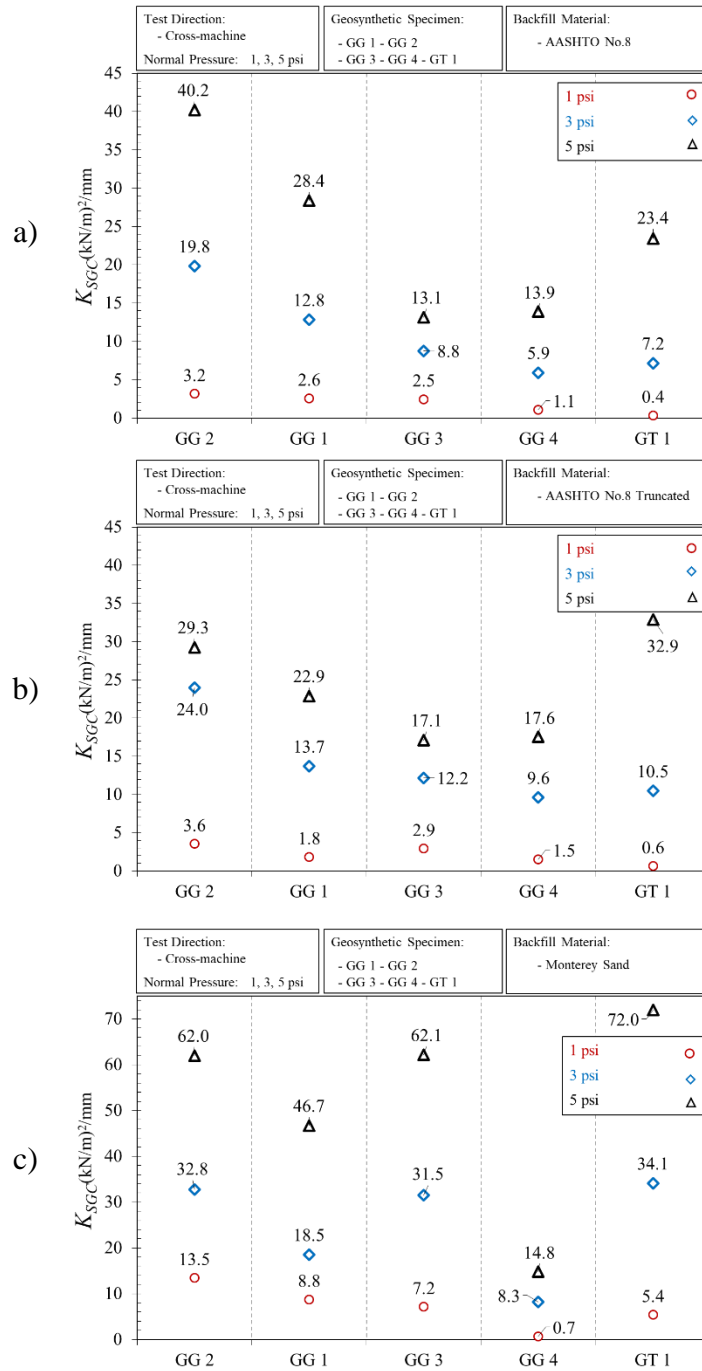


Figure 3.8  $K_{SGC}$  values obtained for the baseline geosynthetics using various backfill materials: a) AASHTO No. 8; b) AASHTO No. 8-Truncated; c) Monterey No. 30 Sand

However, this trend was observed to be different for the sand backfill (i.e., Monterey Sand in Figure 3.8c). Specifically, geogrid GG 3 was found to show a comparatively high  $K_{SGC}$  value when tested with sand. Investigation of the structure of this geogrid revealed that the transverse and longitudinal ribs of this product are composed of multiple coated polyester yarns that are woven together. This design

provided a completely different micro-texture than that in the other integrally formed polypropylene geogrids. The micro texture of geogrid GG 3 makes it particularly suitable to interact with micro-texture of sand backfills. This is similar to interaction between sand and a woven geotextile. Consistent with this observation, it was observed that the  $K_{SGC}$  value for the baseline woven geotextile GT 1 was also significantly higher when tested in sand as compared to testing in gravel.

Because the interaction between geosynthetic and flexible base course can be better represented by gravel-geosynthetic interaction than sand-geosynthetic interaction, “a gravel backfill material” was considered for specification of geosynthetic-stabilized base pavements. Furthermore, since similar trends were observed between results obtained using AASHTO No. 8 and AASHTO No.8-Truncated backfills, “AASHTO No.8-Truncated” was selected to be used for specification of geosynthetic-stabilized base pavements; because this backfill material is comparatively more uniform than AASHTO No.8 and consequently, will be easier to be reproduced.

### 3.4.2. Effect of Normal Stress

Results of the soil-geosynthetic interaction tests conducted under various normal stresses are presented in Figure 3.9a, b, and c, for 1, 3, and 5 psi, respectively. Following the finding regarding the difference between sand-geosynthetic interaction and gravel-geosynthetic interaction, the plots are presented separately for gravel and sand backfills. It was found that for the gravel backfills, the  $K_{SGC}$  values at a normal pressure of 1 psi are comparatively small for all geosynthetics, which made it particularly difficult to differentiate various geosynthetics. The low value of  $K_{SGC}$  under a normal pressure of 1 psi was expected because soil shear strength and stiffness are expected to be particularly low under this normal pressure.

The  $K_{SGC}$  values under normal stress of 3 and 5 psi were, expectedly, found to be higher than that under 1 psi. Both normal stresses were found to provide a reasonably large interaction between geogrids and backfill materials to be able to differentiate various geogrids. However, a 3 psi normal pressure was found to provide a slightly better distinction among the geogrids than 5 psi.

The  $K_{SGC}$  value obtained using baseline geotextile GT 1 could not be fit into the ranking obtained for the baseline geogrids. While under 3 psi, the tests conducted using the geotextile resulted one of the lowest  $K_{SGC}$  values among all geosynthetics, tests conducted under 5 psi resulted a high value for the baseline geotextile as compared to the geogrids. This observation was found in both gravel backfills. Inconsistency between comparison of the geotextile and geogrids based on the  $K_{SGC}$  values under various normal stresses may be attributed to different mechanisms involved in the soil-geogrid interaction as compared to soil-geotextile interaction.

Specifically, soil-geotextile interaction is predominantly governed by friction, while both friction and passive resistances contribute to soil-geogrid interaction.

Based on the discussion presented in this section, a normal pressure of 3 psi was adopted for specifications of geosynthetic-stabilized pavements. It was also concluded that ranking geogrids and geotextiles should be considered separately to account for various interaction mechanisms mobilized in their interaction with backfill materials.

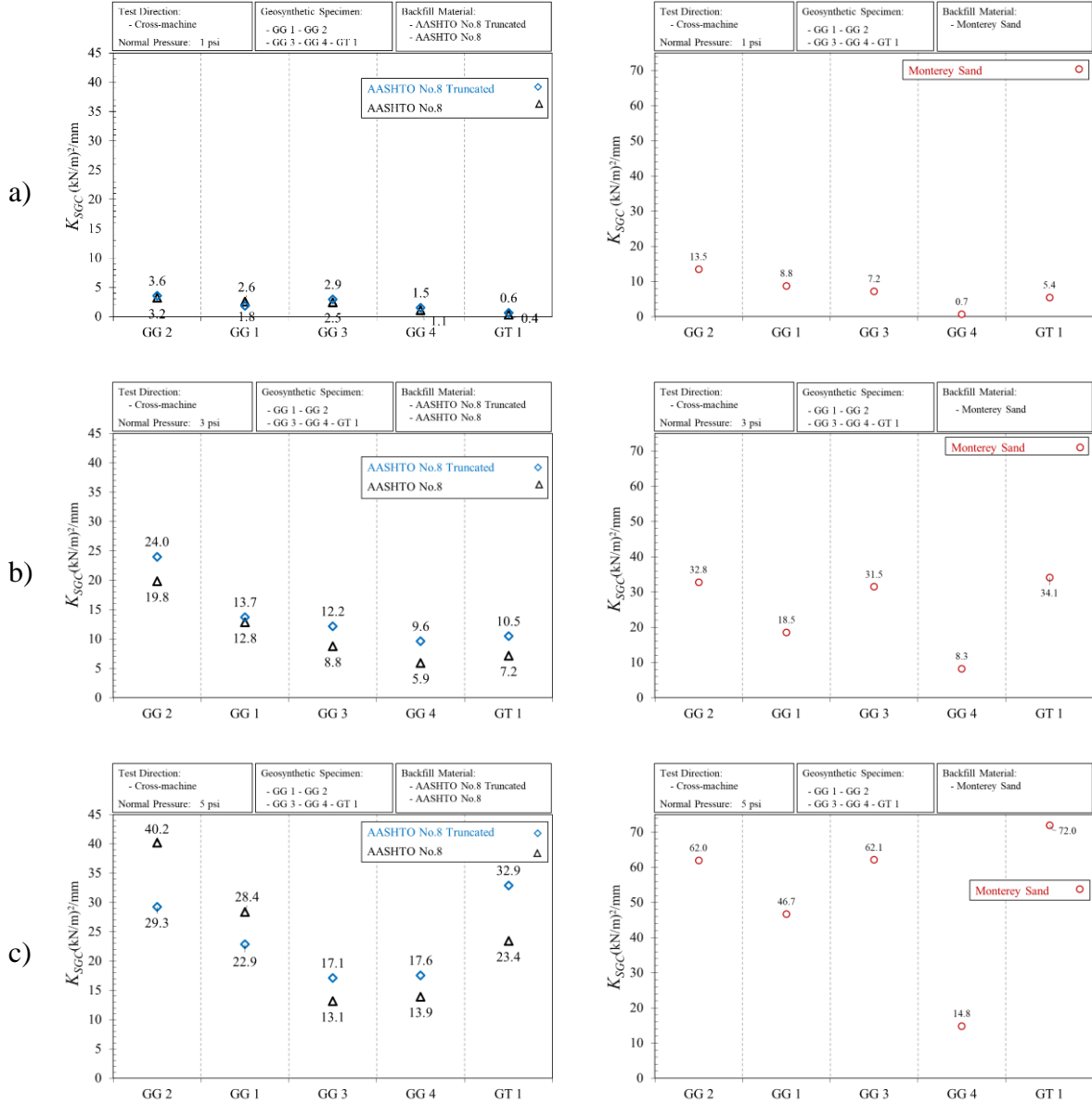


Figure 3.9  $K_{SGC}$  values obtained for the baseline geosynthetics using various normal stresses: a) 1 psi; b) 3 psi; c) 5 psi.

### 3.4.3. Effect of Test Direction

Results of the soil-geosynthetic interaction tests conducted using the target normal stress and backfill materials in different directions of geosynthetic rolls are presented in this section. It should be noted that since physical and mechanical properties of the geosynthetics may not necessarily be the same in the machine and cross-machine directions, different  $K_{SGC}$  values and rankings among the geosynthetics could be expected for the two directions.

Figure 3.10 presents the  $K_{SGC}$  values obtained in both machine and cross machine directions of the five baseline geosynthetics using AASHTO No.8-Truncaed backfill materials and under a normal pressure of 3 psi. Although the  $K_{SGC}$  value obtained for each geogrid in the machine direction was different than its  $K_{SGC}$  in the cross-machine direction, ranking of the geogrids was found to be the same in both directions. For geogrids GG 3 and GG 4, the  $K_{SGC}$  value in the machine direction was found to be slightly smaller than that in the cross-machine direction. The  $K_{SGC}$  value of geogrid GG 1 in the machine direction was found to be approximately the same as that in the cross-machine direction.

The second direction for testing GG 2 (as a triangular geogrid) was selected as the diagonal direction. The  $K_{SGC}$  value obtained for this geogrid in the diagonal direction was found to be considerably smaller than that in the cross-machine direction. This might be partially attributed to the differences in the physical and mechanical characteristics of the geogrid in the two directions, and can also be partially attributed to that geogrid specimens tested in the diagonal directions were collected from a different manufactured roll than the specimens tested in the cross-machine direction.

As the predominant direction of interaction relevant to the performance of geosynthetic-stabilized roadways under environmental loads is the cross-machine direction, this direction was selected for TxDOT specifications. When geosynthetic stabilization of the base course is used to improve road performance under traffic load, both cross-machine and machine directions may be important.

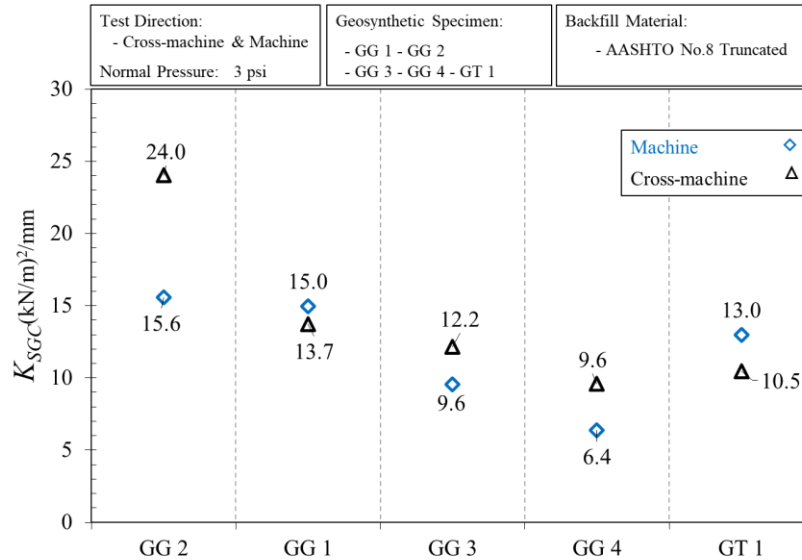


Figure 3.10 Comparison of  $K_{SGC}$  values obtained for the baseline geosynthetics in cross-machine and machine directions using AASHTO No. 8-Truncated backfill materials under 3 psi

### 3.5. Summary and Conclusions

A comprehensive soil-geosynthetic interaction test program was conducted to identify the most relevant test configurations to be used for TxDOT specifications for geosynthetic-stabilized roadways. Specifically, five baseline geosynthetics, including four geogrids and one geotextile, with a wide range of properties were tested using three soil types (two gravels and one sand), three normal pressures (1, 3, and 5 psi), and two testing directions (cross-machine and machine directions).

While large aggregate particles cannot be accommodated in the small-scale soil-geosynthetic interaction box, one sand and two gravel backfill materials (with particle sizes ranging from Sieve No. 4 [4.75 mm] to 3/8" sieve) were used in the testing program. Comparison of the data produced using the sand backfill material to that produced using the gravel backfill materials revealed that a gravel backfill material is necessary for TxDOT specification. Gravel-geosynthetic interaction can better represent the interaction mechanisms between geosynthetic and flexible base materials.

Evaluation of the results obtained using the two gravel backfill materials of different particle sizes indicated that while the absolute value of  $K_{SGC}$  may change, comparative evaluation of geosynthetics may not be affected by characteristics of the gravel backfill. Eventually, the gravel backfill material that had a more uniform particle size distribution was selected for TxDOT specification since this material is expected to be easier to reproduce.

Comparison of the soil-geosynthetic interaction test results for the baseline geotextile to those for the baseline geogrids indicated that the  $K_{SGC}$  values obtained for geotextiles should not be directly compared to those for geogrids. Therefore, geotextiles and geogrids should be separately evaluated for TxDOT specification purposes. This difference can be attributed to the different mechanisms involved in soil-geotextile interaction as compared to soil-geogrid interaction.

$K_{SGC}$  value was found to change with normal stress. A comparatively high normal stress may result in breakage of the geosynthetic specimen in tension before soil-geosynthetic is fully mobilized in the confined length of the geosynthetic. On the other hand, a comparatively small normal stress may not produce  $K_{SGC}$  values large enough to differentiate various geosynthetics. Eventually, a normal pressure of 3 psi was selected for TxDOT specification purposes. This normal stress was found to be a reasonably good estimate of the permanent normal pressure applied to geosynthetics in a geosynthetic-stabilized roadway and also large enough to produce distinctive  $K_{SGC}$  values for various geosynthetics.

Eventually, as the predominant direction of interaction relevant to the performance of geosynthetic-stabilized roadways under environmental loads is the cross-machine direction, this direction was selected for TxDOT specifications.

## Chapter 4. Field Monitoring Program

### 4.1. Introduction

---

This chapter reports on the field-monitoring program conducted to produce field performance data of geosynthetic-stabilized roadways subjected to environmental loads. A total of ten field locations were identified. Field performance measures that are most relevant to assess the performance of stabilized sections versus non-stabilized (control) sections under traffic load and environmental conditions were then identified. Specifically, vertical deflection in the wheel path (rut depth) was identified as the relevant measure to the performance under traffic loads, and the percentage of longitudinal cracks as well as differential vertical movement between the centerline and the shoulders were identified as the relevant measures to the performance under environmental loads.

The data relevant to the performance under environmental loads was then collected on the identified field sections using three procedures: 1) visual condition surveys were conducted to observe, document, and measure the extent and the severity of the surface distresses; 2) total station surveys of the road cross sections were utilized to evaluate the differential movement between the roadway centerlines and shoulders; and 3) the data available in the TxDOT Pavement Management Information System (PMIS) database was collected to evaluate long-term performance of the identified sections.

The field performance data (detailed in this chapter) complemented the experimental data obtained in the soil-geosynthetic interaction testing program (detailed in Chapters 3 and 5) to establish limits for acceptable  $K_{SGC}$  values for selection of geosynthetic for base stabilization under environmental loads.

### 4.2. Performance Evaluation Program

---

A study was conducted to identify field performance measures that can determine potential benefits from geosynthetics in geosynthetic-stabilized roadways. The performance measures were found to be different under various types of loading. Specifically, vertical deflection in the wheel path (rut depth) was identified as the main performance measure under traffic loads (e.g., Distress Identification Manual for the Long-Term Pavement Performance Program (LTPP) [FHWA, 2003], PMIS survey [TxDOT, 2015]). On the other hand, environmental longitudinal cracks were identified as the main distress type caused by the swelling and shrinkage of expansive clay subgrades due to environmental changes (Zornberg et al., 2012a, b; Roodi 2016). In addition, differential vertical movements between the roadway centerline and its edges, which can be characterized by changes in the transverse profile of the road surface, was also identified as an indication of the performance



under subgrade seasonal swelling and shrinkage (Roodi et al., 2016). The performance data was collected through three procedures:

- **Visual Condition Surveys** of the test section were conducted to characterize various types of pavement distresses. The focus of the condition surveys was on characterization of environmental longitudinal cracks.
- **Total Station Surveys** of the transverse profile of the test section surfaces were conducted to characterize the differential vertical movements between the roadway centerline and its edges.
- **TxDOT PMIS Database** of roadways performance data was evaluated. The focus of this evaluation was on the percentage of longitudinal cracks, rut depth data, and the scores relevant to general condition of the roadway.

It should be noted that the performance data for each field location may have been collected from one, two, or all three components of the monitoring program listed above. The main features of each component of the monitoring program along with sample data are presented next.

#### 4.2.1. Visual Condition Surveys

Visual condition surveys were conducted in accordance with the instructions provided by the TxDOT PMIS Rater's Manual (TxDOT, 2015). In particular, the distress data was collected and characterized in the following ten categories recommended by this manual for flexible pavements:

- ***Shallow Rutting and Deep Rutting:*** Rutting was measured as the percentage of the section's total wheel paths area in different severity levels. While shallow rutting is defined as 0.25 to 0.49 in. (6 to 13 mm), deep rutting is determined as 0.5 to 0.99 in. (13 to 25 mm). Severe rutting refers to rut depths as great as 1.0 to 1.99 in. (25 to 51 mm), and failure rutting refers to rut depths exceeding 2.0 in. (51 mm). In this study, rutting of test sections was measured using a 6-foot straight edge and a steel ruler. An example of rutting measurement on the FM2 pavement is illustrated in Figure 4.1.



Figure 4.1 Measurements of rutting in the FM2 pavement

- **Alligator Cracking and Block Cracking:** Alligator (or fatigue) cracks are irregularly shaped interconnected cracks mainly developed in the wheel paths by the traffic load. Block cracks are much larger in dimensions and divide the pavement surface into rectangular shaped blocks. Unlike alligator cracking, block cracking is mainly caused by non-traffic associated reasons such as shrinkage of the asphalt layer or swelling and shrinkage of the base course layer. According to TxDOT PMIS Rater's Manual, alligator cracking should be measured as "the percentage of the rated lane's total wheel path area that is covered by alligator cracking" regardless of the cracks width. This manual does not define any severity level for alligator cracking. Similar to alligator cracking, no severity level has been defined for block cracking in the Rater's Manual. Block cracking shall be measured in terms of the percentage of block cracking area out of the total lane's area.
- **Longitudinal and Transverse Cracking:** As recommended by TxDOT PMIS Rater's Manual, longitudinal and transverse cracks that were wider than 3 mm were considered in the analysis. The cracks were measured in terms of the linear foot of cracking per 100-ft stations, for longitudinal cracking, and the number of cracks per 100-ft stations, for transverse cracking.
- **Patching:** Repairs made to cover distresses appeared on the pavement surfaces are called patches. According to TxDOT PMIS Rater's Manual, patching should be measured in terms of the percentage of the patched area with respect to the total area of the lane.
- **Raveling and Flushing:** Disintegration of the material of the asphalt mix causes the aggregate particles to be exposed on the surface of the pavement. This distress is called raveling and is measured as the percentage of the rated lane's total surface area that is affected by raveling. On the other hand, exposure of the bituminous material on the surface of the pavement is referred to as flushing. This distress shall be quantified as the percentage of flushing area out of the total surface area of the pavement.

- **Failures:** Areas that are severely distressed are counted as failures. Failures may be caused by extreme rutting or widely opened cracks or even high severity alligator cracking.

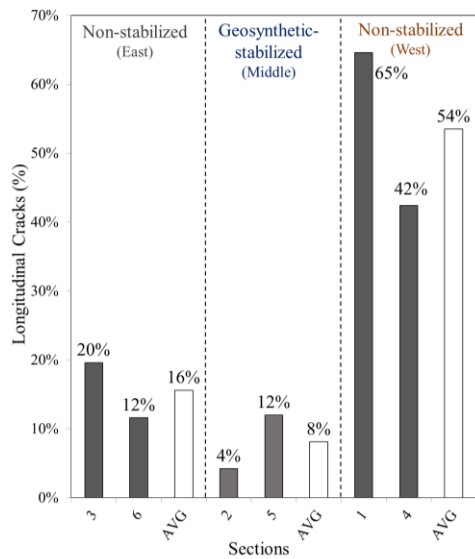
In a number of test sections, including FM 2, FM 1644, and State Highway (SH) 21, comprehensive condition surveys were conducted as part of which distress data was collected in all ten categories described above. In other test sections, the condition surveys were conducted with a focus on characterization of environmental longitudinal cracks, which were identified as the main damage caused by the subgrade swell and shrinkage.

Table 4.1 illustrates an example of visual condition survey forms used by the evaluation team members during the surveys. This example refers to Section #2 from FM 2, which was constructed as a control section. General information of the test section, including section number, geosynthetic type, section length, and starting and ending stations, are summarized on top. Then, the severity and extent of each distress type is detailed in the next rows of the table. In particular, the location of each distress has been recorded by the distance from the beginning of the section or the beginning of the experimental area. Picture numbers associated with each distress are also documented in the next column. Remarks by the road evaluators are also included in the last column of the survey form.

Figure 4.2 illustrates an example of the analysis that was conducted for comparative evaluation of performance in stabilized versus non-stabilized test sections. This example shows the percentage of longitudinal cracks in the FM1644 test sections. The horizontal axis of this graph corresponds to the test section numbers, categorized in stabilized versus non-stabilized groups. The vertical axis presents the percentage of longitudinal cracks calculated from condition survey data. The potential benefit of geosynthetics in mitigating the percentage of cracks in this road is underlined in this example. While the geosynthetic-stabilized test sections located in the middle of the experimental area had a percentage of crack of 8% on average, the non-stabilized test sections located on the west and east sides presented comparatively higher percentage of cracks.

**Table 4.1: Example visual condition survey data collected as part of the monitoring program**

Sect #	Actual		Original		Lane	Starting Station			Start Readg (ft)	Ending Station			Ending Readg (ft)	Section Length (feet)												
	Name	Layout	Name	Layout																						
26	1Eh2	Cont	was 4Eb	GT	K1-1	176	+	50	4050	181	+	50	4500	450												
LOCATION																										
Dist. Readg (ft)	From	To	Length (feet)	Starting at Station	Pic #	@ V.L.	Long Crack		Other Cracks					Patching and Potholes			Surface		Shoulder Drop off	Patched Shoulder	Rutting (mm) W.L. Y.L.	Comments (Water bleeding-Plished aggregate)				
							wheel <3 (L,M,H)	non-wheel <3 (L,M,H)	Alligat. (L,M,H)	Block (L,M,H)	Edge <3 (L,M,H)	Shoulder <3 (L,M,H)	Transverse <3 (L,M,H)	No. (L,M,H)	Patching (L,M,H)	No. (L,M,H)	Width (L,M,H)	Length (L,M,H)					Potholes (min d >150mm) (L,M,H)	No. (L,M,H)	Width (L,M,H)	Length (L,M,H)
4055			---	176 + 55	175-176																					
4055	4187	132	176 + 55	177-78			L																		Might be previous alligator crack	
4065	4187	122	176 + 65	79-80						L																
4200			---	178 + 00	81																					End of Big Patch Area
			---	---	---																					82 Facing Back
4204	4225	21	178 + 04	83-84																						
4190	4302	112	177 + 90																							Aggregate On Shoulder
4320			---	179 + 20																						Ranch Entrance
4382			---	179 + 82	85																					
4440			---	180 + 40	86-87																					
4508			---	End of Sect	88 End																					
			---	---	---																					
4050	4086	36	Start of Sect	8		x	x																			
4090	4139	49	176 + 90	9																						
4139	4306	167	177 + 39																							
4239	4246	7	178 + 39	10																						
4050	4090	40	Start of Sect	7																						



*Figure 4.2 Example analysis for comparative evaluation of performance in geosynthetic-stabilized versus non-stabilized test sections*

## 4.2.2. Total Station Surveys

This section describes the procedure conducted to monitor differential vertical movements between the centerline and shoulders of the roadways constructed on expansive clay subgrades. The mechanism that is expected to result the differential vertical movements is explained first, and the procedure conducted to measure the deflections are discussed next.

### 4.2.2.1. Differential Vertical Movement

As illustrated in Figure 4.3, construction of a relatively impervious pavement structure over expansive clay subgrades restrains the access to water for the area

located beneath the center of the road. However, the shoulder areas have unrestrained access to water. Consequently, while the subgrade soil beneath the shoulders can freely swell and shrink when its moisture content changes, the subgrade beneath the center experiences little change in the moisture; and consequently shows little swelling and shrinkage. Therefore, the edges of the pavement tend to move downward during dry periods and upward during wet periods (Figure 4.4). Cyclic wet and dry periods can then result in a non-uniform uplift loading applied to the pavement structure, and, consequently, impose a differential movement between the center and edges of the road. This leads to points of high compressive stress in wet periods and high tensile stress in dry periods, and, subsequently, generates longitudinal cracks in the pavement. Consistent with this mechanism, longitudinal cracks have been reported to occur or widen towards the end of dry periods and to partly close during wet periods.

It is expected that the geosynthetic layer homogenizes the non-uniform surface movements in the roadway induced by settlement and heave of the expansive clay subgrade. Redistribution of the non-uniform deformations of the roadway surface then minimizes the differential movements across the pavement and transfers the location of the maximum flexion from the paved area to the shoulder areas.

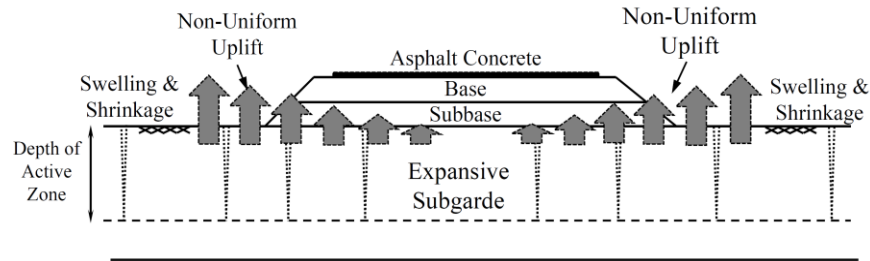


Figure 4.3 Non-uniform environmental loading imposed to road structures by expansive subgrades (Roodi and Zornberg, 2012)

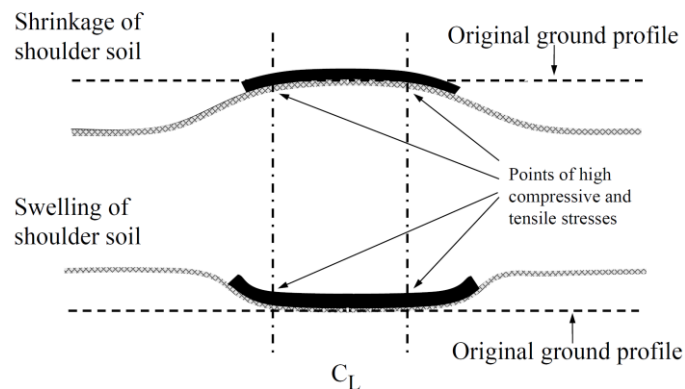


Figure 4.4 Conceptual model for generating environmentally induced longitudinal cracks in pavements

Total station surveys were conducted to evaluate this conceptual model on a select field test sections as described next.

#### 4.2.2.2. Marking Transverse Sections

To monitor vertical movement of the road surface, a number of transverse sections were identified in each test section. The transverse sections were selected from areas that were found to perform well as well as from areas with poor performance in terms of environmental longitudinal cracks. This allowed characterization of the differential vertical movements in well-performed sections as compared to that in poorly performed sections.

Identified transverse sections were marked on pavement surface as illustrated in Figure 4.5. First, a 2- to 3-in. wide transverse stripe was marked perpendicular to the central line of the road using duck tapes (Figure 4.5a). The stripe was then painted with white spray paints as illustrated in Figure 4.5b. Then, starting from the center line, circular orange marks were painted on top of the white stripe with 1-ft spacing toward the edges of the pavement (Figure 4.5c). Vertical movement orange marks were then monitored over time to evaluate changes in the transverse profile of the road surface.

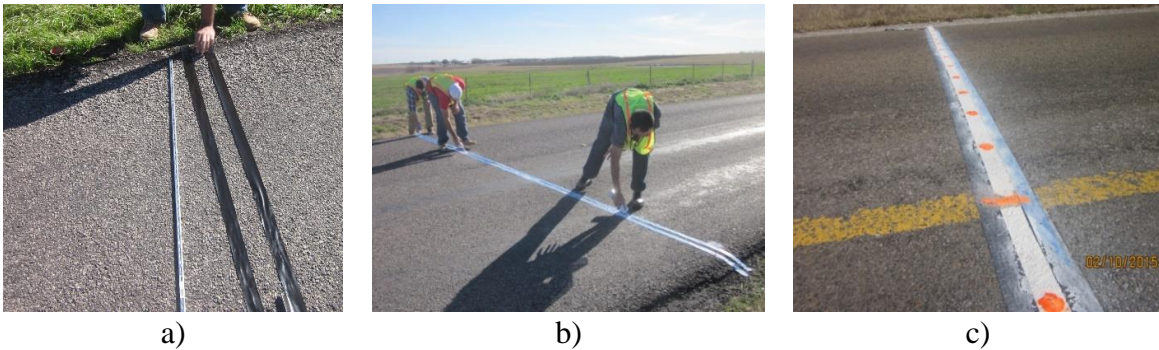


Figure 4.5 Marking transverse test sections a) Marking a stripe with duct tape; b) Painting the stripe with white spray paints; c) Painting circular orange marks on the white stripe

#### 4.2.2.3. Deformation Monitoring with Total Station

Total station instrumentation was used to obtain information on the vertical movement of the marked transverse sections. The instrument model and the distance of shooting were selected to provide a minimum accuracy of 2 mm in reading elevations. As illustrated in Figure 4.6, the operation was first carried out with regular total stations in which a prism should be held at target point. The regular total station was later replaced by a prism-less total station that allowed shooting at target points without prism. The replacement provided the same level of accuracy and a fast and safe operation in the field.

In order to read elevation of the marked transverse sections, a total station was installed on the roadside less than 200 ft away from the marked sections. Then the instrument was pointed at each orange mark along the transverse sections, and the coordinates of the point were recorded. Transverse profile of the road could be obtained by analyzing the recorded coordinates and connecting them accordingly. Transverse profiles were obtained over time for the marked sections on a regular basis and changes in the elevations were evaluated.



*Figure 4.6 Using total station and prism to monitor vertical deformation of the marked transverse sections*

#### **4.2.2.4. Example Results**

The total station has many surveying functions of which the one used for this study is a coordinate output in the northing (X), easting (Y), and Z direction. Each survey was done by shooting the center point marked on the centerline of the road, and continuing toward the shoulder by shooting each marked point in approximately one-foot intervals (Figure 4.7).

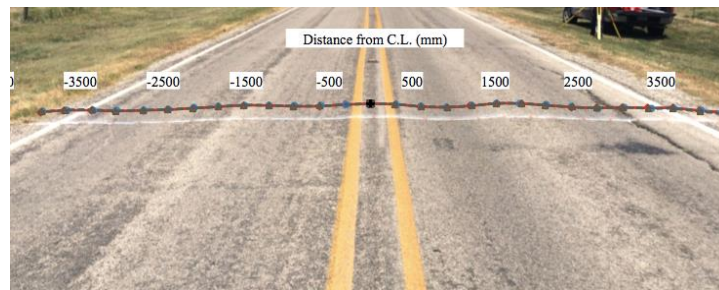


*Figure 4.7 Total station survey of the marked sections in the field*

After performing the total station survey, the coordinate data was downloaded from the total station onto the computer and plotted using a template created in excel. The plots were produced by obtaining the X and Y coordinates of each point relative to the center point. Changes in the transverse profile of the road surface were evaluated by comparison among the profiles produced in consecutive site visits. Changes in the slope of each side of the road were also evaluated. An

example of the results from the total station surveys is shown in Figure 4.8 and Table 4.2.

**Table 4.2. Example results from total station surveys**

FM 1979-Westbound Readings-Section#8-Visit #1							FM 1979-Eastbound Readings-Section#8-Visit #1						
Total Station Coordinate Reading Relative to center line			Modified coordination for cross section of the road				Total Station Coordinate Reading Relative to center line			Modified coordination for cross section of the road			
	Z	X	Y	Z	X	Y		Z	X	Y	Z	X	Y
Pt.	m	m	m	mm	mm	mm	Pt.	m	m	m	mm	mm	mm
1	0	0	0	0	0	0	1	0	0	0	0	0	0
2	-0.00762	0.217932	0.224028	-7.62	313	0	2	-0.0061	-0.19812	-0.22403	-6.096	299	0
3	-0.01981	0.428244	0.44196	-19.812	615	0	3	-0.02286	-0.39472	-0.4511	-22.86	599	0
4	-0.02134	0.641604	0.673608	-21.336	930	0	4	-0.02896	-0.61265	-0.67208	-28.956	909	0
5	-0.01524	0.839724	0.897636	-15.24	1229	0	5	-0.01829	-0.80467	-0.89002	-18.288	1200	0
6	-0.01372	1.042416	1.124712	-13.716	1533	0	6	0.001524	-1.03327	-1.11404	1.524	1519	0
7	-0.02591	1.260348	1.344168	-25.908	1843	0	7	0	-1.23292	-1.33807	0	1819	0
8	-0.03658	1.444752	1.56972	-36.576	2133	0	8	-0.01372	-1.43256	-1.54991	-13.716	2111	0
9	-0.04877	1.674876	1.7907	-48.768	2452	0	9	-0.02743	-1.6322	-1.7907	-27.432	2423	0
10	-0.05334	1.868424	2.013204	-53.34	2747	0	10	-0.03505	-1.83032	-2.01168	-35.052	2720	0
11	-0.05944	2.112264	2.25552	-59.436	3090	0	11	-0.03048	-2.04673	-2.24028	-30.48	3034	0
12	-0.05334	2.289048	2.465832	-53.34	3365	0	12	-0.03505	-2.2479	-2.4704	-35.052	3340	0
13	-0.05486	2.526792	2.692908	-54.864	3693	0	13	-0.03505	-2.45212	-2.68834	-35.052	3639	0
14	-0.06706	2.706624	2.912364	-67.056	3976	0	14	-0.05486	-2.67919	-2.91084	-54.864	3956	0
15	2.717292	-12.7559	3.003804	2717.292	13105	0	15	-0.0701	-2.87426	-3.14554	-70.104	4261	0

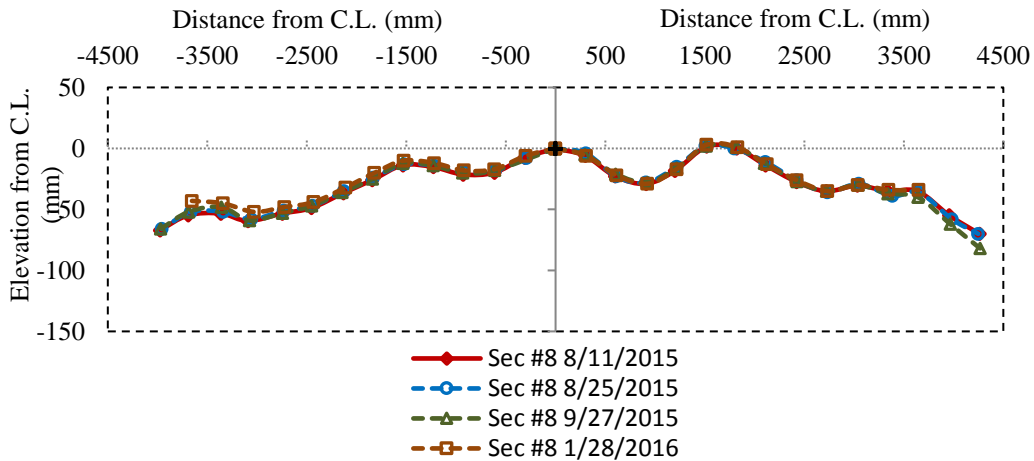


Figure 4.8 Example transverse profile of the road surface generated using total station data

### 4.2.3. PMIS Data

As part of TxDOT’s PMIS, road performance data has been collected and stored in databases in a manner that can quickly be retrieved and analyzed. The performance data has been summarized for 0.5-mile data collection sections in five categories of (1) visual distresses, (2) ride quality, (3) rutting data, (4) deflection, and (5) skid resistance. While PMIS requires distress, rutting, and ride quality data to be collected annually for 100% of state-maintained highways, collection of deflection data is optional and skid resistance data must be collected on 25 to 50% of the roads. Visual distress data is transformed into corresponding ratings including ratings for



rutting, patching, failures, block cracking, alligator cracking, longitudinal cracking, transverse cracking, raveling, and flushing. Rutting measurements are reported as shallow rutting percentage, deep rutting percentage, and average rut depth. The PMIS also produces five scores to describe the quality of Texas pavements in an orderly and consistent manner. The scores include Distress Score (ranging from 1 to 100), Ride Score (ranging from 0.1 to 5), Condition Score (ranging from 1 to 100), Structural Strength Index (SSI) Score (ranging from 1 to 100), and Skid Score (ranging from 1 to 99). These scores are defined as utility factors to adjust the ratings and other performance data into a uniform scale for comparison purposes.

As part of the monitoring program of the field sections, the PMIS data available on and around the location of the field sections was collected and evaluated. Texas Road Marker (TRM) numbers were identified at each field location and the corresponding performance data was downloaded in spreadsheet format from the TxDOT PMIS database. In particular, consistent with the identified performance measures in this project, the following information types were collected from the TxDOT PMIS database:

- **Longitudinal Cracking** that is characterized as part of PMIS visual distress evaluation and is reported with a designated distress rating. The rating method for longitudinal cracking involves using length per 100-ft station scale, which can range from 0 to 999.
- **Rutting Data** that is measured from the actual pavement surface by a TxDOT profiler/rutbar vehicle. Rutting measurements are reported as shallow rutting percentage, deep rutting percentage, and average rut depth.
- **Condition Score** that is identified based on pavement overall condition in terms of distress and ride quality. This score ranges from 1 (worst condition) to 100 (best condition) with the five classes varying from Class A (Very Good), for Condition Scores of 90 to 100, to Class F (Very Poor), for Condition Scores below 34.

Table 4.3 illustrates an example of the performance data collected from TxDOT PMIS database. This example refers to the FM 1774 project, which is composed of three test sections: two geogrid-stabilized sections and one control section. As illustrated on top, TRM numbers were identified for the limits of the test sections and the PMIS results of longitudinal cracking percentage were collected between 1994 and 2015.

**Table 4.3. Example PMIS data collected as part of the monitoring program**

FM1774 K													
ACP_LONGITUDE_CRACKING_PCT													
	TRM												
Year	427	427.5	428	428.5	429	429.5	430	430.5	431	431.5	432	432.5	433
1994													
1995	0	0	2	0	0	0	0	0	0	0	0	0	0
1996	0	0	2	0	0	0	0	0	0	0	0	0	0
1997	0	6	10	0	1	2	3	2	5	1	0	4	0
1998	0	3	0	0	2	2	2	2	8	8	3	0	5
1999	0	0	2	0	0	0	0	0	0	0	0	3	0
2000	0	0	0	2	2	9	0	0	2	0	0	18	3
2001	0	0	3	2	0	9	9	21	3	0	0	0	0
2002	0	3	0	2	5	3	3	5	0	0	0	0	0
2003	2	2	0	3	2	8	2	26	0	0	0	0	0
2004									0	0	0	0	0
2005	0	0	0	0	0	0	0	0	1	1	0	1	5
2006	0	0	0	0	0	0	0	0	15	12	0	12	0
2007	0	0	0	0	5	0	0	0	21	21	0	27	6
2008	0	0	0	0	0	0	0	0	9	6	0	3	0
2009	0	0	0	0	2	3	8	3	12	8	0	3	5
2010	0	0	0	0	0	0	0	3	27	18	0	6	3
2011	0	0	0	0	0	0	0	0	0	0	0	0	0
2012	0	0	3	3	6	10	2	2	6	12	0	0	8
2013	0	0	3	3	0	0	3	0	5	8	0	0	0
2014	0	0	0	0	0	0	0	0	0	4	0	4	3
2015													

Figure 4.9 illustrates an example of the analysis that was conducted for comparative evaluation of performance in geosynthetic-stabilized versus non-stabilized test sections using the collected PMIS data. In this example, average percentage of longitudinal cracks for Data Collection Sections is illustrated on the vertical axis and the TRM numbers are presented on the horizontal axis. Limits of the three test sections are also specified in this graph. Evaluation of the data presented in this graph for various years provides insight on comparative performance of geosynthetic stabilized versus non-stabilized test sections as well as on the comparative performance of various types of geosynthetic reinforcements.

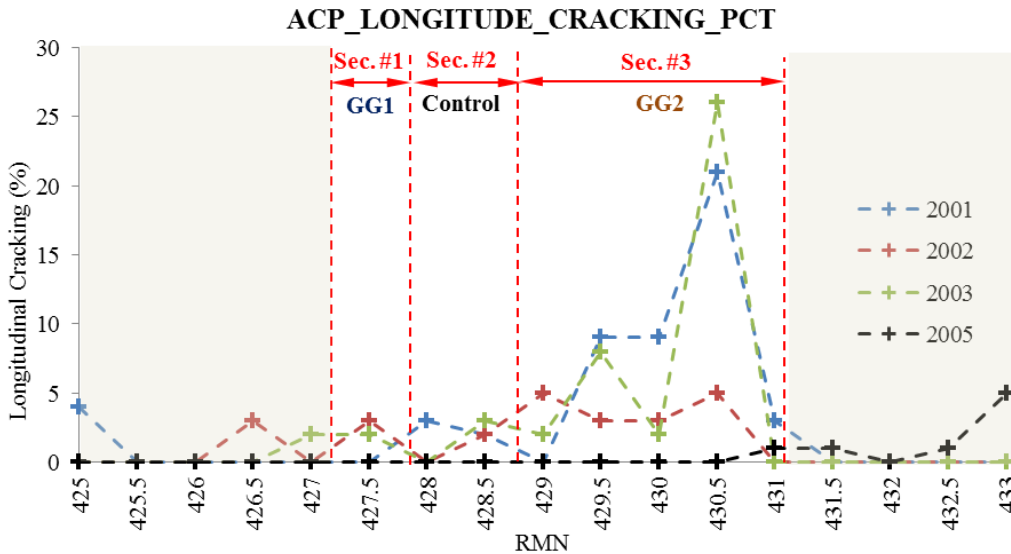


Figure 4.9 Example analysis for comparative evaluation of performance in geosynthetic-stabilized versus non-stabilized test sections using PMIS data

## **4.3. Field Performance of Experimental Test Sections**

---

Results obtained from evaluation of the field performance of experimental test sections are presented in this section.

### **4.3.1. Identification of Field Test Sections**

Ten sites were identified through collaboration between the University of Texas and TxDOT. Table 4.4 summarizes the main features of the field test sections at each site. The sites were selected from among the roads with varying levels of traffic (from low volume to high volume roads) and with a wide range of subgrade soil properties.

Characteristics of the subgrade soil were determined by evaluation of the soil characterization data available to TxDOT or to the research team. Additional subgrade soil samples were also collected and characterized at locations where soil characterization data was not available.

Geosynthetics that have been used at each location were also identified and characterized according to the requirements of the existing TxDOT Department Material Specifications DMS-6240. Table 4.5 summarizes characteristics of the geosynthetics as compared to the requirements of DMS-6240.

**Table 4.4: Main features of the identified field test sections**

	TxDOT District	Texas County	Number of Test Sections	Performance Years	Geosynthetic Types	Geosynthetic Location	Subgrade Soil USCS Class	Approximate Range of Subgrade Soil Plasticity (PI)
FM 2	Bryan	Grimes	32	10	GG 1 GG 5 GT 2	Base-Subbase Interface	CL and CH	20 to 55
FM 1644	Bryan	Robertson	6	4	GG 6	Base-Subbase Interface	CH	25 to 40
FM 1915	Bryan	Milam	3	20	GG 1	Base-Subbase Interface	CH	40 to 55
FM 1774	Bryan	Grimes	3	14	GG 1 GG 4	Base-Subbase Interface	CH	40
SH 21	Austin	Lee	7	5	GG 1 GG 7 GG 8 GG 9 GG 10	Base-Subbase Interface	CH	25 to 50
FM 2924	San Antonio	Atascosa	7	>3	GG 1	Base-Subbase Interface	CH	40 to 55
FM 1979	San Antonio	Guadalupe	8	>3	GG 1	Base-Subbase Interface	CL	55 to 60
Cabeza Road	Yoakum	DeWitt	3	>3	GG 7 GG 9	Base-Subbase Interface	CL, CH	20 to 40
FM 972	Austin	Williamson	6	>3	Non-stabilized	--	CH	40 to 50
Turnersville Rd.	Austin	Travis	6	>3	Non-stabilized	--	CH	35

**Table 4.5: Characterization of geosynthetics used in the field test sections in accordance with the requirements of TxDOT DMS-6240**

Product acronym used in this project	Aperture Size, in. (mm)	Percent Open Area, %	Thickness of Ribs, in. (mm)			Tensile Modulus @2% elongation, kips/ft (kN/m)		Junction Efficiency, % of rib ultimate tensile strength
			MD Ribs	CMD Ribs	Junctions	MD	CMD	
	1.0-2.0 (25-51)	> 70%	0.03 (0.77)	0.025 (0.64)	0.06 (1.50)	>14 (205)	>14 (205)	> 90%
GG 1	1.0x1.3 (25x33)	75	0.03 (0.76)	0.03 (0.76)	0.06 (1.50)	14 (205)	22.5 (330)	93%
GG 2	1.6x1.6x1.6 (40x40x40)	> 70	0.07 (1.8)	0.06 (1.5)	0.13 (3.4)	20.5 (300) (Radial stiffness @ 0.5% strain)		93%
GG 4	1.73x1.73 (44x44)	75%	> 0.03 (0.77)	> 0.03 (0.77)	> 0.06 (1.5)	20.5 (300)	68.5 (500)	35%
GG 5	1.0x1.0 (25x25)	70				25 (365)	25 (365)	
GG 6	0.6x0.6 (15x15)					17.5 (250)	24 (350)	
GG 7	1.3x1.3x1.3 (33x33x33)	> 70	0.06 (1.5)	0.05 (1.2)	0.12 (3.1)	15.1 (200) (Radial stiffness @ 0.5% strain)		93%
GG 8	1.3x1.3 (33x33)	> 70	0.03 (0.76)	0.03 (0.76)		13.5 (200)	19 (275)	93%
GG 9	1.6x1.6x1.6 (40x40x40)	> 70	0.05 (1.3)	0.05 (1.2)	0.13 (3.4)			93%
GG 10	1.6x1.6x1.6 (40x40x40)	> 70	0.08 (2.0)	0.06 (1.6)	0.15 (3.8)			93%
GT 2	--	--	--	--	--	48 (700)	66 (965)	--

GG 1 =Tensar Biaxial Geogrid BX1100; GG 2 = Tensar Triaxial Geogrid TX160; GG 4 = Colbond Enkagrid Max20; GG 5 = Tencare Mirafi BasXgrid 11; GG 6 = Huesker Fornit 20; GG 7 = Tensar Triaxial Geogrid TX130s; GG 8 = Tensar Biaxial Geogrid BX4100; GG 9 = Tensar Triaxial Geogrid TX5; GG 10 = Tensar Triaxial Geogrid TX7; GT 2 = Tencate Geolon HP570.

## 4.3.2. Site 1: Farm-to-Market Road 2 (FM 2)

### 4.3.2.1. Project Description

FM 2 is a two-lane light traffic road with trucks being the major traffic on the road. The speed limit is 55 mph. FM 2 starts from 2 miles west of Highway 6 at Courtney eastward to FM 362 in Grimes County, Texas. The total distance is about 6.4 miles. Major problems with ride quality and different types of distresses, particularly in form of longitudinal cracks, had been reported for the section between Highway 6 and FM 362. Following the falling weight deflectometer and rolling dynamic deflectometer tests in this portion of the road, a major rehabilitation plan was designed in 2006. The length of this section is about 4.4 miles (Figure 4.10).

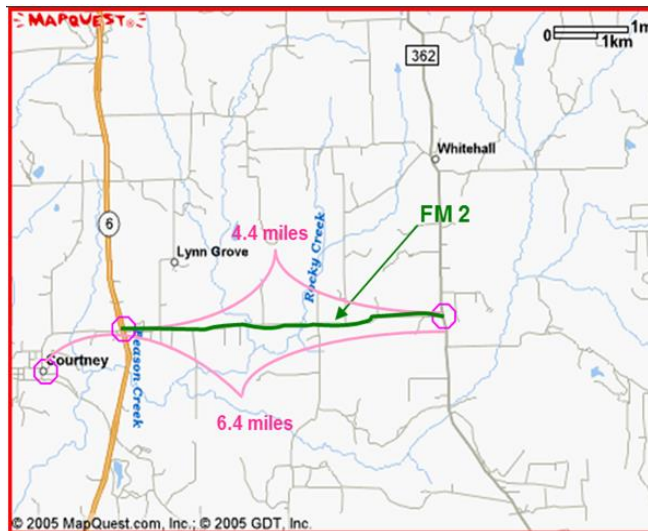


Figure 4.10 Location of FM 2 and the rehabilitation area

### 4.3.2.2. Test Sections Design

Four pavement cores were taken from FM 2 in summer 2003 by TxDOT, which indicated a light pavement structure. It included a 1-in. asphalt concrete layer as the top cover of the road and up to 15-in. iron ore base course (Figure 4.11). The rehabilitation design in 2006 involved 10-in. scarification and remix of the old base course and construction of a new 7-in. base layer. As part of rehabilitation plan, 32 test sections were designed at two sections of the road as illustrated in Figure 4.12. Four different repair schemes (with multiple replicates for each scheme) were designed for the test sections that include (1) non-stabilized (control) sections, (2) lime-stabilized sections, (3) geosynthetic-stabilized sections, and (4) combined geosynthetic- and lime-stabilized sections (Figure 4.13).

Scheme (1) (control sections) was constructed using a 10-in.-thick subbase layer composed of the original pavement materials that were scarified, remixed, and re-

compacted. A new 5-in.-thick base layer was constructed on top of the subbase. In Schemes (2) and (4) the 10-in.-thick subbase was stabilized using 4 to 6% lime. In Schemes (3) and (4) one layer of geosynthetic was placed at the interface between the 10-in.-thick subbase course and the 7-in.-thick new base course. Three geosynthetics were used including two geogrids (GG 1 and GG 5) and one geotextile (GT 2).

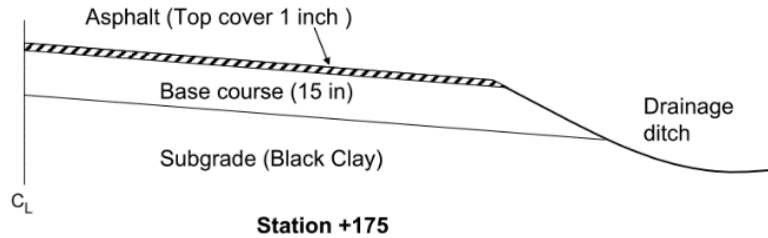


Figure 4.11 Design profile of FM 2 before reconstruction



Figure 4.12 Location of the test sections at FM 2

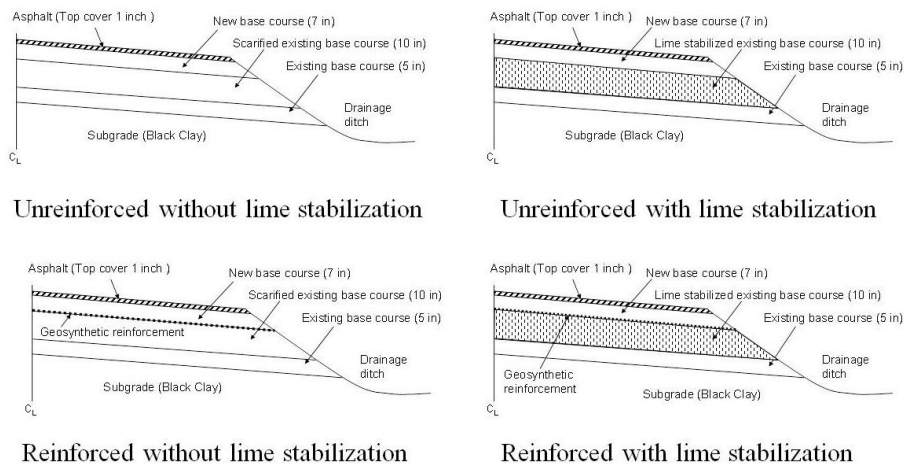


Figure 4.13 Four repair schemes used in the FM2 project

### 4.3.2.3. Performance Result

Performance of the test sections in FM 2 has been evaluated using a comprehensive monitoring program for more than 10 years. As part of the monitoring program in this project, a new conditions survey was conducted on FM 2 and the extents of the longitudinal cracks were evaluated. The results obtained in this conditions survey are presented in Figure 4.14. Geosynthetic-stabilized sections were found to perform significantly better than the control section. While the average percentage of longitudinal cracks were found to be below 30% in the geosynthetic-stabilized sections, the average percentage of longitudinal cracks in the control sections exceeded 85%. The test sections constructed with three different geosynthetic products showed similar performance.

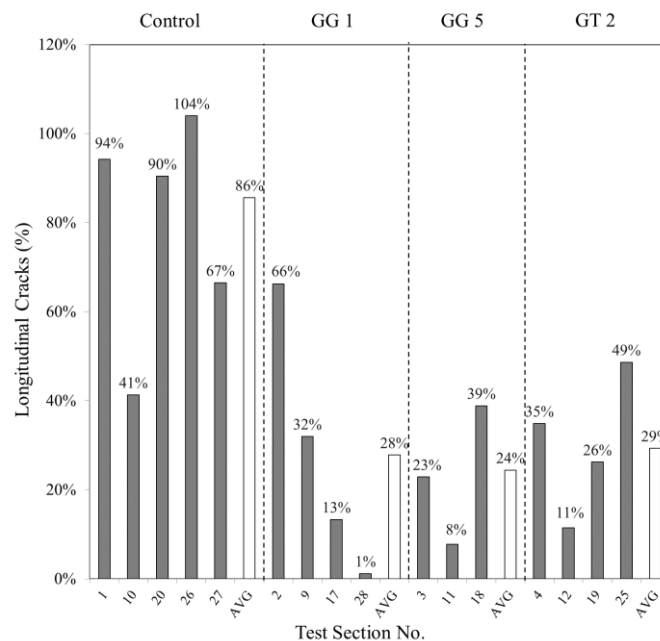


Figure 4.14 Percentage of environmental longitudinal cracks at the FM2 test sections

## 4.3.3. Site 2: Farm-to-Market Road 1644 (FM 1644)

### 4.3.3.1. Project Description

As an extension to the FM2 experiment, additional test sections were identified and reconstructed in 2010 in FM 1644, Robertson County, Texas. FM 1644 starts from US 190 southwest of Calvert and extend 24 miles to Franklin. Test sections are located approximately 4 miles east of SH 6 at Calvert that were among the areas founded on expansive subgrades with reportedly poor performance before reconstruction (Figure 4.15).





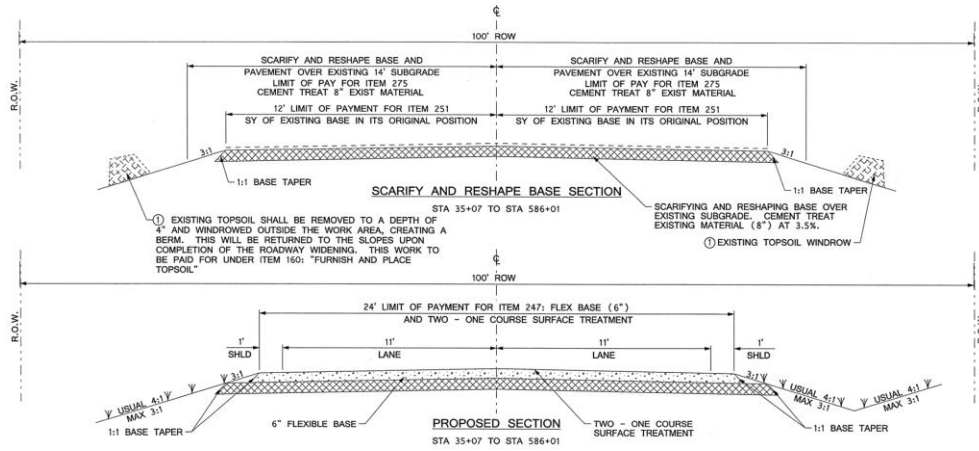


Figure 4.17 Design of the test sections at FM 1644

#### 4.3.3.3. Performance Result

Performance of the test sections in FM 1644 has been monitored by conducting condition surveys for more than 7 years. As part of the field monitoring program in this project, an additional condition survey was conducted on FM 1644 and longitudinal cracks in different test sections were characterized. Results obtained in this condition survey are presented in Figure 4.18. It was found that the geosynthetic-stabilized sections performed significantly better than the other sections. Specifically, the percentage of longitudinal cracks in the geosynthetic-stabilized sections was below 10%. However, the percentage of longitudinal cracks in the control sections exceeded 15 and 50% for the test sections located on the east and west of the geosynthetic-reinforced sections, respectively.

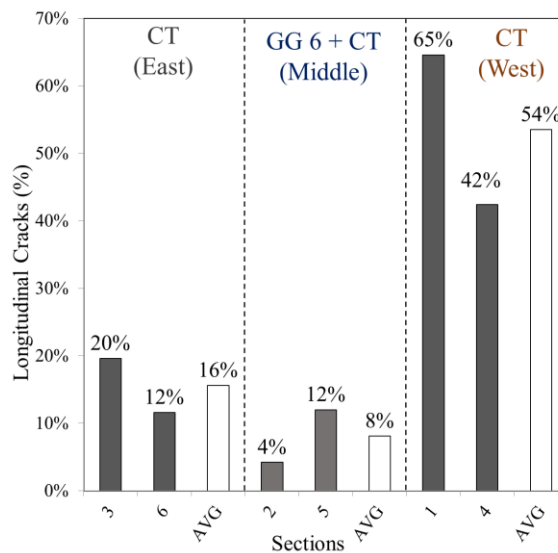


Figure 4.18 Percentage of environmental longitudinal cracks at the FM1644 test sections

Figure 4.19 shows example pictures taken during the condition surveys conducted on FM 1644. Comparison of the pictures presented in Figure 4.19a and b indicate a comparatively good performance of the section stabilized with geogrid (Figure 4.19a) as compared to the control section (Figure 4.19b).

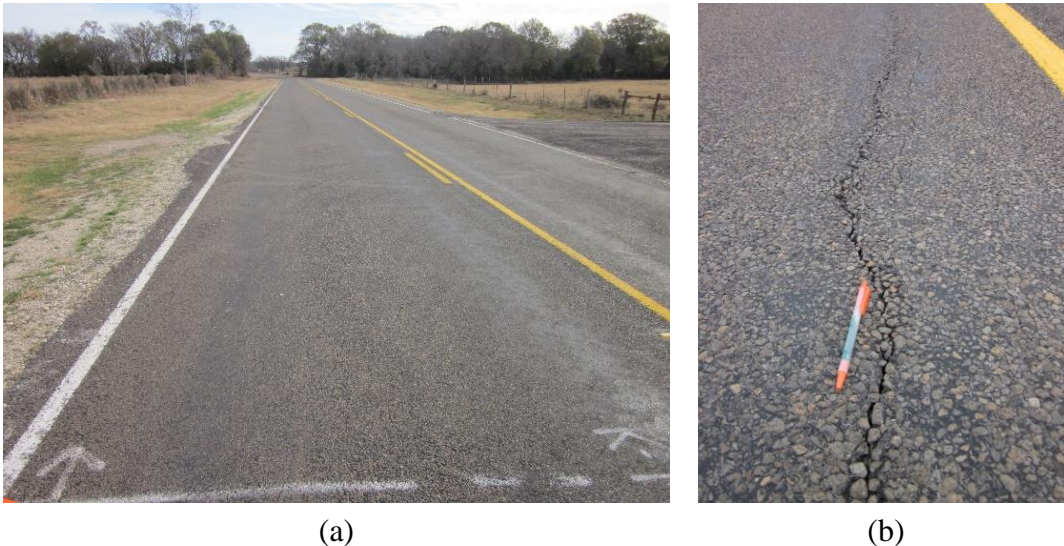


Figure 4.19 Example pictures from test sections at FM 1644: a) Section 2 (geosynthetic-stabilized section); b) Section 4 (control section)

### 4.3.4. Site 3: Farm-to-Market Road 1915 (FM 1915)

#### 4.3.4.1. Project Description and Test Sections Design

FM 1915 is located in Milam County, Texas. Significant longitudinal cracks had been reported in a 2.5 miles (4 km)-long section of this road extending from Little River Relief Bridge to the west. The subgrade soil in this section has been reported as high plasticity clay. As part of a rehabilitation plan conducted in 1996 the old pavement was entirely removed and the recycled material from the old road was used to build a 10 in. (0.25 m)-thick subbase stabilized using 5% lime. As presented in Figure 4.20 and Table 4.6, the new pavement was divided into three test sections with different design schemes aiming at evaluating the performance of geogrid-stabilized pavements. The middle section (Section 2) was constructed as a control section (i.e., without using geosynthetic) using an 8 in. (0.20m)-thick base layer, whereas a biaxial geogrid (GG 1) was placed at the interface of the subgrade and base layers in Sections 1 and 3. While Section 1 was constructed using the same base thickness as the control section, Section 2 was constructed using a reduced thickness of 5 in. (0.127 m) to further evaluate the impact on the performance of the reduced base thickness.

**Table 4.6. Main features of three test sections constructed at FM 1915**

	Section 1	Control section	Section 2
Material used	Geogrid	No Geogrid	Geogrid
Base course thickness, inch (m)	8 (0.20)	8 (0.20)	5 (0.127)
Extent of test section	0.038–0.827 miles	0.827–1.663 miles	<b>1.663</b> –2.480 miles
Total length, ft (km)	4150 (1.26)	4397 (1.34)	4297 (1.31)

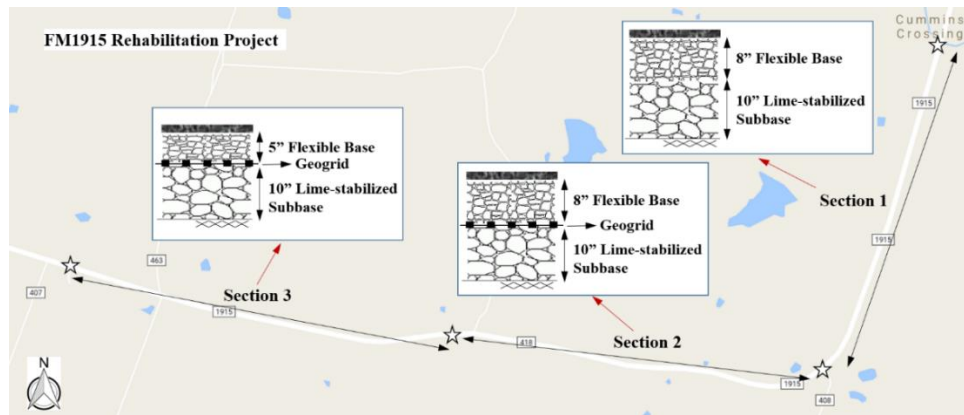


*Figure 4.20 Extensions and designs of the test sections at FM 1915*

#### 4.3.4.2. Performance Result

As part of the field monitoring program in this project, a condition survey was conducted on FM 1915 and longitudinal cracks in different test sections were characterized. Results obtained in this condition survey are presented in Figure 4.21. It was found that both geosynthetic-stabilized sections performed significantly better than the control section. Specifically, the percentage of longitudinal cracks in the geogrid-stabilized section that was constructed using the same base thickness as the control section was very small. The percentage of longitudinal cracks in the geogrid-stabilized section that was constructed with reduced base thickness was found to be 10%, which was significantly lower than the percentage of longitudinal cracks in the control sections. It should be noted that over the past years surface rehabilitation might have been conducted on the test sections. Therefore, the cracks characterized in the condition survey represented comparatively wider cracks that have been reflected through the new surface.

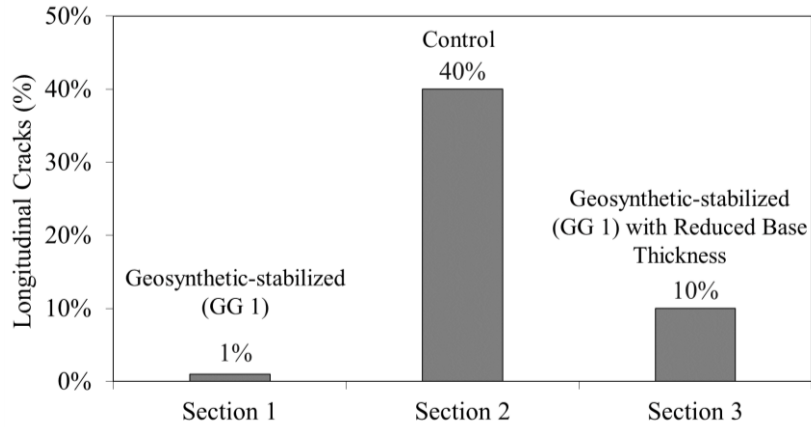


Figure 4.21 Percentage of environmental longitudinal cracks at FM 1915 test sections

Example pictures from condition survey conducted at FM 1915 are presented in Figure 4.22. Figure 4.22a presents a picture from geosynthetic-stabilized sections (Section 1) and Figure 4.22b presents an example picture from the control section (Section 2).

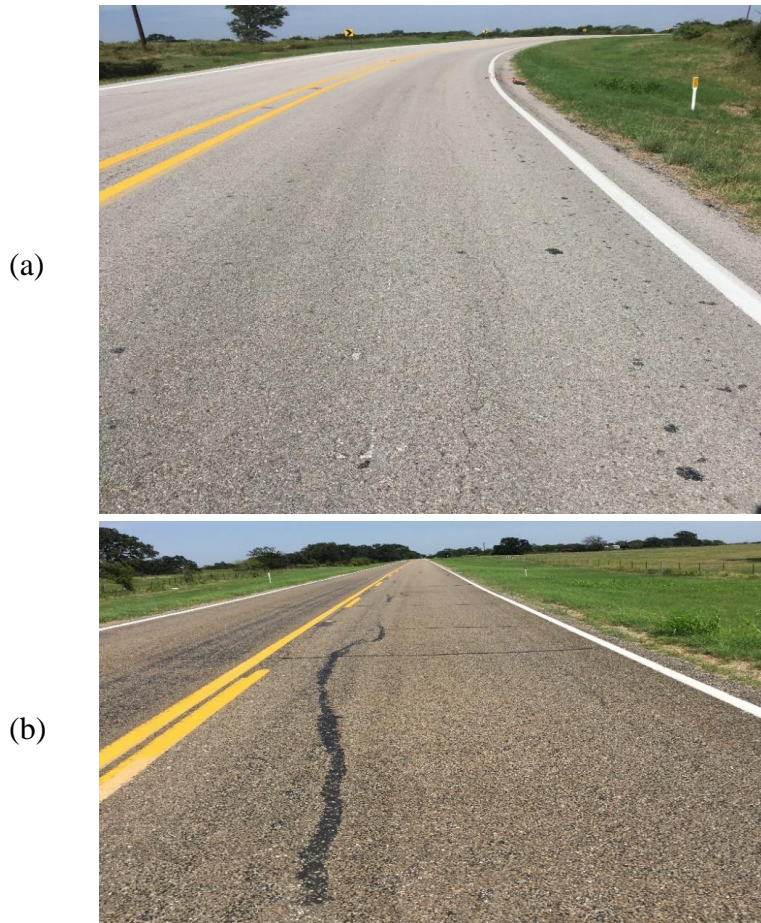


Figure 4.22 Example pictures from test sections at FM 1915: a) Section 1 (geosynthetic-stabilized section); b) Section 2 (control section)

### 4.3.5. Site 4: Farm-to-Market Road 1774 (FM 1774)

#### 4.3.5.1. Project Description and Test Sections Design

As part of restoration of distressed roads in Grimes County, Texas, over 9 miles (14 km) of FM 1774 extending from SH 90 to FM 2445 was reconstructed in August 2002. The old road was fully excavated and leveled and the recycled material was used to form a 10 in. (0.25 m)-thick lime-stabilized subbase. A new 7-in. (0.18 m)-thick flexible base was then constructed overlain by a thin course of asphalt surface layer. Preliminary site investigation and soil testing showed presence of high plasticity subgrade clay (PI=40) in a 3.5-mile-long extension of the road. In order to further stabilize this section of the road, a geogrid layer was installed at the subbase-base interface. To evaluate comparative performance of road sections stabilized with geogrids of different properties, three test sections were constructed. Sections 1 and 3 (0.4 and 2.1 miles in length, respectively) were constructed using two geogrids of different properties, whereas Section 2 (0.9 mile in length) was constructed without geosynthetic. Section 1 was constructed using GG 1 and Section 3 was constructed using GG 4. Figure 4.23 schematically illustrates the design of the road in the geogrid-stabilized sections.

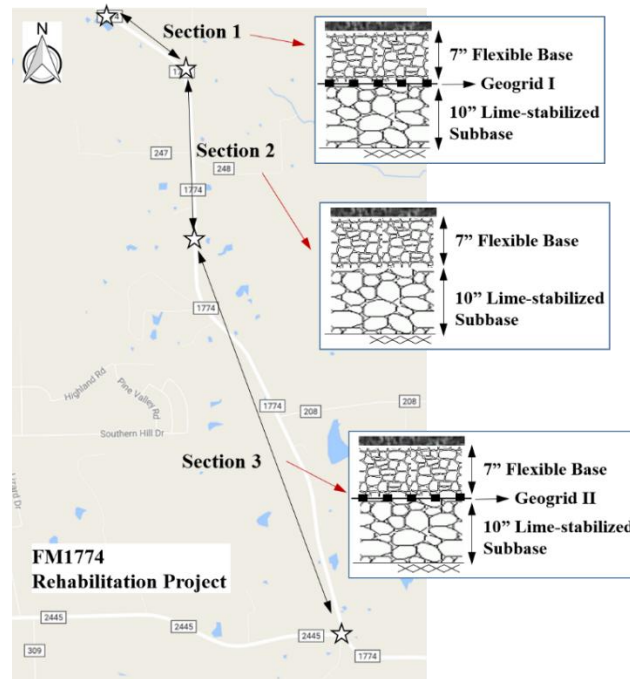
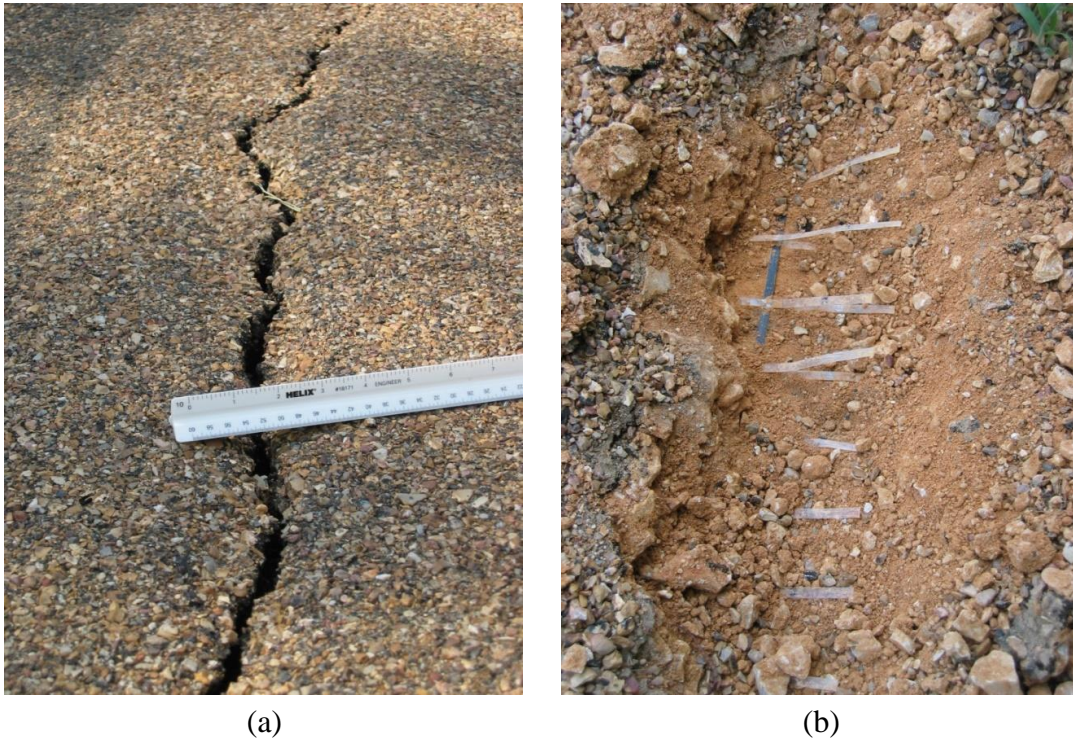


Figure 4.23 Extensions and designs of the test sections in FM 1774

#### 4.3.5.2. Performance Result

In summer 2004, longitudinal cracks were seen in a section stabilized using GG 4. On excavating the cracked road sections of the pavement stabilized with GG 4, it was observed that there was no longer a bond between the longitudinal and

transverse elements of the geogrid. Longitudinal cracks and slippage at junction of the geogrid in the section stabilized using GG 4 are as shown in Figures 4.24a and b, respectively.



*Figure 4.24 Example pictures of the field performance of the test section stabilized using GG 4: a) longitudinal crack on the pavement; b) slippage between longitudinal and transverse ribs at junction of geogrid*

However, an evaluation of the test section stabilized using GG 1 indicated that this section was performing well. An example picture of the performance of this section is presented in Figure 4.25.



*Figure 4.25 Example picture of the field performance of the test section stabilized using GG 1 at FM 1774*

As an additional effort to evaluate performance of the test sections constructed at FM 1774, performance data available in the TxDOT PMIS database was evaluated. Specifically, condition score of the road at the location of the test sections was evaluated. It was found that Section 1 (stabilized using GG 1) extends from TRM number 427 to 427.5, Section 2 (Control section) extends from TRM number 428 to 428.5, and Section 3 (stabilized using GG 4) extends from TRM number 429 to 431. Figure 4.26 presents variation of the condition score of FM 1774 from TRM = 427 to TRM = 431 from 1995 to 2014. Reconstruction of the road in 2004 led to restoration of the condition score to 100 in 2005 for all sections. However, evaluation of the condition score data from 2005 to 2014 indicates that Section 3 (stabilized using GG 4) continuously showed a poor performance.



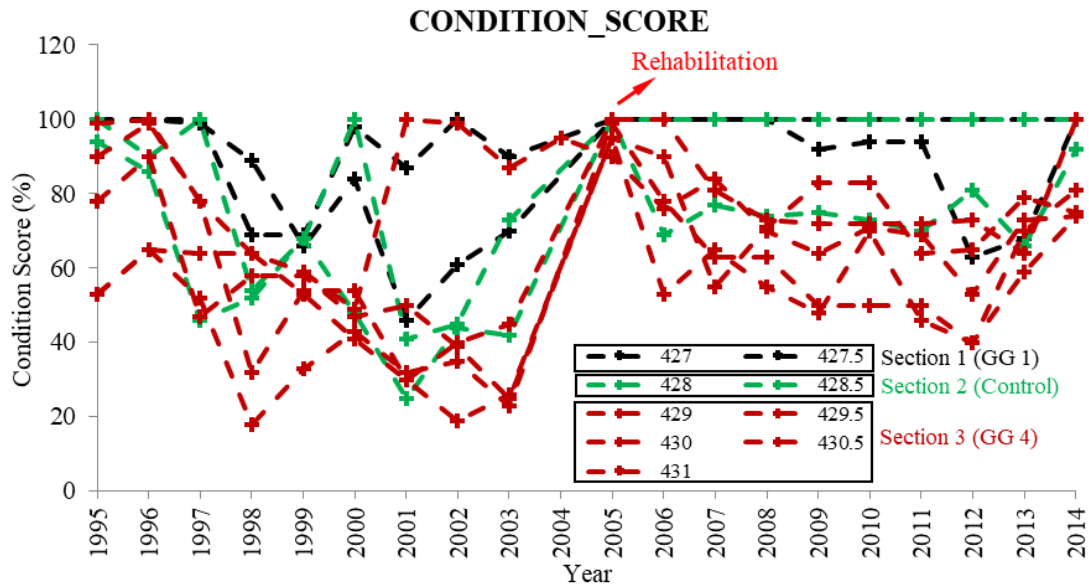


Figure 4.26 Condition score of the test sections at FM 1774 from 1995 to 2014

### 4.3.6. Site 5: State Highway 21 (SH 21)

#### 4.3.6.1. Project Description

A section of SH 21 extended from US 290 to FM 2440 had severe drop off at the edge of pavement as well as several ride issues. As part of the rehabilitation plan in 2011, a few test sections were designed from Lee County line extending to the east (Figure 4.27). Specifically, the outer lane of the test sections was stabilized using different types of geogrid and the shoulder width was extended.

#### 4.3.6.2. Test Sections Design

A total of five geosynthetic stabilized test sections were constructed in SH 21 using five different types of geogrids, including three triangular (GG 7, GG 9, and GG 10) and two biaxial (GG 1 and GG 8) geogrids (Figure 4.28). Road sections before and after reconstruction are illustrated in Figure 4.29. The existing 12-in.-thick base course in 2011 was excavated in the outer lane and replaced by a 6-in.-thick cement-treated subbase layer overlain by a new 6-in.-thick flex base course. The shoulder was reshaped and widened 5 ft to provide additional lateral support for pavement layers. The geogrid layer was installed at the interface between the subbase and the new base layer.



Figure 4.27 Location of SH 21 and the test sections

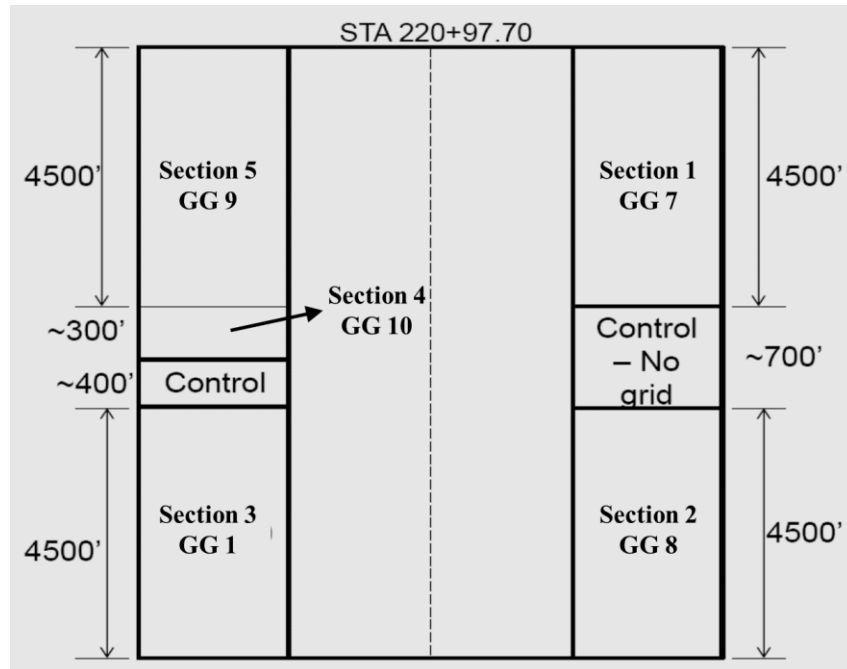


Figure 4.28 Layout of test sections at SH 21

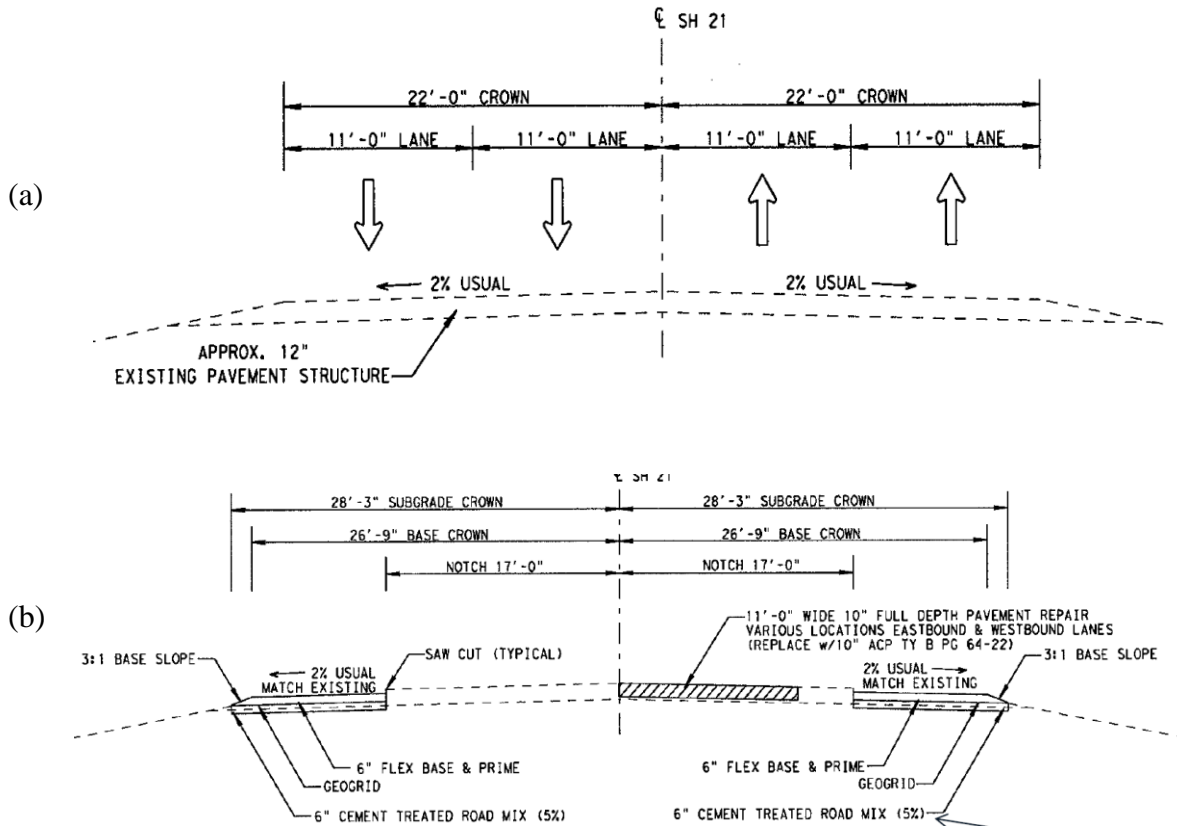


Figure 4.29 Test sections design in the SH21 reconstruction project: a) before reconstruction; b) after reconstruction

#### 4.3.6.3. Performance Result

As part of the field monitoring program in this project, a condition survey was conducted on SH 21 and the extent of longitudinal cracks in different test sections was determined. Results obtained in this condition survey are presented in Figure 4.30. The test sections stabilized using triangular geogrids (i.e., Sections 1, 4, and 5) were found to perform significantly better than the sections stabilized using biaxial geogrids (i.e., Sections 2 and 3). While the percentage of longitudinal cracks in Sections 1, 4 and 5, was found to be below 4%, this percentage in Sections 2 and 3 was 9 and 8%, respectively.

Among the sections stabilized using triangular geogrid, the section stabilized using a geogrid with comparatively high rib thickness (i.e., Section 4 that was stabilized using GG 10) was found to perform comparatively better than the other two sections. Example pictures of the test sections at SH 21 are presented in Figure 4.31. Figure 4.31a, b, and c present example pictures from Sections 1, 4, and 5, respectively, which were stabilized using triangular geogrids. Figure 4.31d presents example picture of cracks observed in Sections 3, which was stabilized using a biaxial geogrids.

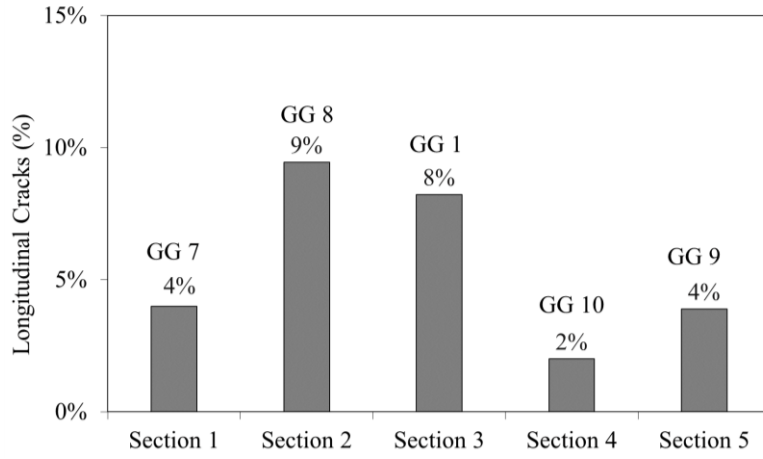


Figure 4.30 Percentage of environmental longitudinal cracks at SH21 test sections

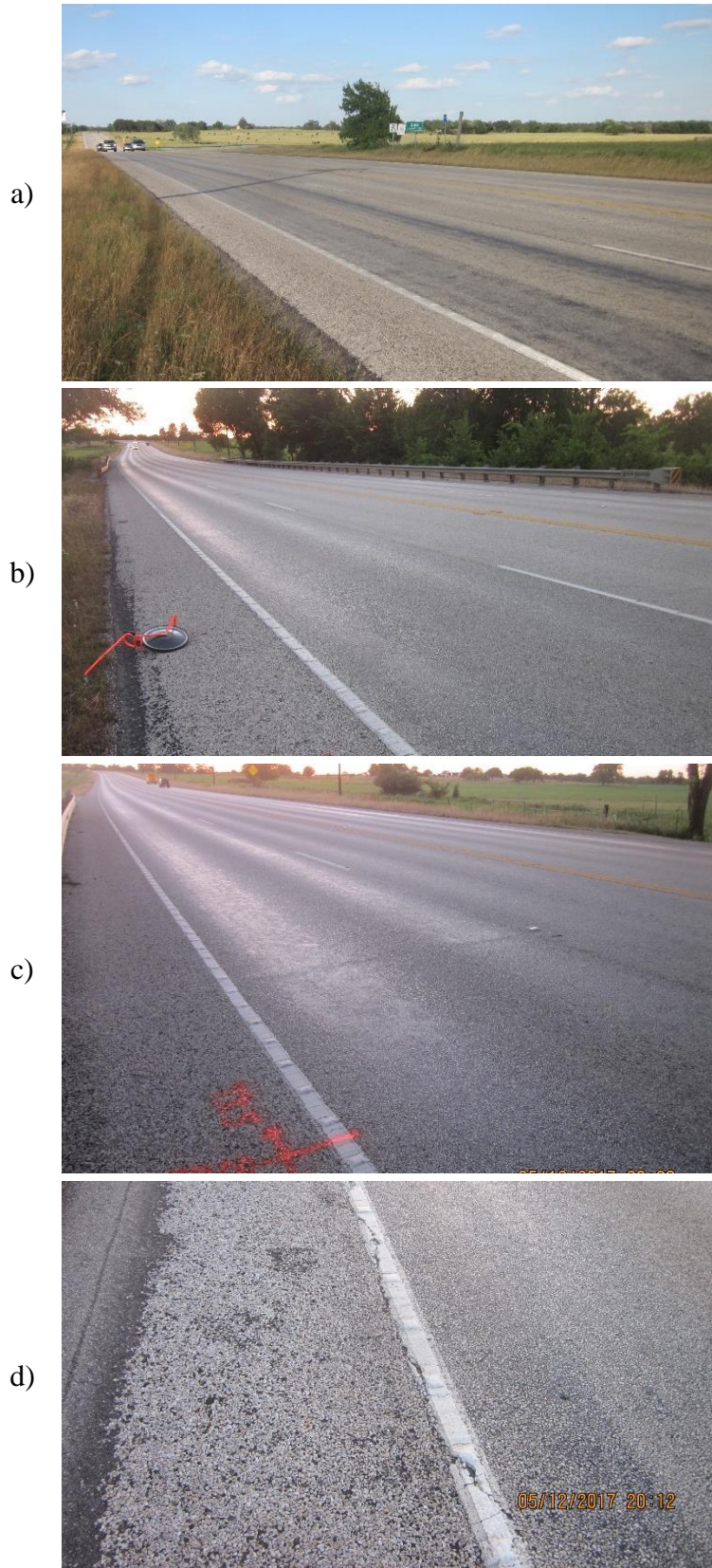


Figure 4.31 Example pictures from test sections at SH 21: a) Section 1; b) Section 4; c) Section 5; d) Section 3

### 4.3.7. Site 6: Farm-to-Market Road 2924 (FM 2924)

#### 4.3.7.1. Project Description

FM 2924 is a two-lane road in Atascosa County located about 70 miles south of San Antonio. It is within TxDOT's San Antonio District and extends about 4.14 miles from FM 791 in the southeast direction to FM 99. It is a road primarily traveled by heavy traffic underlain by an expansive subgrade. The performance of the road has been reported to be particularly poor before stabilization of the pavement by a biaxial geogrid (GG 1) (Figure 4.32). The subgrade soil was characterized as high expansive clay.

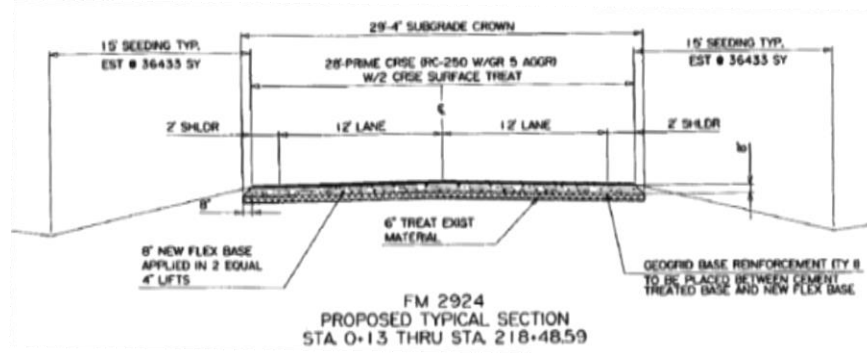


Figure 4.32 Design of test sections at FM 2924

#### 4.3.7.2. Test Section Design

A section of the road extended for approximately 1,100 feet was selected (Figure 4.33). This section was split into six test sections that were divided by white stripe markings in the transverse direction. Orange circles were also added to the white stripe markings every foot from the centerline to shoulder to be used for total station monitoring. The first marked transverse section (Transverse Section 1) is located on the northwest side approximately 2 miles from FM 791. The last marked transverse section (Transverse Section 7) is located on the southeast side of the road (Figure 4.33). The locations for the transverse sections were chosen based on the existing pavement condition along the roadway such that Sections 2, 4, 5, and 6 are considered as poorly performed test sections and Section 1, 3, and 7 are found to be well-performed sections.

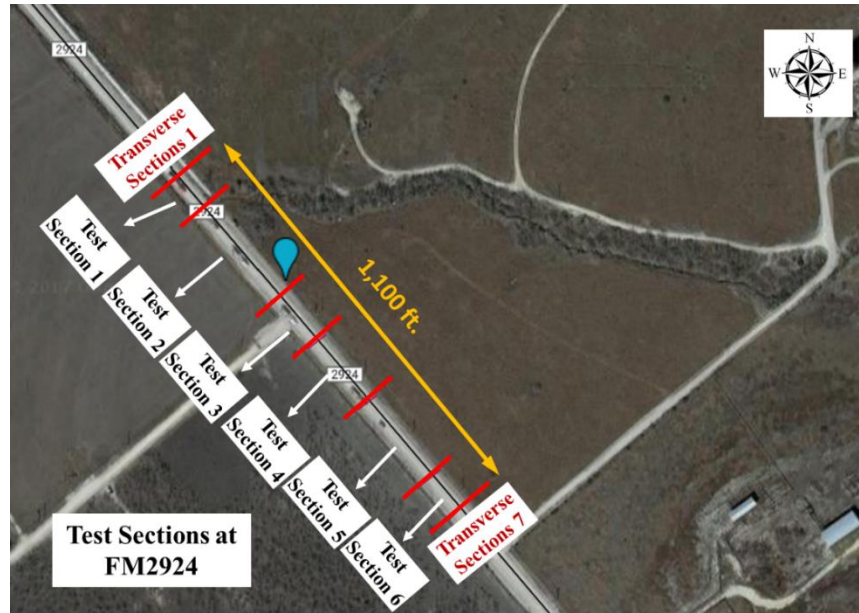


Figure 4.33 Layout of the test sections at FM 2924

#### 4.3.7.3. Performance Result

As part of the field monitoring program in this project, condition surveys were conducted to evaluate extension of longitudinal cracks in test sections at FM 2924. In addition, vertical movement of the marked transverse sections was monitored using total station instrument.

As shown in Figure 4.34, it was found that longitudinal cracks were extended only along the edge of the road where the paved area ends. This area is expected to be the location where the geosynthetic layer also ends. Since no major longitudinal crack was observed in the paved area (i.e., in middle of the road), it can be concluded that the presence of geosynthetic layer could transfer the location of the cracks from the inner parts of the road to the edges. This observation is consistent with the anticipated mechanism associated with the benefits from geosynthetic stabilization layer in roadways.



*Figure 4.34 Example pictures of the longitudinal cracks developed at the edges of test sections at FM 2924*

Example results obtained from monitoring vertical movements of the marked transverse sections at FM 2924 are presented in Figure 4.35. Vertical movement of Transverse Sections 2, 4 and 6 are presented in Figures 4.35 a, b, and c, respectively, from 2015 to 2017. Consistent with the mechanism explained for differential vertical movements in roadways founded on expansive clay subgrades, the edges of the road was found to move comparatively more than the center. This resulted the differential vertical movements between the center and shoulders. In the absence of geosynthetic layer, the differential vertical movements between the center and edges might have led to development of longitudinal cracks in the pavement. However, as previously discussed, the presence of geosynthetic layer could transfer the location of cracks to outside of the paved area.



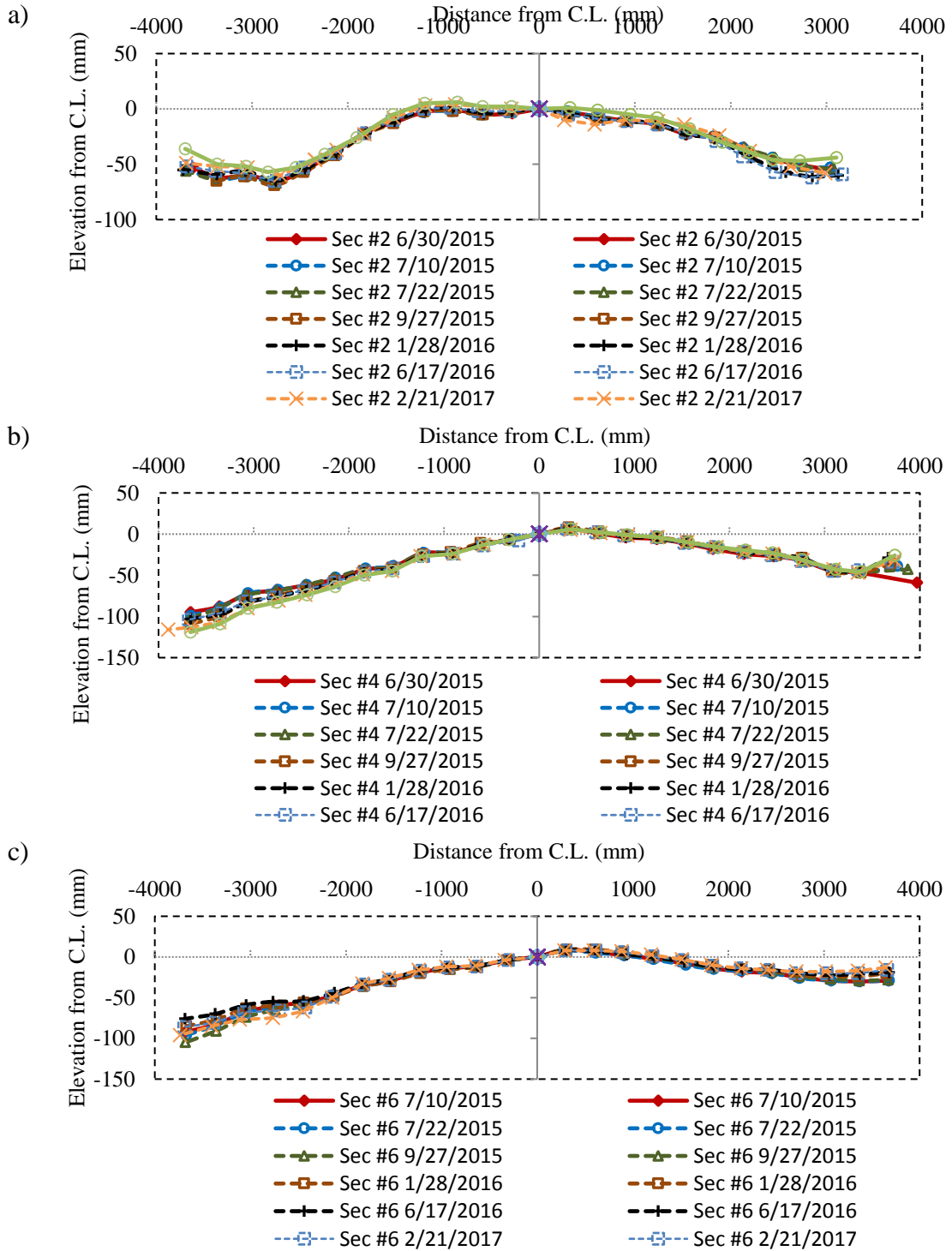


Figure 4.35 Elevation of marked transverse sections at FM 2924 from 2015 to 2017: a) Transverse Section 2; b) Transverse Section 4; c) Transverse Section 6

### 4.3.8. Site 7: Farm-to-Market Road 1979 (FM 1979)

#### 4.3.8.1. Project Description

FM 1979 is a two-lane road in Geronimo, Guadalupe County near Martindale, TX. It is within TxDOT's San Antonio District and extends about 9.2 miles between TX 80 and TX 123 (Figure 4.36). It is a road primarily traveled by civilian traffic underlain by an expansive subgrade and has a biaxial pavement stabilization layer. Average daily traffic in 2008 was 1,700 and the predicted traffic in 2028 is 2,900. The total number of equivalent 18k single-axle loads for a 20-year period is 691,000 for flexible pavement and 908,000 for rigid pavement with a structure number of 3. The subgrade soil was characterized as expansive clay.

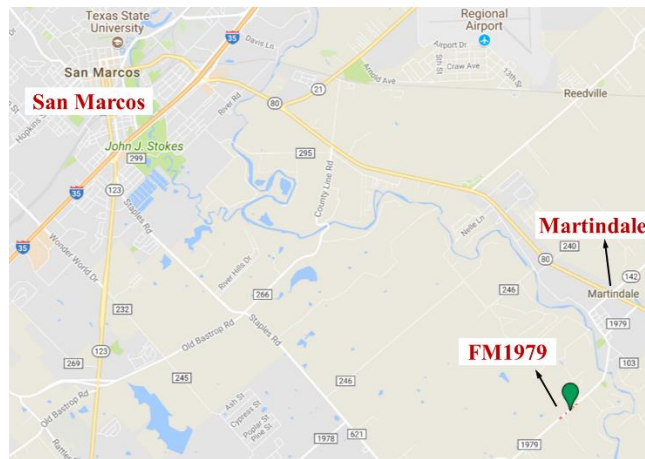


Figure 4.36 Location of FM 1979 relative to San Marcos and Martindale

#### 4.3.8.2. Test Section Design

A total of eight transverse sections were marked along FM 1979 starting with Section 1 about 1.5 miles from TX 80 and ending with Section 8 in the westbound direction. The total length of the area of interest is about 0.26 miles (Figure 4.37). The test sections were marked along areas where there were poor pavement conditions and consist of Sections 2, 3, 5, and 8. Sections 1, 4, 6, and 7 are comparatively better performed sections for the site and are located near each of the test sections.

#### 4.3.8.3. Performance Result

As part of the field monitoring program in this project, condition surveys were conducted to evaluate extension of longitudinal cracks in test sections at FM 1979. In addition, vertical movement of the marked transverse sections was monitored using total station instruments.

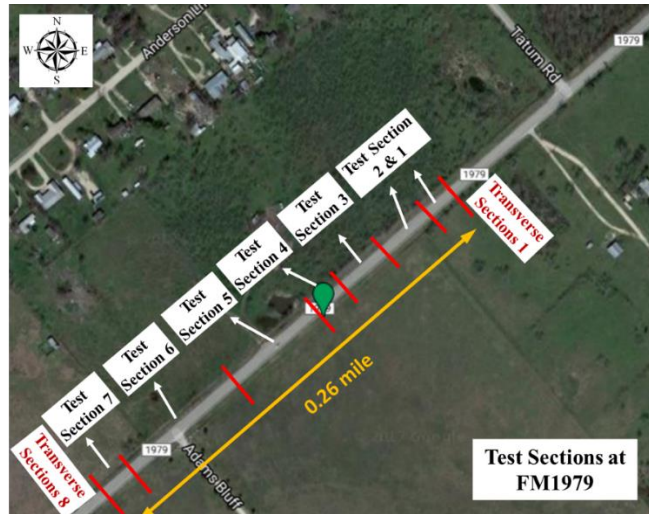


Figure 4.37 Layout of test sections at FM 1979

Results obtained in the condition surveys are presented in Figure 4.38. Except for Section 2, the average percentage of longitudinal cracks among other sections was found to be approximately 20%. The percentage of longitudinal cracks in Section 2 was found to be 57%. Potential reason for unusually high percentage of longitudinal cracks in Section 2 was explored by evaluation of the vertical movement data recorded using total station at Transverse Section 3.

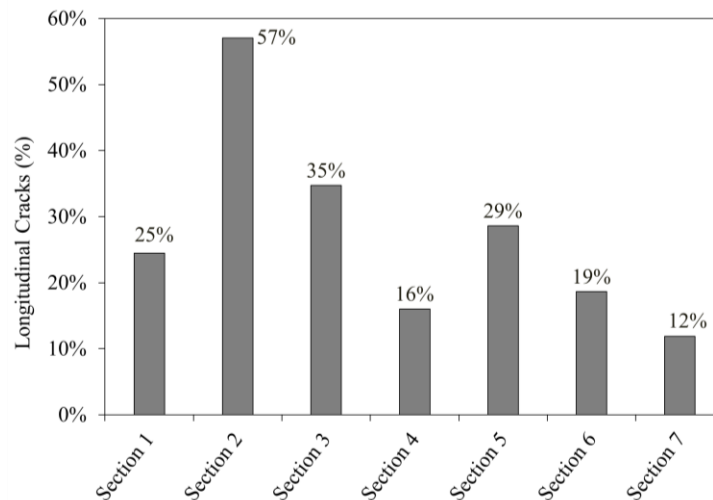


Figure 4.38 Percentage of environmental longitudinal cracks at the FM1979 test sections

As presented in Figure 4.39a, the data recorded by total station from 2015 to 2017 shows that the left lane at this section has had comparatively large vertical movements from the middle of the lane towards the edge. Exploration of the picture of this section presented in Figure 4.39b indicates that the shoulder at the left side has a steep slope. Further evaluation of this picture also reveals that road layers may have had shear failure at this location. Therefore, a comparatively high percentage of longitudinal cracks at this section may partially be attributed to the shear failure.

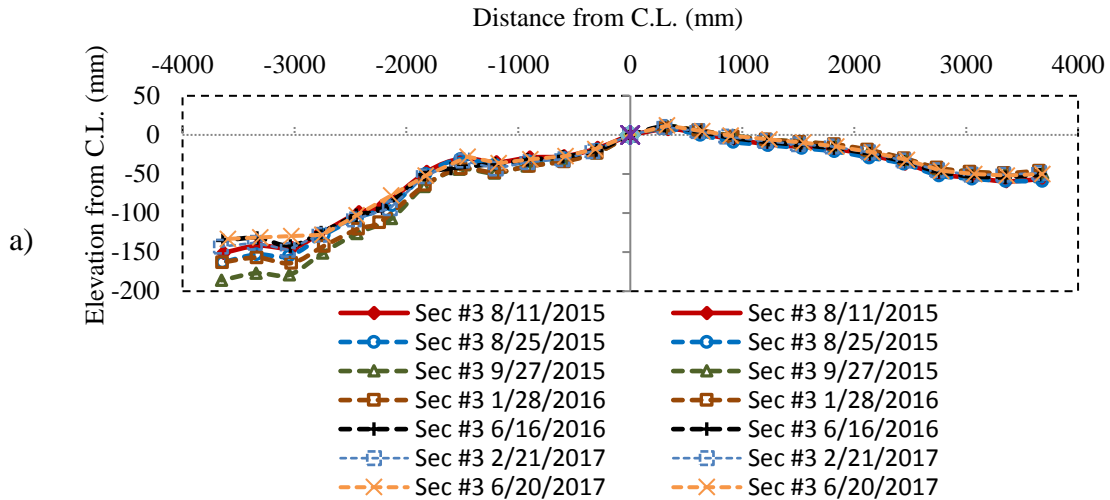


Figure 4.39 Transverse Section 3 at FM 1979: a) variation of the elevation from 2015 to 2017 from data recorded using total station; b) picture of the transverse section

Variation of the road elevation at Transverse Section 7 is presented in Figure 4.40. This transverse section is located close to test Section 7, which has shown the lowest percentage of longitudinal cracks as 12%. Evaluation of the data presented in Figure 4.40 indicates that elevation of the road edge on both sides relative to the centerline of the road has been continually changing. This observation further underlines the presence of differential vertical movement between the center and edges due to subgrade swelling and shrinkage beneath the shoulders. The differential movement might have led to development of severe environmental longitudinal cracks on the road. However, geogrid-stabilization was found to be effective in mitigating the development of such cracks.

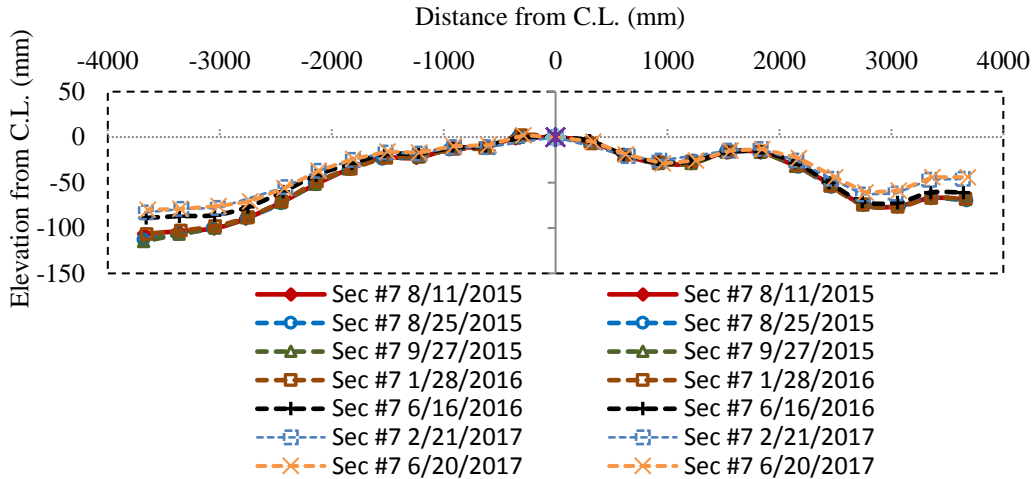


Figure 4.40 Variation of the road elevation at Transverse Section 7

### 4.3.9. Site 8: Cabeza Road

#### 4.3.9.1. Project Description

Cabeza Road is located approximately 84 miles east of San Antonio close to Nordheim, Dewitt County, Texas (Figure 4.41). Cabeza Road is a county road (Dewitt County 324 Rd) connecting Ckodore Road (Dewitt County 352 Rd) and Texas SH 72 with a total length of 8.93 miles. The test sections are located along a north-south direction with a total length of 910 ft (Figure 4.42).

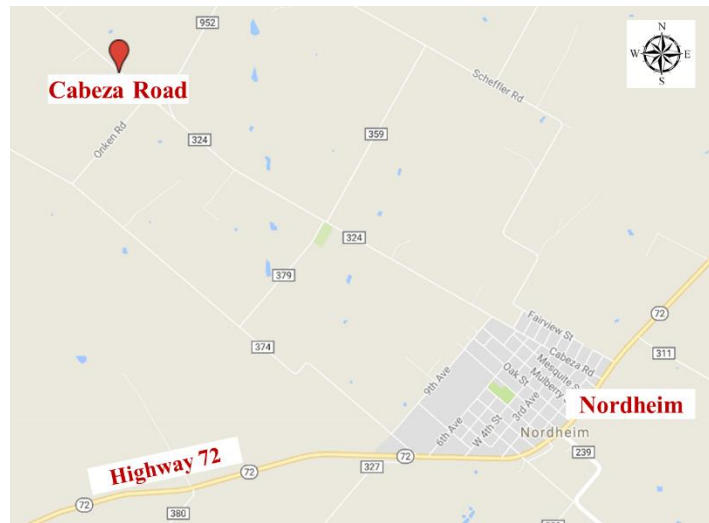


Figure 4.41 Location of Cabeza Rd. relative to Nordheim

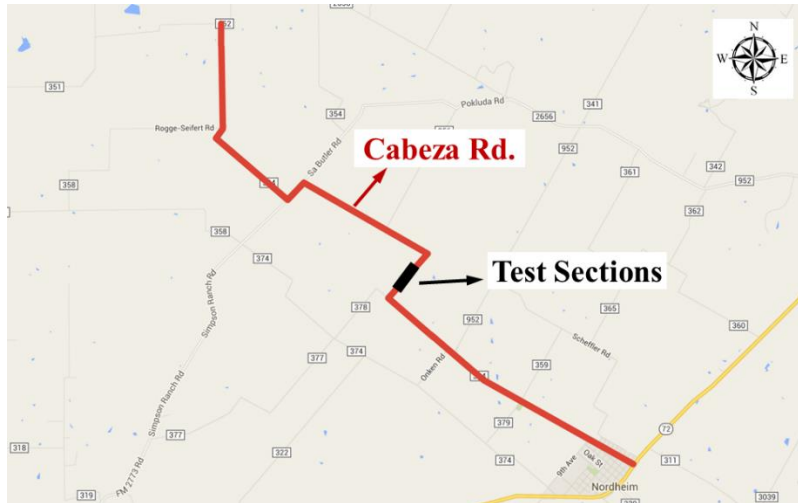


Figure 4.42 Location of test sections along Cabeza Rd.

#### 4.3.9.2. Test Section Design

Three test sections were constructed in Cabeza Road, including a 246-ft-long section stabilized using triangular geogrid GG 7, a 246-ft-long control section without geosynthetic stabilization, and a 417-ft-long section stabilized using triangular geogrids GG 9 (Figure 4.43). A gas facility is located at the north side of the test sections that may cause comparatively higher traffic volumes at its entrance. The section design involved an asphalt chip seal at the surface supported with 6 in. of flexible base layer, underlain by 6 to 8 in. of cement-stabilized subbase. The geosynthetic layer was placed at the interface of the subbase and base course (Figure 4.44).

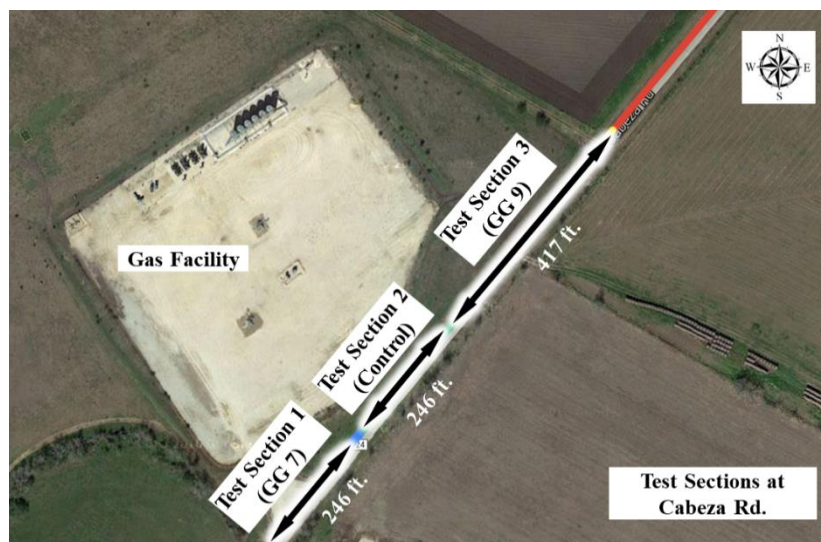


Figure 4.43 Layout of test sections at Cabeza Rd.

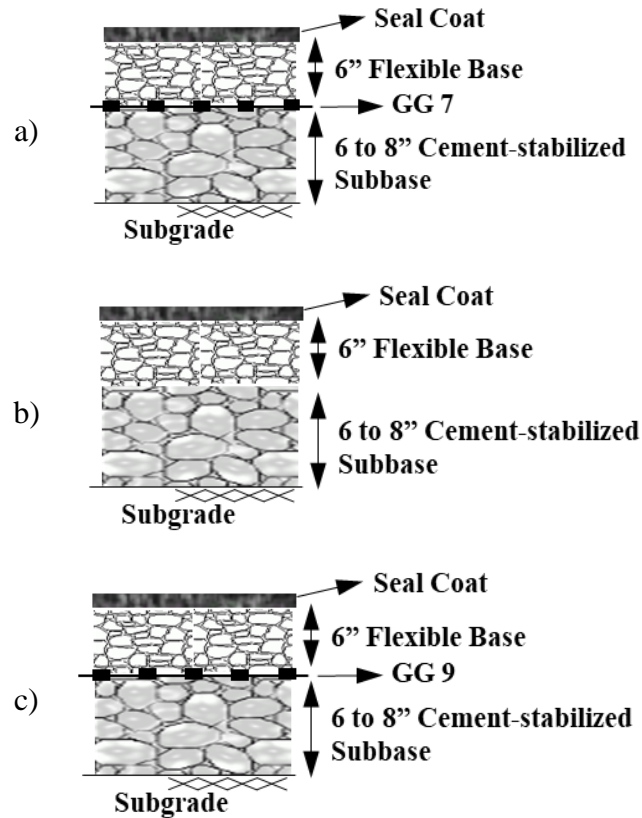


Figure 4.44 Design of test sections at Cabeza Rd.: a) Section 1 (geosynthetic-stabilized); b) control; c) geosynthetic-stabilized

#### 4.3.9.3. Performance Result

As part of the field monitoring program in this project, condition surveys were conducted to evaluate extension of longitudinal cracks in test sections at Cabeza Rd. Results obtained in condition surveys are presented in Figure 4.45. The best performance among the three sections was observed in test Section 3. This section was stabilized using a triangular geogrid with comparatively larger rib thickness than that in triangular geogrid used in test Section 1. Section 2, which was not stabilized with geosynthetic, showed particularly poor performance. Example pictures of longitudinal cracks observed in the control section are presented in Figure 4.46.

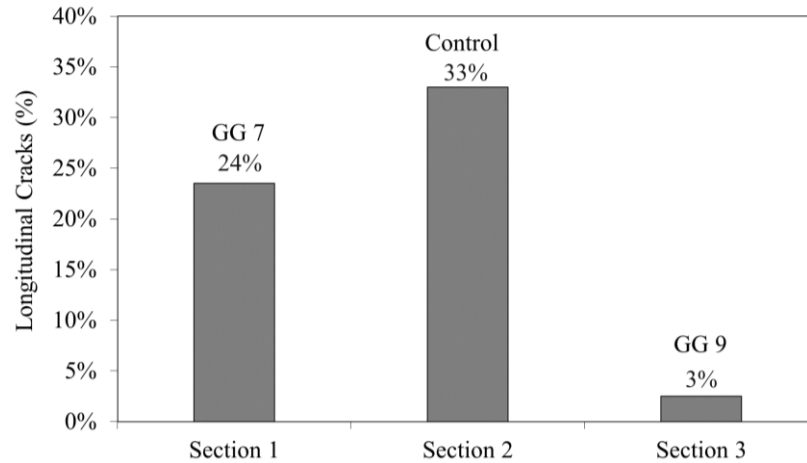


Figure 4.45 Percentage of environmental longitudinal cracks at SH21 test sections



Figure 4.46 Example pictures of longitudinal cracks in control section at Cabeza Rd.

Five transverse sections were also marked along Cabeza Rd. test sections and their vertical movements were monitored using total station. Figure 4.47 presents an example of vertical movements observed in Transverse Section 5 located within test Section 3 (GG 9). Consistent with the explained mechanism for differential vertical movement of the roads founded on expansive clay subgrades, the data presented in this figure indicates upward movement of both edges of the road relative to the center between the two total station reading conducted in 2015 and 2016. It can be anticipated that the road had experienced a comparatively wet period



between the two visits, which led to the swelling of the subgrades on the edges of the road. However, the presence of triangular geogrid GG 9 could mitigate development of environmental longitudinal crack on the road.

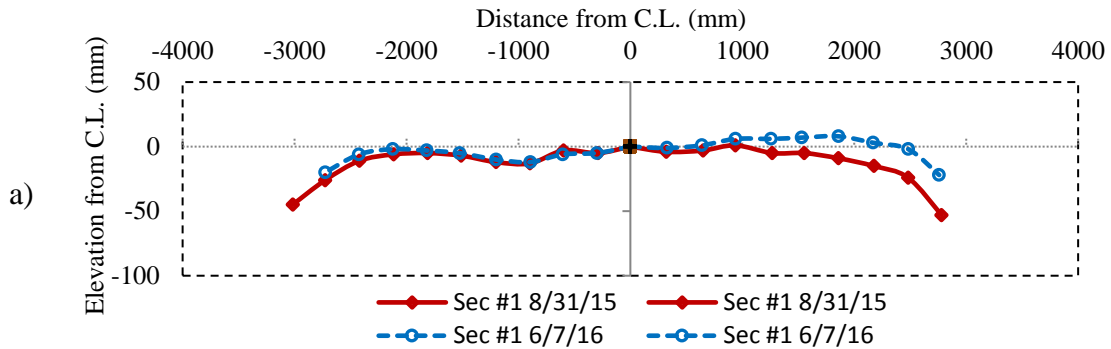


Figure 4.47 Transverse Section 5 at Cabeza Rd. located within test Section 3: a) variation of the elevation from 2015 to 2016 from data recorded using total station; b) picture of the transverse section

### 4.3.10. Site 9: Farm-to-Market Road 972 (FM 972)

#### 4.3.10.1. Project Description

FM 972 is a two-lane road in Williamson County near Georgetown, TX. It is within TxDOT’s Austin District and became an area of interest in February 2015 based on the existing pavement conditions, low traffic volume, and potentially expansive subgrade. The test sections are located approximately 0.25 miles west of SH 95. This area was found to have longitudinal cracking close to the outer wheel path without any other major form of distress.

Soil samples were collected from subgrade soil in FM 972 and their plasticity properties were characterized. The liquid limit of the samples was found to range from 70 to 77, the plastic limit was found to vary from 24 to 27, and, thus, the plasticity index (PI) was found to vary from 43 to 53. The subgrade soil in FM 972

is classified as high to very high expansive soil. In-situ moisture content of collected soil samples was also found to vary from 36 to 39, which indicates that the subgrade soil was in relatively wet condition.

#### 4.3.10.2. Test Section Design

A total of seven transverse sections were marked on the road to be monitored using total station. The first marked transverse section (Transverse Section 1) is located on the east side, closer to SH 95, and the last transverse section (Transverse Section 7) is located on the west end approximately 1,200 ft from Transverse Section 1 (Figure 4.48). Each section was marked by a painted white stripe with orange circles extending every foot from the centerline to the shoulders. Table 4.7 summarizes characteristics of the transverse sections at FM 972. Four of the transverse sections, including Sections #2, #3, #5, and #6, were selected on areas that were in poor condition with severe longitudinal cracking or faults. The other three transverse sections were selected on areas that were in good condition.

The transverse sections were chosen based on the presence of longitudinal cracking and each of them have a control section nearby for comparison purposes. Sections 1, 4, and 7 were chosen as the control and Sections 2, 3, 5, and 6 were selected on existing longitudinal cracks.

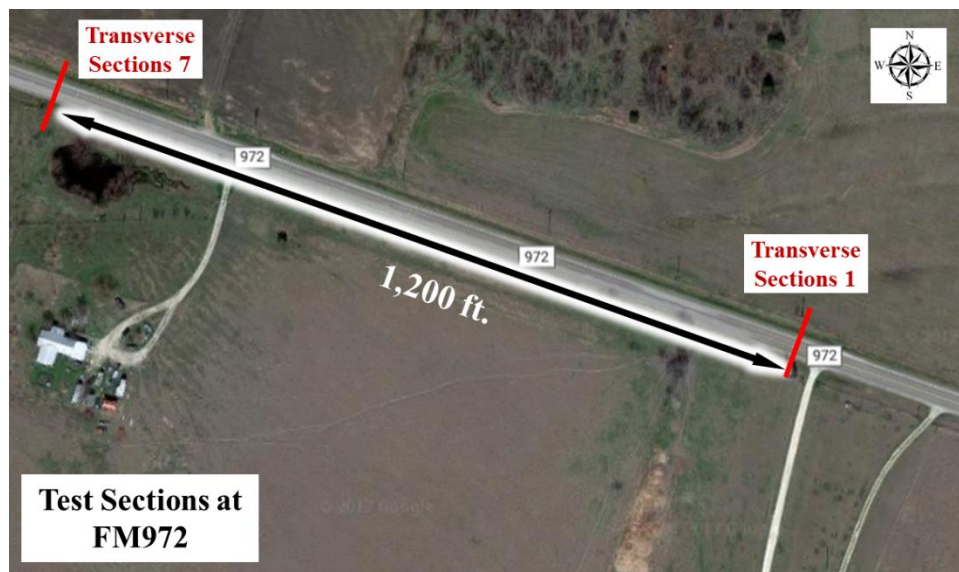


Figure 4.48 Layout of test sections at FM 972

#### 4.3.10.3. Performance Result

Road condition at the FM972 site was surveyed over a period of 134 days in 2015. Total station surveys were also conducted. Results are illustrated in Figure 4.49 and Table 4.7. The profiles illustrated on the right side of the centerline represent the eastbound of the road and the profiles on the left represent the westbound.

Evaluation of the data presented in Figure 4.49 indicates different vertical movements in transverse sections with observed good condition as compared to sections with poor condition. The transverse profiles of the east and west bounds were found to be essentially unchanged in sections with observed good conditions (Sections #1, #4, and #7). However, in all sections with observed poor performance (i.e., Sections #2, #3, #5, and #6) significant vertical deflections have been recorded. The vertical movements were found to be positive, i.e., in upward direction, and to be more significant in the edges of the pavement. This is consistent with the mechanism explained for vertical movement of the roads founded on expansive clay subgrades. According to this mechanism, edges of pavements founded on expansive subgrades tend to heave during wet season, when the subgrade soil expands in the shoulder area, and to settle during dry season, when the subgrade soil tend to shrink. This cycle of upward and downward vertical movements in the edges leads to the development of longitudinal cracks in pavements, particularly close to the edges. As illustrated in Figure 4.49, poor condition of Sections #2, #3, #5, and #6 are attributed to the cracks observed on the edges of the eastbound of the road (i.e., the right lane on the profiles), whereas the westbound lanes are found to be in good condition. Vertical deflections were also found to be significant only in the edge of the eastbound lanes. It can be envisioned that cycles of heave and settlement that have been repeated over time have been the main reason for development of the observed cracks. Maximum upward movements between first and last surveys were found to be 18, 16, 9, and 20 mm, respectively for Transverse Sections #2, #3, #5, and #6.

The differential vertical movements of the test sections were evaluated with the initial transverse slopes and changes in the slopes summarized in Table 4.7. Although the initial transverse slopes were different among the marked sections, all westbound sections exhibited almost zero change in the slope. This is consistent with the good conditions have been observed in the westbound sections. The slope of the eastbound sections, however, has changed in the sections with the observed poor condition. The changes were found to be negative indicating reduction in the slope magnitude.

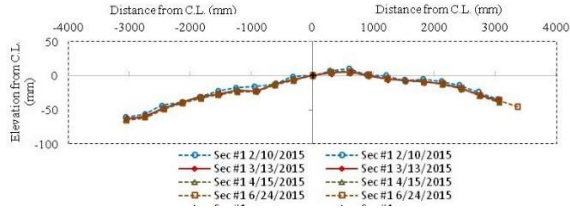
**Table 4.7. Summary of monitoring program and results for transverse test sections in FM 972—Segment II**

Transverse Section No.	Distance to Next Section (ft)	Observed Performance*	Surveys Period (days)	Transverse Profile Characteristics			
				Left Lane** (West Bound)		Right Lane** (East Bound)	
				Initial Slope	Change in Slope	Initial Slope	Change in Slope
Section 1	200	Well	134	2%	~ 0%	1.6%	~ 0%
Section 2	440	Poor	134	0.3%	~ 0%	1.5%	-0.5%
Section 3	70	Poor	134	1.5%	~ 0%	1.4%	-0.3%
Section 4	250	Well	134	1.7%	~ 0%	0.6%	~ 0%
Section 5	170	Poor	134	1.1%	~ 0%	1.3%	~ 0%
Section 6	90	Poor	134	1.2%	~ 0%	un-cracked portion 2.1%	un-cracked portion -0.3
Section 7	--	Well	134	0.1%	~ 0%	un-cracked portion 1.1%	un-cracked portion ~ 0%

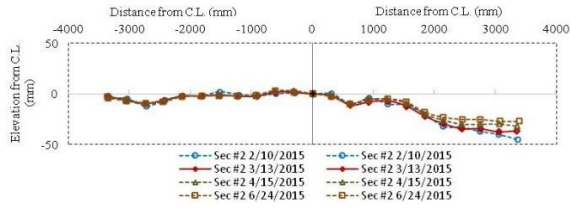
\* Observed Performance: Good = zero or very minor cracks; Fair = slightly cracked; Poor = severely cracked.

\*\* Left and Right lanes are referred to sides as depicted in the transverse profile sketches

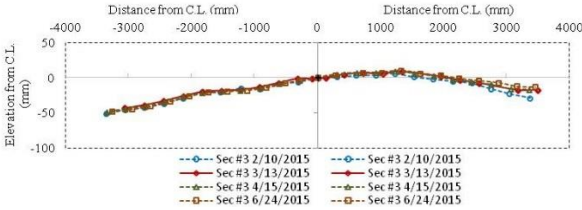
Section 1



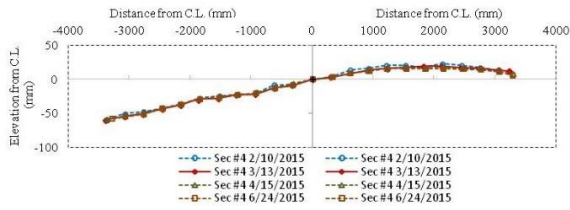
Section 2



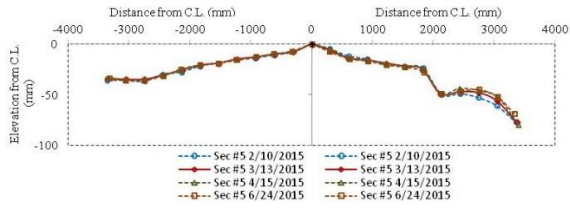
Section 3



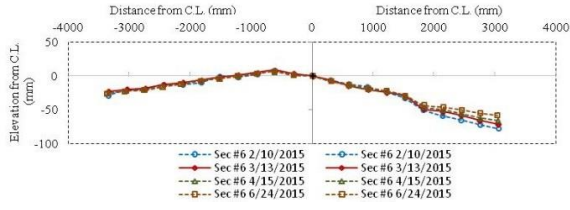
Section 4



Section 5



Section 6



Section 7

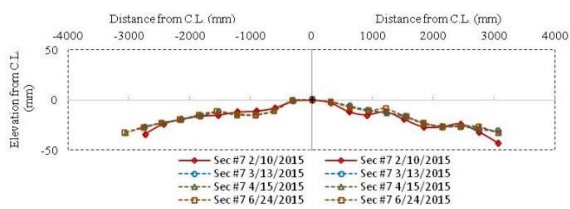


Figure 4.49 Results of total station surveys and road conditions at FM 972

### 4.3.11. Site 10: Turnersville Road

#### 4.3.11.1. Project Description

Turnersville Road is a two-lane road in Travis County about 17 miles south of downtown Austin. It extends from IH 35 on the west side to Williamson Road on the east. The area of interest along this road is located about 2.5 miles from IH 35 and extends about 1.1 miles to the east. The site became of interest due to its poor pavement condition, expansive subgrade, and low traffic volume. The road is primarily used by lightweight vehicles.

Atterberg limit tests conducted on soil samples collected from Turnersville Road subgrade resulted in the liquid limit, the plastic limit, and the plasticity index (PI) of 57, 20, and 37, respectively. Therefore, similar to subgrade soil at FM 972, the subgrade soil at Turnersville Road was classified as high to very high expansive soil.

#### 4.3.11.2. Test Section Design

Seven transverse sections were marked along Turnersville Road (Figure 4.50). Transverse Section 1 is located on the east end of the site and Transverse Section 7 is located approximately 0.3 miles away on the west end of the site. The sections were chosen based on pavement performance and visibility of traffic. The transverse sections were selected from areas with good, fair, or poor performance. Sections #3, #5, and #6 have exhibited severe cracks and faulting, whereas Sections #2, #4, and #7 were found to be slightly cracked. Section #1 was been observed to be in good condition.



Figure 4.50 Layout of test sections at Turnersville Road

### 4.3.11.3. Performance Result

Turnersville Road condition was surveyed over a period of 134 days in 2015. Total station surveys were also conducted. Results are illustrated in Figure 4.51 and Table 4.8. The profiles illustrated on the right side of the centerline represent the eastbound of the road and the profiles on the left represent the westbound.

Vertical movement of the road surface was found to be different among the seven transverse sections. Similar to the sections in good condition at FM 972, it was found that Section #1 in Turnersville Road has exhibited very limited vertical deflection. As illustrated in Figure 4.51, minor change was observed in the elevation of the painted points in Section #1. The slope of both right and left lanes did not change significantly in this section (Table 4.8). Transverse slopes in Section #2 were also found to remain essentially unchanged.

Sections #3, #4, and #5 exhibited significant decrease in their right lane elevations. The significantly wide crack on the road surface in Section 3 indicates that the settlement observed in this section may be attributed to shear failure of the shoulder. However, changes in the elevation of the road in Sections 4 and 5 can be attributed to the shrinkage of the expansive clay subgrade. The maximum settlement was found to be at the edges of the pavement, which is consistent with the described mechanism for pavements constructed on expansive clay subgrades. The maximum settlements were measured as 55, 49, and 28 mm in Sections #3, #4, and #5, respectively. As presented in Table 4.8, as a result of the settlements, significant increase was observed in the right lane transverse slopes. The increase was found to be as large as +2 and +1.7% for Sections #3 and #4, respectively. It should be noted that the wide crack on the right lane of Section #3 could potentially provide a faster and easier access to water for pavement base and subbase layers as well as for the expansive subgrade. This could result slope stability issues as well as exacerbating impact from expansive clay subgrade.

In contrast with the settlements observed in other sections, left lanes in Sections 6 and 7 exhibited upward vertical movement, which indicates swelling of the expansive clay subgrades in this area (Figure 4.51). Maximum vertical movement was recorded as +18 and +30 mm in Sections 6 and 7, respectively, which has led to reduction of -0.5 and -1% in the slope of the left lanes. However, the right lanes of Sections 6 and 7 exhibited zero or negative change in the elevation, which is consistent with the shrinkage observed in the other sections. The expansion of the subgrade soil observed in the left lanes of Sections 6 and 7 may be attributed to the geographical features in this area. As seen in Figure 4.51, left side of the road in Sections 6 and 7 is bound by residential areas. A natural pond for accumulation of rain water or other runoffs has been created in this area. The impact of this natural pond can clearly be seen in the difference in the vegetation of the right side of the road as compared to the left side. Accumulation of water in the pond could

potentially provide additional access to water for the adjacent subgrade soil, which has led to the observed swelling.



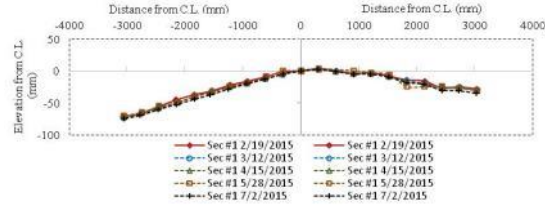
**Table 4.8. Summary of monitoring program and results for transverse test sections in Turnersville Road**

Transverse Section No.	Distance to Next Section (ft)	Observed Performance*	Surveys Period (Days)	Transverse Profile Characteristics			
				Left Lane** (West Bound)		Right Lane** (East Bound)	
				Initial Slope	Change in Slope	Initial Slope	Change in Slope
Section 1	70	Good	134	2.4%	~ 0%	1.2%	+0.2%
Section 2	190	Fair	134	5.6%	-0.4%	1.7%	-0.2%
Section 3	650	Poor	134	3.6%	-0.1%	0.2%	+2% un-cracked portion
Section 4	170	Fair	134	3.2%	+0.3%	1.2%	+1.7%
Section 5	430	Poor	134	2.9%	+0.2%	3.8%	+0.7%
Section 6	100	Poor	134	-1.6%	-0.5%	1.2%	+0.2%
Section 7	--	Fair	134	-0.9%	-1%	1.2%	~ 0%

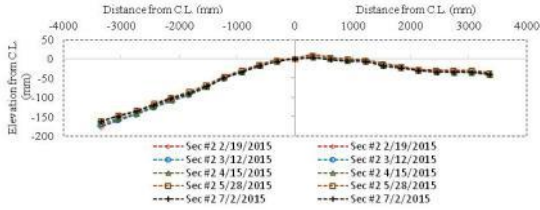
\* Observed Performance: Good = zero or very minor cracks; Fair = slightly cracked; Poor = severely cracked.

\*\* Left and Right lanes are referred to sides as depicted in the transverse profile sketches.

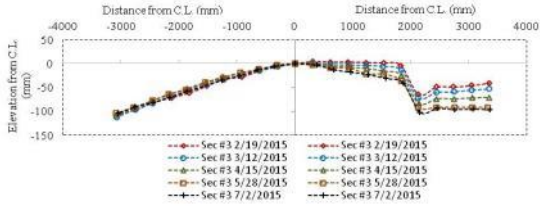
Section 1



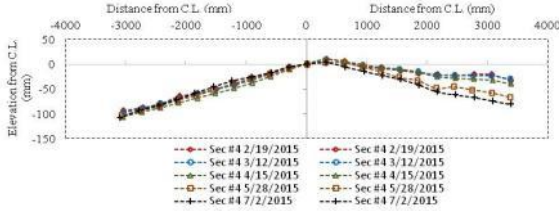
Section 2



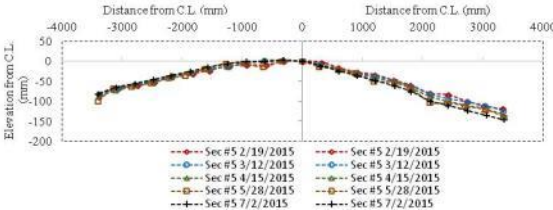
Section 3



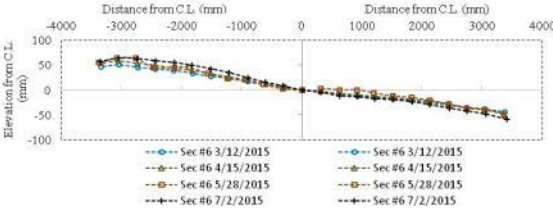
Section 4



Section 5



Section 6



Section 7

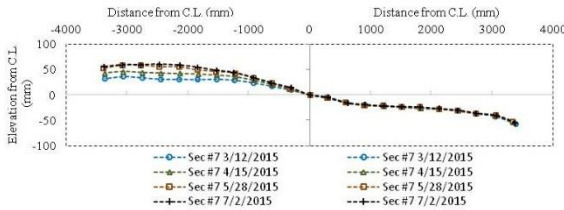


Figure 4.51 Results of total station surveys and road conditions in Turnersville Road

An additional condition survey was conducted in 2017 to evaluate performance of the test sections at Turnersville Road. Results of this condition survey are presented

in Figure 4.52. All test sections were found to be severely cracked. The lowest percentage of longitudinal cracks was found to be 70% and the average percentage of longitudinal cracks was found to exceed 100%. Comparison of these numbers with the percentage of longitudinal cracks in similar sections that were stabilized with geosynthetics (e.g., FM 2924, FM 1979) underscores the significance of using geosynthetic stabilization. Example pictures from cracks observed at Turnersville Road test sections are presented in Figure 4.53.

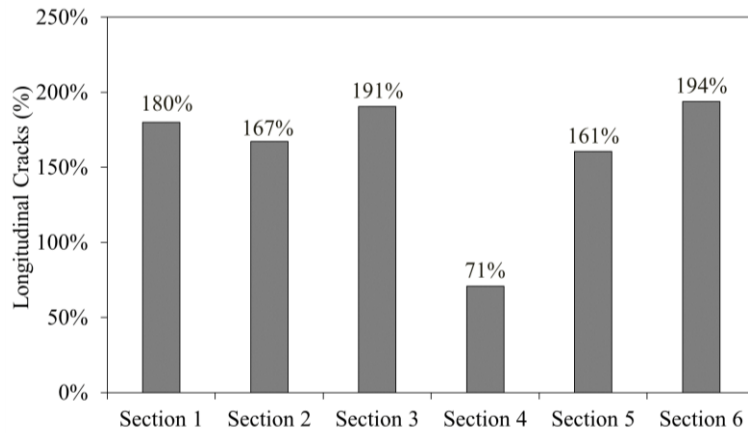


Figure 4.52 Percentage of environmental longitudinal cracks at Turnersville Road test sections



Figure 4.53 Example pictures of longitudinal cracks observed at Turnersville Road test sections in 2017

## 4.4. Summary and Conclusions

---

Field performance of over 80 test sections located at 10 sites founded on expansive clay subgrades were evaluated. Performance data was collected through three sources, including 1) visual condition survey of the road surface, 2) total station survey of the road transverse section, and 3) TxDOT PMIS Database. Overall, it was found that geosynthetic stabilization significantly improved field performance of the test sections under environmental loads result from expansive clay subgrades. The percentage of longitudinal cracks was found to be significantly lower in test sections stabilized using geosynthetics as compared to control (non-stabilized) sections.

Potential benefits from geosynthetic in mitigation of damages results from environmental loads were observed for both biaxial geogrids and triangular geogrids. A comparatively good performance was also observed in the only test section stabilized with a woven geotextile. For the specific geogrid products used in the evaluated test sections in this project, field performance of the sections stabilized using triangular geogrids were comparatively better than those stabilized using biaxial geogrids. Furthermore, the triangular geogrids with comparatively higher rib depths were found to enhance the road performance more than other triangular geogrids.

One of the geosynthetic-stabilized sections was found to show particularly poor performance. This section was stabilized using a laser-bonded biaxial geogrid with comparatively high ultimate tensile strength and tensile modulus.

Enhancement in the field performance results from geosynthetics was found not to be directly correlated with the geosynthetic properties characterized in-isolation (i.e., without involvement of soil). Specifically, the unconfined tensile modulus of geosynthetics or ultimate tensile strength was found not to be correlated with the field performance of geosynthetic-stabilized roads.

The results obtained from total station surveys of the transverse sections of roads founded on expansive clay subgrades showed swelling and shrinkage in the subgrade soil are reflected at the road surface in terms of settlement and heave. Consistent with the expectations hypothesized for this movement, it was found that the vertical movements are comparatively higher at the edges of the roads relative to the center.

The differential vertical movements result from successive swelling and shrinkage of the edges of the roads was found to occur in both roadways constructed with and without geosynthetic layer. However, while the presence of the geosynthetic layer can mitigate initiation and propagation of longitudinal cracks resulting from the differential movements (e.g., FM 2924, FM 1979, Cabeza Rd.—geosynthetic-

stabilized sections), the absence of a geosynthetic layer results in the development of severe longitudinal cracks (e.g., Turnersville Rd., FM 972, Cabeza Rd.—control section).

# **Chapter 5. Specifications for Selection of Geosynthetic for Base Stabilization of Roadways Subjected to Environmental Loads**

## **5.1. Introduction**

---

This chapter reports on the activities conducted to refine TxDOT specifications for selection of geosynthetics for geosynthetic-stabilized pavements. The existing TxDOT departmental material specifications relevant to the selection of geosynthetics for base stabilizations were first evaluated. Then, a complementary experimental program was conducted using the final testing configurations identified in the Chapter 3. Specifically, 15 geosynthetics were evaluated and their ranking based on the  $K_{SGC}$  values was determined. Findings from field monitoring program were then reassessed to obtain evidences for field performance of the sections stabilized using the geosynthetics tested. By comparing the field performance and experimental data, a threshold  $K_{SGC}$  value was established. Geosynthetic products with a  $K_{SGC}$  value above the threshold are expected to show a satisfactory field performance in geosynthetic-stabilized roadways subjected to environmental loads. Finally, recommendations were made to TxDOT to refine its specification for selection of geosynthetics for base stabilization.

## **5.2. Review of the Existing Specifications**

---

Existing TxDOT Departmental Material Specifications relevant to the selection of geosynthetics for base stabilizations include TxDOT DMS-6240 (Geogrid for Base/Embankment Reinforcement) and TxDOT DMS-6270 (Biaxial Geogrid for Environmental Cracking). As identified in the title of both specifications, their objective is to specify only geogrids. Although geotextiles have also been widely used for base stabilization, TxDOT specifications that specify geotextiles were not found.

On the other hand, although geosynthetic stabilization has predominantly used by TxDOT to mitigate damages caused by environmental loads (mostly environmental longitudinal cracks), the specifications that are often referred to for selection of geosynthetics involves DMS-6240, which appears to be originally developed for “base/embankment reinforcement” not “environmental cracking.”

TxDOT DMS-6240 and DMS-6270 summarize the main requirements that shall be used to specify geogrids in their “Table 1: Geogrid Requirements.” These tables are presented in Table 5.1 and 5.2 in this report. TxDOT DMS-6240 specifies two grades of geogrids, Types 1 and 2, for different load levels. However, load levels and expected benefits from each geogrid grade have not been specified in the

specification. TxDOT DMS-6270 specifies a single geogrid grade. The requirements specified by TxDOT DMS-6270 are intended to provide a basis for a geogrid that can “intercept cracks and prevent the transmission of cracking to other pavement layers above the grid.” However, as previously explained in this report, the actual mechanism involved in the benefits results from geosynthetics may completely be different from that indicated by TxDOT DMS-6270.

Evaluation of the requirements by TxDOT specifications listed in Tables 5.1 and 5.2, indicates that all geosynthetic properties that are currently listed by these specifications are determined in-isolation (i.e., without involvement of surrounding backfill materials). For example, as presented in Table 5.1, requirements by TxDOT DMS-6240 include index geometrical properties of aperture size, percent open area, aperture shape, number of nodes, and rib thicknesses as well as unconfined index properties of tensile modulus and junction efficiency. However, these properties are not adequate for specification of soil-geosynthetic interaction in stabilized base courses. The actual performance of geosynthetic-stabilized systems shall be determined by accounting for the interaction between geosynthetic and surrounding soil.

**Table 5.1 Geogrid requirements in accordance with TxDOT DMS-6240**

Property	Type 1	Type 2	
Aperture Size, mm (in.)	25–51 (1.0–2.0)	25–51 (1.0–2.0)	
Percent Open Area, %	70 Min	70 Min	
Thickness, mm (in.)			
MD ribs	0.77 (0.03) Min	1.27 (0.05) Min	
CMD ribs	0.64 (0.025) Min	1.15 (0.045) Min	
Junctions	1.50 (0.06) Min	2.54 (0.10) Min	
Junction Efficiency, % of rib ultimate tensile strength			
MD & CMD	90 Min	90 Min	
Aperture Shape	Square or Rectangular	Square or Rectangular	Equilateral Triangular
Ribs per Node	4	4	6
Tensile Modulus @ 2% elongation <sup>1</sup> , N/m (lb./ft.)			
MD & CMD	204,260 (14,000) Min	291,000 (20,000) Min	175,080 (12,000) Min

1. Determined as a secant modulus without offset allowances.

Note—MD and CMD do not necessarily refer to the machine (warp) and cross machine (fill) directions in the manufacturing process. They refer, for drawn products, to the more (CMD) or less (MD) highly drawn ribs where the aperture dimensions are unequal.

**Table 5.2 Geogrid requirements in accordance with TxDOT DMS-6270**

Property	Test Method	Requirements
<b>Ultimate Tensile Strength (lb./ft.)</b> MD <sup>2</sup> and CMD <sup>2</sup>	Tex-621-J	850 minimum
<b>Tensile Strength at 2% strain (lb./ft.)</b> MD and CMD	Tex-621-J	270 minimum
<b>Junction Strength (lb./junction)</b> MD and CMD	Tex-621-J	20 minimum
<b>Aperture Size (in.)</b> Range in either MD or CMD	Tex-621-J	0.5–2.0
<b>Percent Open Area</b>	Tex-621-J	60% minimum
<b>Resistance to Installation Damage</b> a. Ribs b. Junctions c. Retained tensile strength ratio	Tex -629-J	≤ 2 ruptured ≤ 2 displaced or ruptured 75%

1. Machine direction (MD) and cross-machine direction (CMD) refers to the warp (machine) and fill (cross machine) directions in the manufacturing process.
2. Determined as a secant modulus without offset allowance.

### 5.3. Experimental Program to Produce Soil-geosynthetic Interaction Data

A complementary soil-geosynthetic interaction testing program was conducted to produce specific data required for establishment of threshold for selection of geosynthetics for base stabilization. This program is discussed in this section.

#### 5.3.1. Geosynthetic Products

Fifteen geosynthetics were selected to produce data to support TxDOT design of geosynthetic-stabilized roadways. These geosynthetics were selected from among those products that have been used in the experimental test sections so that evidence regarding their field performance would also be available. This allowed the results of the testing program to be related to the findings obtained in the evaluation of the field performance of the test sections.

Characteristics of the selected geosynthetics as compared to the material requirements of TxDOT DMS-6240 are listed in Table 5.3. The selected geosynthetics included three woven geotextiles, eight biaxial geogrids (including three integrally formed and five woven or laser bonded geogrids), and four triangular geogrids. All products have expectedly been designed by manufacturers to be used in roadway stabilization applications to fulfill stiffening/reinforcement functions. Therefore, it can be expected that they all can be classified in a reasonably narrow range of physical and mechanical properties. Geotextiles may



also be used to fulfill additional functions such as separation, filtration, and drainage.

The geosynthetics were selected from among seven manufacturers. Similar to the baseline geosynthetics, these products were selected from both polymer types of polypropylene and polyester. Furthermore, they have been made by a wide range of manufacturing processes including extrusion, weaving, and welding.

The last column of the table indicates whether evidence is available of the field performance of test sections in which each geosynthetic was used. As many of these products have not widely been used in roadway construction projects in Texas, the field performance of road sections stabilized with them remains to be unexplored. However, the results of this soil-geosynthetic interaction program can be an indication of their expected field performance.

As a representative of a particularly weak material, specimens from Mylar sheets that have been used on the inner sides of the box were also tested as the sixteenth product (Figure 5.1). The Mylar sheets were used to minimize the friction between soil and the inner sides of the box, thus, they are expected to have very weak interaction with soil. Consequently, the  $K_{SGC}$  value obtained in the interaction test conducted using Mylar sheets can be assumed as an index for a possible low value for  $K_{SGC}$ .

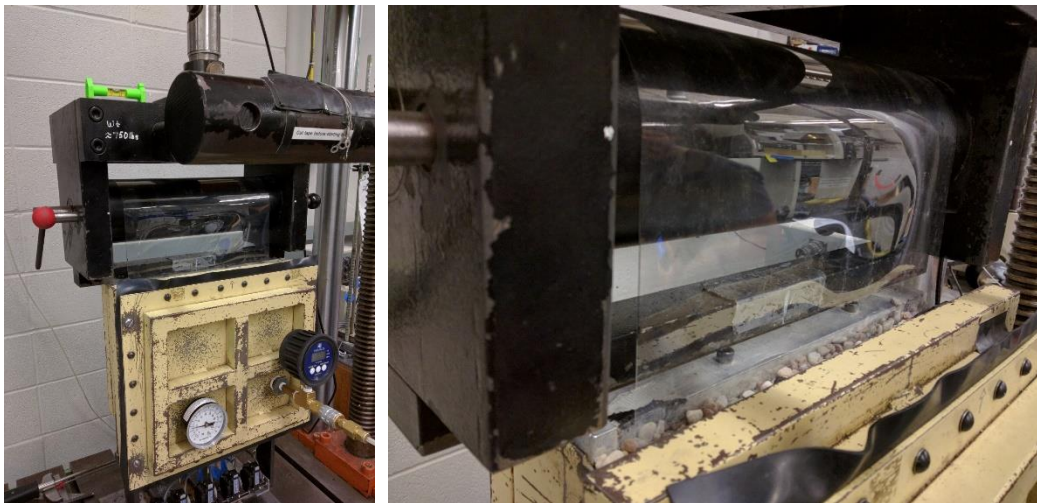


*Figure 5.1 Interaction test conducted using Mylar sheets as an index for a product with particularly weak interaction properties*

**Table 5.3: Characterization of the selected geosynthetic reinforcements in accordance with the requirements of DMS-6240**

DMS-6240 Material Requirements for Type 1 Geogrid									
Geosynthetics	Aperture Size in., (mm)	Percent Open Area, %	Thickness of Ribs, in. (mm)			Tensile Modulus @2% elongation, kips/ft (kN/m)		Junction Efficiency, % of rib ultimate tensile strength	Availability of Field Performance
			MD Ribs	CMD Ribs	Junctions	MD	CMD		
	1.0-2.0 (25-51)	> 70%	0.03 (0.77)	0.025 (0.64)	0.06 (1.50)	>14 (205)	>14 (205)	> 90%	
GG 1	1.0x1.3 (25x33)	75%	0.03 (0.76)	0.03 (0.76)	0.06 (1.50)	14 (205)	22.5 (330)	93%	✓
GG 2	1.6x1.6x1.6 (40x40x40)	>70%	0.07 (1.8) In diagonal	0.06 (1.5) In transverse	0.13 (3.4)	20.5 (300) (Radial stiffness @ 0.5% strain)	93%	--	
GG 3	1.0x1.0 (25x25)	>70%	> 0.03 (0.77)	> 0.03 (0.77)	> 0.06 (1.5)	26.3 (385)	28.9 (422)	100% in CD 201% in MD	--
GG 4	1.73x1.73 (44x44)	75%	> 0.03 (0.77)	> 0.03 (0.77)	> 0.06 (1.5)	20.5 (300)	68.5 (500)	35%	✓
GG 5	1.0x1.0 (25x25)	>70%				25 (365)	25 (365)	93%	✓
GG 6	0.6x0.6 (15x15)	>70%				17 (250)	24 (350)		✓
GG 7	1.3x1.3x1.3 (33x33x33)	>70%	0.06 (1.5) In diagonal	0.05 (1.2) In transverse	0.12 (3.1)	15.1 (200) (Radial stiffness @ 0.5% strain)	93%	✓	
GG 9	1.6x1.6x1.6 (40x40x40)	>70%	0.05 (1.3) In diagonal	0.05 (1.2) In transverse	0.13 (3.4)			93%	✓

DMS-6240 Material Requirements for Type 1 Geogrid									
Geosynthetics	Aperture Size in., (mm)	Percent Open Area, %	Thickness of Ribs, in. (mm)			Tensile Modulus @2% elongation, kips/ft (kN/m)		Junction Efficiency, % of rib ultimate tensile strength	Availability of Field Performance
			MD Ribs	CMD Ribs	Junctions	MD	CMD		
	1.0-2.0 (25-51)	> 70%	0.03 (0.77)	0.025 (0.64)	0.06 (1.50)	>14 (205)	>14 (205)	> 90%	
GG 10	1.6x1.6x1.6 (40x40x40)	>70%	0.08 (2.0) In diagonal	0.06 (1.6) In transverse	0.15 (3.8)			93%	✓
GG 11	1.0x1.3 (25x33)	75%	0.05 (1.27)	0.05 (1.27)	0.1 (2.54)	20.5 (300)	30.7 (450)	93%	--
GG 12	1.26x1.26 (32x32)	>70%				41 (600)	41 (600)		--
GG 13	1.65x1.96 (42x50)	>70%	0.05 (1.27)	0.05 (1.27)		7.5 (110)	11.25 (165)	93%	--
GT 1	--	--	--	--	--	24 (350)	90 (1313)	--	--
GT 2	--	--	--	--	--	48 (700)	66 (965)	--	✓
GT 3	--	--	--	--	--	27 (395)	90 (1313)	--	--

GG 1 =Tensar Biaxial Geogrid BX1100; GG 2 = Tensar Triaxial Geogrid TX160; GG 3 = Synteen SF11; GG 4 = Colbond Enkagrid Max20; GG 5 = Tencare Mirafi BasXgrid 11; GG 6 = Huesker Fornit 20; GG 7 = Tensar Triaxial Geogrid TX130s; GG 9 = Tensar Triaxial Geogrid TX5; GG 10 = Tensar Triaxial Geogrid TX7; GG 11 = Tensar Biaxial Geogrid BX1200; GG 12 = Naue Secugrid 30/30; GG 13 = Tenax MS110; GT 1 = Tencate Mirafi RS580i; GT 2 = Tencate Geolon HP570; GT 3 = Tencate Mirafi H2Ri.

### 5.3.2. Test Configurations

The test configurations used in this complementary testing program was that selected following completion of the comprehensive testing matrix for the baseline geosynthetics reported in Chapter 3. Specifically, as summarized in Table 5.4, the final testing matrix involved testing geosynthetics in *cross-machine direction* under a *normal stress of 3 psi* using *AASHTO No. 8-Truncated backfill material*. All tests were conducted using the refinements made in the testing procedure and data analysis as detailed in Chapter 2. A minimum of six repeat tests were conducted for each geosynthetic. Additional repeat tests were also conducted as needed following evaluation of the test results obtained for each geosynthetic.

**Table 5.4: Final testing matrix for the additional ten geosynthetics**

Soil Type	Confining Pressure (psi)	Testing Direction	No. of Geosynthetics	Number of repeats	Total Number of Tests
AASHTO No.8-Truncated	3	CD	15 + 1 (Mylar sheet)	>5	>100

### 5.3.3. Sources of Uncertainty in the Test Results

Variation in the properties of the geosynthetic specimens was identified as one of the potential sources for scatter in the test results. Specifically, the variation was observed in physical properties of the specimens (including aperture shape and sizes, and rib width and thickness) as well as their mechanical properties. While the source of such variations may be limitations in controlling characteristics of the final products in the manufacturing process, specific efforts were made to minimize the effect of such variations on the soil-geosynthetic interaction test results. These efforts are summarized in the following subsections.

#### 5.3.3.1. Documentation of Geosynthetic Lot and Roll Numbers

The manufacturer lot and roll numbers of the geosynthetic rolls received at the University of Texas laboratory for testing were carefully documented. Accordingly, the lot and roll numbers correspond to the specimen used in every test was also documented. This documentation was found necessary as part of the scatter observed among the results of repeat tests conducted using the same geosynthetic product was due to the variation of the specimens cut from different geosynthetic rolls.

### **5.3.3.2. Inspection of Geosynthetic Rolls**

Every geosynthetic roll was also carefully inspected before cutting the specimens. Specimens were cut from sections of geosynthetic rolls that are homogeneously manufactured.

### **5.3.3.3. Template Specimens**

In order to further minimize uncertainties arise from variations within a geosynthetic roll, template specimens were cut from homogeneous sections of all rolls. Geosynthetic specimen used in each test was then matched with the template specimen and was discarded if they did not match. When necessary, the thickness of the ribs of the testing specimens was also measured and compared to the template specimens.

Locations of tell-tale attachments were also marked on the template specimens. The markings allowed all operators to attach tell-tales to the same locations and minimized scatter in the results that may arise from measuring displacements at different locations.

### **5.3.3.4. Additional Characterization of Testing Specimens**

In cases that the properties of the geosynthetic specimens were found to deviate from the specifications provided by the manufacturers, additional characterizations were conducted to determine specifications of the specific specimens tested. In particular, tensile properties in the unconfined portions of the specimens were characterized in such specimens. Furthermore, when available, the manufacturer quality control report for the specific geosynthetic lot was also requested and the property values reported by the manufacturer were compared to those obtained in the characterization program.

## **5.3.4. Data Reduction Protocol**

As an additional effort to identify outliers and improve the quality of the produced data, a protocol was used to reduce the data. The protocol involved two procedure as follows: selection of  $K_{SGC}$  in a single test and trimming outliers among repeat tests.

### **5.3.4.1. Selection of $K_{SGC}$ in a Single Test**

As previously discussed, a total of five telltales (Telltales 1 to 5) were attached to the confined portion of each geosynthetic specimen to measure displacement. However, to minimize potential effect on the results of the boundary conditions, the data recorded at the telltales closest to the front and the back of the specimens

(Telltale 1 and 5) were not used to estimate  $K_{SGC}$ . The data recorded by these two telltales were used only for quality control of the tests.

Three  $K_{SGC}$  values (i.e.,  $K_{SGC-2}$ ,  $K_{SGC-3}$ ,  $K_{SGC-4}$ ) were estimated using the data recorded at the location of the three middle telltales (Telltale 2, 3, and 4). Theoretically, the three values should be identical or reasonably close. However, in comparatively less-stiff products that cannot effectively develop soil-geosynthetic interaction along their entire length, the front portion of the geosynthetic may excessively elongate while the back portion does not displace. In such cases, an unusually high difference between the three  $K_{SGC}$  may be observed. To account for the weak interaction of such products, the following protocol was adopted in the data reduction process:

If the highest value among the three  $K_{SGC}$ s was larger than twice the lowest value, the lowest  $K_{SGC}$  value was used.

Otherwise,  $K_{SGC}$  was estimated at the center of the unconfined portion of the geosynthetic according to the procedure detailed in data analysis.

#### **5.3.4.2. Trimming Outliers among Repeat Tests**

A mild outlier elimination procedure was adopted to eliminate outliers among the multiple repeat tests conducted using the same test configurations. According to this procedure:

If more than 10 repeat tests were conducted, tests that their ultimate pullout load or  $K_{SGC}$  values were out of the “Average  $\pm$  1.5 $\times$ Standard Deviation” window were eliminated.

If between 5 and 10 repeat tests were conducted, a test was eliminated if its ultimate pullout load deviates more than 20% from the average or if its  $K_{SGC}$  value deviates more than 50% from the average.

### **5.4. Establishment of Threshold Value for $K_{SGC}$**

---

In this section, results from the complementary experimental program using the fifteen identified geosynthetics were evaluated along with the field performance of the test sections stabilized with each geosynthetic. Then limits of acceptable  $K_{SGC}$  values were established.

#### **5.4.1. Comparison of $K_{SGC}$ Values**

The  $K_{SGC}$  values obtained for the geogrid products are summarized in Figure 5.2. On the horizontal axis, geogrids are sorted from those with the highest  $K_{SGC}$  to those with the lowest  $K_{SGC}$ . The vertical axis represents the  $K_{SGC}$  values. Overall,

triangular geogrids showed comparatively larger  $K_{SGC}$  values than the biaxial geogrids. The highest  $K_{SGC}$  was found to be 32.7 for triangular geogrid GG 10, which has the largest rib thickness among the triangular geogrids. The triangular geogrids with the second and third largest rib thickness (i.e., GG 2 and GG 9) were found to have larger  $K_{SGC}$  value than the triangular geogrid with the lowest rib thickness (GG 7). The  $K_{SGC}$  values for these products

The  $K_{SGC}$  values for the biaxial geogrids were found to range from 17.2 for the integrally formed polypropylene geogrid GG 11 to 9.6 for two geogrids including GG 13 (an extruded polypropylene geogrid) and GG 4 (a laser-bonded polypropylene geogrid).

The plot presented in Figure 5.2 also shows the  $K_{SGC}$  value found for Mylar sheet as 4.7. This value is potentially one of the lowest possible values that can be obtained for the stiffness of soil-geosynthetic composite in this testing configuration. As the last item listed on the horizontal axis, the plot schematically shows  $K_{SGC} = 0$  for the case that no geosynthetic was used.

It should be noted that the  $K_{SGC}$  values presented herein were determined using the specimens obtained from the specific rolls that were received from the manufacturers. The presented  $K_{SGC}$  value shall not be considered as a suggestion for manufacturers' specifications or for design. The  $K_{SGC}$  value shall be determined based on the tests conducted on project-specific geosynthetic lots and rolls.

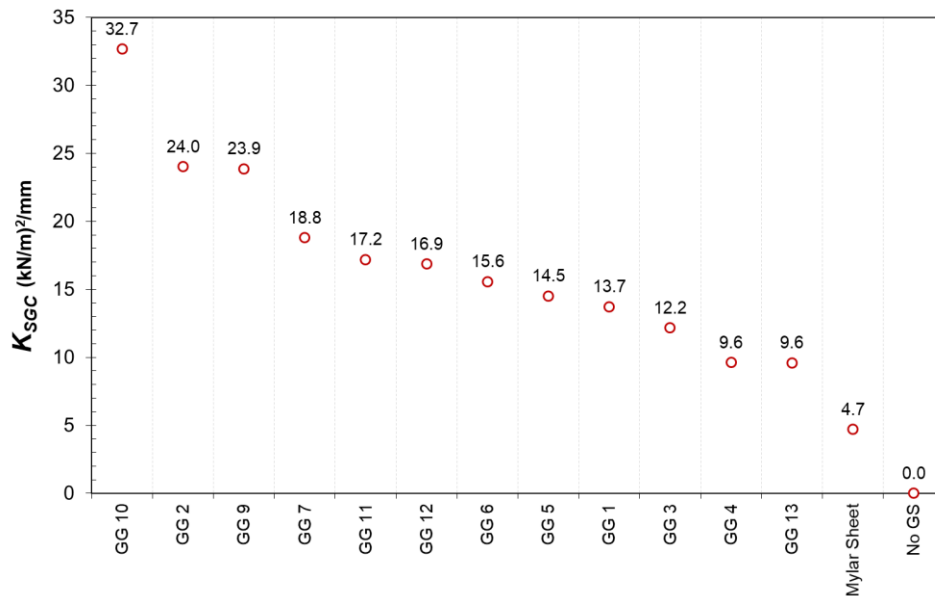


Figure 5.2 The  $K_{SGC}$  values obtained for the identified geosynthetics using test configurations recommended for TxDOT specifications

### 5.4.2. Qualitative Evaluation of Field Performance

As listed in Table 5.3, evidence of field performance was available for eight out of the fifteen geosynthetics tested in the soil-geosynthetic interaction testing program. These geosynthetics include: GG 1, GG 4, GG 7, GG 9, GG 10, GT 2, GG 5, and GG 6. Field performance of the test sections constructed using each of these eight geosynthetics was discussed in details in Chapter 4. In this section, the data presented in Chapter 4 was reassessed to establish qualitative ranking of the field performance among the eight products.

From evaluation of the field performance of the test sections constructed at SH 21, it can be concluded that field performance of GG 10 was considerably better than both GG 9 and GG 7. Furthermore, all triangular geogrids used in this road was found to perform better the biaxial geogrid GG 1. Therefore, comparative field performance of the geosynthetics used in SH 21 can be qualitatively sorted as below:

GG 10 (best performance) > GG 9 = GG 7 > GG 1

From evaluation of the field performance of the test sections constructed at Cabeza Road, it can be concluded that the field performance of GG 9 was better than both GG 7:

GG 9 (better performance) > GG 7

From evaluation of the field performance of the test sections constructed at FM 2, it can be concluded that GG 1, GG 5, and GT 2 equally performed well:

GG 1 = GG 5 = GT 2

From evaluation of the field performance of the test sections constructed at FM 1774, it can be concluded that GG 4 performed particularly poor as compared to GG 1:

GG 1 >> GG 4

Comparison of the field performance of the test section constructed at FM 1644 using GG 6 to the field performance of the test sections constructed at FM 2, indicates that GG 6 performed slightly better than the test sections at FM 2:

GG 6 > GG 1

In addition to the observed performance of the experimental test sections, geogrid GG 13 was also known to result in particularly poor performance in the field. Manufacturer of this product does not recommend that it is used as a single layer (as tested in this project). Instead, the manufacturer bundles two or more layers of



this product to be used for base stabilization. Therefore, geosynthetic GG 13 can also classify as a poorly performed product in the field.

### 5.4.3. Recommended Threshold Value for $K_{SGC}$

Comparisons made above between the field performance of the test sections constructed using each of the eight geosynthetics are summarized in Table 5.5 using a qualitative description of the field performances ranging from “Poor” to “Excellent.” The  $K_{SGC}$  values obtained for each geosynthetic is also listed in this table.

**Table 5.5 Qualitative field performance of geosynthetics as compared to their  $K_{SGC}$  value**

		Qualitative Field Performance							
	Excellent	Excellent	Very Good	Very Good	Good	Good	Good	Poor	Poor
Geosynthetic	GG 10	GG 9	GG 7	GG 6	GG 5	GT 2	GG 1	GG 4	GG 13
$K_{SGC}$	32.7	23.9	18.8	15.6	14.5	--	13.7	9.6	9.6

Evaluation of the data presented in Table 5.5 indicates a reasonable agreement between the  $K_{SGC}$  value of geosynthetics and qualitative performance observed from their performance in the field. As the  $K_{SGC}$  value for geosynthetic increases, the field performance of the section constructed with that geosynthetic also improves. Specifically, poor field performance was observed for geosynthetics that had a  $K_{SGC}$  value below 10.

This observation is consistent with the existing geogrid grades in TxDOT DMS-6240. GG 1, which is the baseline geogrid Type 1 according to TxDOT DMS-6240, was found to be the first geosynthetic classified above the threshold value of  $K_{SGC} > 10$ .

## 5.5. Refinement of TxDOT DMS-6240

In this section, findings from experimental program and field performance monitoring were used to provide recommendations for refinements of TxDOT DMS-6240. The recommendations provided in this section are only in the form of additions to the existing specifications based on the results directly obtained from activities conducted as part of this project. The authors have not provided comments or recommended corrections on other aspects of the specifications.

As presented next, two alternative refinement scenarios are recommended. First alternative involves maintaining two geogrid grades Types 1 and 2, and the second alternative involves adding a new geogrid grade (Type 3) to the specifications. The threshold  $K_{SGC}$  value for each geogrid grade is presented.

### 5.5.1. Alternative 1 – Two Geogrid Grades: Types 1 and 2

The information used to support this alternative is summarized in Figure 5.3. The  $K_{SGC}$  values of all geosynthetics are presented along with the qualitative field performance of the test section constructed using the geosynthetics. The threshold value of  $K_{SGC} > 10$  set the criterion for acceptance of a geogrid to be used for base stabilization. As comparatively better field performance was observed for geosynthetics that have  $K_{SGC}$  values above 15, it is recommended that the threshold value between geogrid grades 1 and 2 (Types 1 and 2) be set as 15. As illustrated in Figure 5.3, this specification is consistent with the baseline Types I and II geogrids according to the existing TxDOT specification.

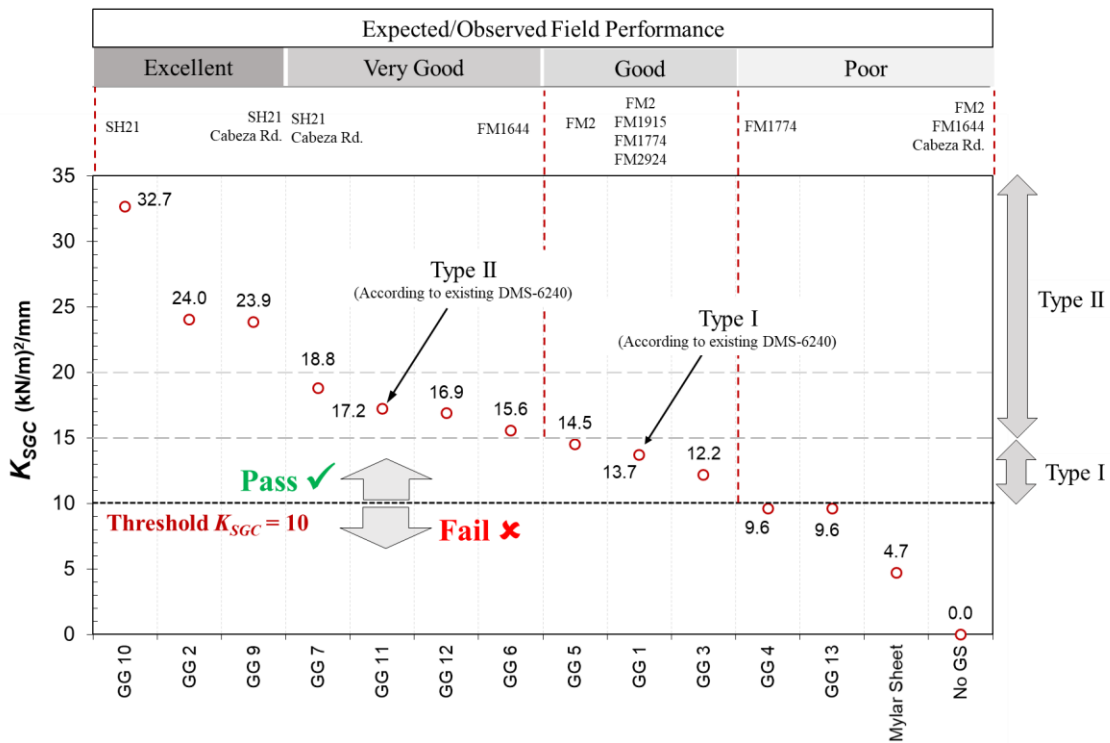


Figure 5.3 Alternative 1 - Adopting two geogrid grades in the refined TxDOT DMS-6240 specification

The refinements in the TxDOT DMS-6240 that are consistent with this alternative are presented in Figure 5.4. A revised version of the specifications consistent with this alternative was also submitted as a separate document (5-4829-03-P1-v.1).

**Table 1  
Geogrid Requirements**

Property	Test Method	Type 1	Type 2	
Aperture Size, mm (in.)	Tex-621-J	25–51 (1.0–2.0)	25–51 (1.0–2.0)	
Percent Open Area, %	Tex-621-J	70 Min	70 Min	
Thickness, mm (in.)				
MD ribs	Tex-621-J	0.77 (0.03) Min	1.27 (0.05) Min	
CMD ribs		0.64 (0.025) Min	1.15 (0.045) Min	
Junctions		1.50 (0.06) Min	2.54 (0.10) Min	
Junction Efficiency, % of rib ultimate tensile strength				
MD & CMD	Tex-621-J	90 Min	90 Min	
Stiffness of soil-geosynthetic composite ( $K_{SGC}$ ) <sup>2</sup> , (kN/m) <sup>2</sup> /mm				
CMD	Tex-1xx-E	10 Min	15 Min	
Aperture Shape	---	Square or Rectangular	Square or Rectangular	Equilateral Triangular
Ribs per Node	---	4	4	6
Tensile Modulus @ 2% elongation <sup>1</sup> , N/m (lb./ft.)				
MD & CMD	Tex-621-J	204,260 (14,000) Min	291,000 (20,000) Min	175,080 (12,000) Min

1. Determined as a secant modulus without offset allowances.
2. Determined using washed and dried aggregates with rounded particles that retain between ¼" (6.35 mm) sieve and Sieve No.4 (4.75 mm). A dry density of 102.5 pcf and a normal stress of 3 psi shall be used. A minimum of 6 repeat tests shall be conducted.

Note—MD and CMD do not necessarily refer to the machine (warp) and cross machine (fill) directions in the manufacturing process. They refer, for drawn products, to the more (CMD) or less (MD) highly drawn ribs where the aperture dimensions are unequal.

*Figure 5.4 Refinement in TxDOT DMS-6240 specification according to Alternative 1*

## 5.5.2. Alternative 2 – Three Geogrid Grades: Types 1, 2, and 3

In addition to the refinements recommended in Alternative 1, in Alternative 2, a third geogrid grade (Type 3) is recommended to be added to TxDOT DMS-6240. Rationale for adding this new grade is explained in Figure 5.5. As the three triangular geogrids with  $K_{SGC}$  values above 20 were found to perform considerably better than the other geosynthetics, it is recommended to define a third geogrid grade with the threshold  $K_{SGC}$  value of 20. It should be noted that the thickness of the ribs and the junctions in these three triangular geogrids are comparatively higher than the other triangular geogrid specified as Type 2. Therefore, the minimum thickness of the ribs and junctions of these three triangular geogrids are recommended to be used as the threshold thickness values for geogrid Type 3.

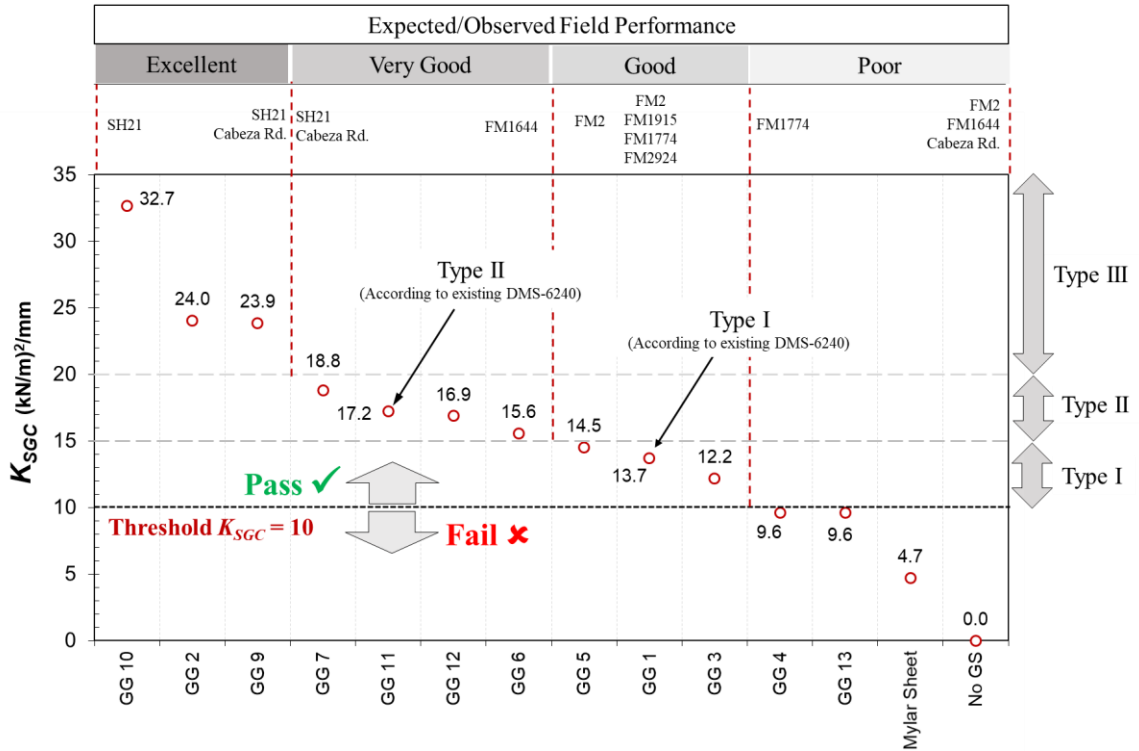


Figure 5.5 Alternative 2 - Adopting three geogrid grades in the refined TxDOT DMS-6240 specifications

The refinements in the TxDOT DMS-6240 that are consistent with this alternative are presented in Figure 5.6. A revised version of the specifications consistent with this alternative was also submitted as a separate document (5-4829-03-P1-v.2).

**Table 1  
Geogrid Requirements**

Property	Test Method	Type 1	Type 2		Type 3	
Aperture Size, mm (in.)	Tex-621-J	25–51 (1.0–2.0)	25–51 (1.0–2.0)		25–51 (1.0–2.0)	
Percent Open Area, %	Tex-621-J	70 Min	70 Min		70 Min	
Thickness, mm (in.)						
MD ribs	Tex-621-J	0.77 (0.03) Min	1.27 (0.05) Min		1.4 (0.055) Min	
CMD ribs		0.64 (0.025) Min	1.15 (0.045) Min		1.4 (0.055) Min	
Junctions		1.50 (0.06) Min	2.54 (0.10) Min		3.5 (0.14) Min	
Junction Efficiency, % of rib ultimate tensile strength MD & CMD	Tex-621-J	90 Min	90 Min		90 Min	
Stiffness of soil-geosynthetic composite ( $K_{SGC}$ ) <sup>2</sup> , (kN/m) <sup>2</sup> /mm CMD	Tex-1xx-E	10 Min	15 Min		20 Min	
Aperture Shape	---	Square or Rectangular	Square or Rectangular	Equilateral Triangular	Square or Rectangular	Equilateral Triangular
Ribs per Node	---	4	4	6	4	6
Tensile Modulus @ 2% elongation <sup>1</sup> , N/m (lb./ft.) MD & CMD	Tex-621-J	204,260 (14,000) Min	291,000 (20,000) Min	175,080 (12,000) Min	291,000 (20,000) Min	175,080 (12,000) Min

1. Determined as a secant modulus without offset allowances.
2. Determined using washed and dried aggregates with rounded particles that retain between ¼" (6.35 mm) sieve and Sieve No.4 (4.75 mm). A dry density of 102.5 pcf and a normal stress of 3 psi shall be used. A minimum of 6 repeat tests shall be conducted.

Note—MD and CMD do not necessarily refer to the machine (warp) and cross machine (fill) directions in the manufacturing process. They refer, for drawn products, to the more (CMD) or less (MD) highly drawn ribs where the aperture dimensions are unequal.

*Figure 5.6 Refinement in TxDOT DMS-6240 specification according to Alternative 2*

## Chapter 6. Conclusions

A comprehensive soil-geosynthetic interaction test program was conducted to identify the most relevant test configurations to be used for TxDOT specifications for geosynthetic-stabilized roadways. The final testing matrix involved testing geosynthetics in cross-machine direction under a normal stress of 3 psi using AASHTO No. 8-Truncated backfill material. Using the identified test configurations, a complementary testing program was conducted using 15 geosynthetics to produce data to support refinement of TxDOT specifications for geosynthetic-stabilized roadways. The geosynthetics were characterized and sorted on the basis of their  $K_{SGC}$  values.

Field performance of over 80 test sections located at 10 sites founded on expansive clay subgrades were also evaluated. Performance data was collected through three sources, including 1) visual condition survey of the road surface, 2) total station survey of the road transverse section, and 3) TxDOT PMIS Database. Overall, it was found that geosynthetic stabilization significantly improved field performance of the test sections under environmental loads resulting from expansive clay subgrades. The percentage of longitudinal cracks was found to be significantly lower in test sections stabilized using geosynthetics as compared to control (non-stabilized) sections.

Results from the experimental program using the 15 identified geosynthetics were evaluated along with the field performance of the test sections stabilized using each geosynthetic. The limit of acceptable  $K_{SGC}$  value was then established as  $K_{SGC} > 10$ .

Findings from experimental and field performance monitoring of this project were then used to provide TxDOT with recommendations for refinement of TxDOT DMS-6240. Two alternative refinement scenarios were recommended. The first alternative involved maintaining two geogrid grades (Types 1 and 2), and the second alternative involved adding a new geogrid grade (Type 3) to the existing specifications. The threshold  $K_{SGC}$  value for geogrid grades 1, 2, and 3 (Types 1, 2, and 3) were established as  $>10$ ,  $>15$ , and  $>20$ , respectively.

## References

- AASHTO. (2012). "Standard specification for classification of soils and soil-aggregate mixtures for highway construction purposes." AASHTO M145-91 (12), Washington, DC.
- AASHTO. (2013). "Standard specification for sizes of aggregate for road and bridge construction." AASHTO M43-05 (13), Washington, DC.
- ASTM. (2007a). "Standard test method for measuring geosynthetic pullout resistance in soil." ASTM D6706-01(07), West Conshohocken, PA.
- ASTM. (2007b). "Standard test methods for particle-size analysis of soils." ASTM D422, West Conshohocken, PA.
- ASTM. (2011). "Standard practice for classification of soils for engineering purposes (Unified Soil Classification System)." ASTM D2487-11, West Conshohocken, PA.
- ASTM. (2012). "Standard classification for sizes of aggregate for road and bridge construction." ASTM D448-12, West Conshohocken, PA.
- ASTM. (2014). "Standard test method for specific gravity of soil solids by water pycnometer." ASTM D854-14, West Conshohocken, PA.
- ASTM. (2015). "Standard practice for classification of soils and soil aggregate mixtures for highway construction purposes." ASTM D3282-15, West Conshohocken, PA.
- ASTM. (2016a). "Standard test methods for maximum index density and unit weight of soils using a vibratory table." ASTM D4253-16, West Conshohocken, PA.
- ASTM. (2016b). "Standard test methods for minimum index density and unit weight of soils and calculation of relative density." ASTM D4254-16, West Conshohocken, PA.
- FHWA (2003). "Distress Identification Manual for the Long-Term Pavement Performance Program (LTPP)." *U.S. Department of Transportation, Federal Highway Administration*, Publication No. FHWA-RD-03-031, Washington, D.C., USA, 168p.
- Roodi, G.H. (2016). "Analytical, experimental, and field evaluations of soil-geosynthetic interaction under small displacements." Ph.D. dissertation, The Univ. of Texas, Austin, Texas, USA.
- Roodi, G. H., Phillips, J. R., and Zornberg, J. G. (2016). "Evaluation of Vertical Deflections in Geosynthetic Reinforced Pavements Constructed on Expansive Subgrades." Proc., *3<sup>rd</sup> Pan-American Conference on Geosynthetics, Geo-Americas 2016*, Miami Beach, FL, USA, Vol. 2, pp. 1970 to 1987.

- Roodi, G. H., and Zornberg, J. G. (2012). "Effect of geosynthetic reinforcements on mitigation of environmentally induced cracks in pavements." *Proc., EuroGeo5: 5th European Geosynthetics Conference*, Valencia, Spain, 611–616.
- Roodi, G.H., & Zornberg, J.G. (2017). "Stiffness of Soil-Geosynthetic Composite under Small Displacements: II. Experimental Evaluation" *J. Geotech. Geoenviron. Eng.*, 143(10).
- TxDOT (2015). "Pavement Management Information System, Rater's Manual." *Texas Department of Transportation*, Austin, Texas, USA, 126 p.
- TxDOT DMS-6270 (2017). "Biaxial Geogrid for Environmental Cracking." *Texas Department of Transportation, Departmental Material Specification 6240*, Austin, Texas, USA.
- TxDOT DMS-6240 (2017). "Geogrid for Base/Embankment Reinforcement." *Texas Department of Transportation, Departmental Material Specification 6240*, Austin, Texas, USA.
- Zornberg, J.G., Roodi, G.H., & Gupta, R. (2017). "Stiffness of Soil-Geosynthetic Composite under Small Displacements: I. Model Development" *J. Geotech. Geoenviron. Eng.*, 143(10).
- Zornberg, J.G., Ferreira, J.A.Z., Gupta, R., Joshi, R.V., & Roodi, G.H. (2012a). "Geosynthetic-reinforced unbound base courses: quantification of the reinforcement benefits." *Rep. No. FHWA/TX-10/5-4829-01-1*, Center for Transportation Research (CTR), Austin, Texas.
- Zornberg, J. G., Roodi, G. H., Ferreira, J. & Gupta, R. (2012b). "Monitoring performance of geosynthetic-reinforced and lime-treated low-volume roads under traffic loading and environmental conditions." *Proc. Geo-Congress 2012*, 1310–1319.